GENERATION OF CONDITIONAL MUTANTS TO DISSECT ESSENTIAL GENE FUNCTION IN *CHLAMYDIA TRACHOMATIS*

Julie Ann Brothwell

Submitted to the faculty of the University Graduate School
in partial fulfillment of the requirements
for the degree
Doctor of Philosophy
in the Department of Microbiology and Immunology,
Indiana University
April 2017

Accepted by the Graduate Faculty, Indiana University, in partial fulfillment of the requirements for the degree of Doctor of Philosophy.

Doctoral Committee

David E. Nelson, Ph.D., Chair

Margaret E. Bauer, Ph.D.

Stacey D. Gilk, Ph.D.

William J. Sullivan, Jr., Ph.D.

December 7, 2016

Acknowledgements

"Vitality shows in not only the ability to persist, but the ability to start over."

-F. Scott Fitzgerald

Life is full of challenges, and graduate school is certainly no exception. Luckily I have been blessed with numerous people who have helped to encourage me during the oh-so-many frustrating times. I would like to take this opportunity to thank some of those people that either directly or indirectly contributed to my success.

I thank my research advisor, Dr. David Nelson, for giving me the opportunity to work in his lab. It is in his lab that I learned the power of high risk, high reward projects and to be resilient when experiments just did not work out. I learned the value of pushing the boundaries of what has been done, and this has made me look at research in a different way.

I am also indebted to numerous committee members over the years that have helped to guide my work. My committee members when our lab was at Indiana University-Bloomington (Drs. Melanie Marketon, Cheng Kao, and Claire Walzcak), provided important guidance when I was working on how *C. trachomatis* impacts cytokeratin 17 organization. Although the project did not pan out, I am grateful to have gained skills required to address pathogenesis from the host's perspective.

I would also like to thank my committee members at Indiana University School of Medicine for their insight into my projects. Although he moved following my prelim defense, Dr. Raymond Johnson helped to put the importance of developing genetic tools in chlamydia from a clinical perspective. We will soon be able to test one of his first

written qualifying exam questions regarding tropism of L2::MoPn chimeras in mice. Insight from Drs. Stacey Gilk and William Sullivan has opened my eyes as to how other intracellular pathogens survive and proliferate in host cells. Dr. Margaret Bauer has been helpful in better understanding bacterial genetics and helping guide me through the graduate school process.

Many thanks go out to Janis Stringer, Cathleen Collins, and Cynthia Booth for helping me navigate a multitude of forms and numerous travel arrangements and for making me smile.

Finally, I would be remiss to not thank my lab mates, friends, and family for listening to me complain about failed experiments and for helping me celebrate when they finally went right. It was difficult to move to a place I had never been before where I knew no one, but their support from both near and afar over the years has been truly invaluable.

Julie Ann Brothwell

GENERATION OF CONDITIONAL MUTANTS TO DISSECT ESSENTIAL GENE FUNCTION IN *CHLAMYDIA TRACHOMATIS*

Chlamydia trachomatis is the leading cause of bacterial sexually transmitted disease. *Chlamydia* spp. are all obligate intracellular organisms that undergo a biphasic developmental cycle within a vacuole termed the inclusion. Infectious, non-metabolically active elementary bodies (EBs) are endocytosed and differentiate into non-infectious, metabolically active reticulate bodies (RBs) before re-differentiating back into EBs. The chlamydial factors that mediate these differentiation events are mostly unknown. Comparative genomics revealed that *Chlamydia* spp. have small, highly conserved genomes, suggesting that many of their genes may be essential. Genetic manipulation strategies for *Chlamydia* spp. are in their infancy, and most of these cannot be used to inactivate essential genes. We generated a clonal ethyl methanesulfonate (EMS)-mutagenized *C. trachomatis* library and screened it for temperature sensitive (TS) mutants that produced fewer inclusions at either 32°C or 40°C compared to 37°C. Because EMS mutagenesis elicited multiple mutations in most of the library isolates, we also developed a novel lateral gene transfer strategy for mapping mutations linked to TS phenotypes. We identified TS alleles of genes that are essential in other bacteria and that are involved in diverse biological processes including DNA replication, protein synthesis, carbohydrate metabolism, fatty acid biosynthesis, and energy generation, as well as in

highly conserved chlamydial hypothetical genes. TS DNA polymerase (*dnaE*^{ts}) and glutamyl-tRNA synthestase (*gltX*^{ts}) mutants were characterized further. Both the *dnaE*^{ts} and *gltX*^{ts} mutants failed to replicate their genomes at 40°C but exhibited unique signs of stress. Chlamydial DNA replication begins by 12 hpi and protein synthesis begins by 2 hpi. However, inclusion expansion and replication of both of the mutants could be rescued by shifting to them to 37°C prior to mid-late development. Since *gltX*^{ts} is likely unable to produce aminoacyl-tRNAs at 40°C, our observation suggests that *de novo* chlamydial translation uses a pre-existing pool of aminoacyl-tRNA in EBs. Genetic suppressor analysis indicated that the inability of the *dnaE*^{ts} mutant to replicate its genome at 40°C might be linked to an inability of mutant DnaE to bind the DNA template. The tools and mutants we have identified will be invaluable assets for investigating many essential aspects of chlamydial biology.

David E. Nelson, Ph.D., Chair

Table of Contents

List of Tables

Table of Figures

List of Abbreviations

(p)ppGpp ..... guanosine pentaphosphate

aaRS ..... aminoacyl-tRNA synthetase

CDC ..... Centers for Disease Control

CERT ..... ceramide transport protein

CFP ..... cyan fluorescent protein

CFTR..... cystic fibrosis transmembrane receptor

COMC..... cysteine-rich outer membrane complex

CPn..... *C. pneumoniae*

CS..... cold sensitive

EB ..... elementary body

EF..... elongation factor

EMS ..... ethyl methanesulfonate

ENU ..... N-ethyl-N-nitrosourea

ER ..... endoplasmic reticulum

FRAEM..... fluoresence reported allelic exchange mutagenesis

gDNA..... genomic DNA

GFP ..... green fluorescent protein

glucose-6P..... glucose-6-phosphate

GPIC ..... *C. caviae*

HhH..... helix-hairpin-helix

hpi ..... hours post infection

HS ..... heat sensitive

IB ..... intermediate body

IF ..... initiation factor

IFN ..... interferon

IFU ..... inclusion forming unit

Indels ..... insertion and deletion mutations

L2 ..... *C. trachomatis* serovar L2

LGT ..... lateral gene transfer

LGV ..... lymphogranuloma venereum

mG ..... methylguanosine

MOI ..... multiplicity of infection

MoPn ..... *C. muridarum*

mRNA ..... messenger RNA

NIH ..... National Institutes of Health

nt ..... nucleotide

NTG ..... N-methyl-N'-nitro-N-nitrosoguanidine

OB ..... oligonucleotide-binding

ORF ..... open reading frame

PCR ..... polymerase chain reaction

PDGFR ..... platelet-derived growth factor receptor

PHP ..... polymerase and histidinol phosphatase

Pmp ..... polymorphic membrane protein

PTM ..... post-translational modification

RB ..... reticulate body

RF.....release factor

rif^R.....rifampicin resistance

rRNA.....ribosomal RNA

SNARF.....seminaphthorhodafluors

SPG.....sucrose phosphate glutamic acid buffer

STI.....sexually transmitted infection

t .....threonyl

T3SS.....type III secretion system

TCA.....tricarboxylic acid cycle

TILLING..... targeting induced local lesions in genomes

tRNA.....transfer RNA

TrpAB ..... tryptophan synthase

TS..... temperature sensitive

ψ .....pseudouridine

CHAPTER I: Introduction

Section I: Chlamydial Disease and Pathogenesis

The Chlamydiales are obligate intracellular pathogens

Bacteria in the phylum Chlamydiae have been evolving with their respective hosts for over 700 million years. The first Chlamydiae were obligate intracellular symbionts in amoebae and are termed the environmental chlamydia. Genome sequences of chlamydia isolated from *Acanthamoebae*, such as the *Parachlamydiae*, share high sequence similarity with today's medically relevant, pathogenic *Chlamydia* spp. (1). This indicates that the early chlamydiae evolved to parasitize higher order organisms only recently. Examples of these animal pathogens include *Chlamydia psittaci*, *C. abortus*, *C. caviae*, and *C. muridarum*, which naturally infect birds, sheep, guinea pigs, and mice, respectively. At least three species in the genus *Chlamydia*—*C. pneumoniae*, *C. trachomatis*, and *C. psittaci*—naturally infect humans.

Chlamydiae can also exhibit distinct tissue tropisms in the same natural host. *C. pneumoniae*, *C. psittaci*, and *C. muridarum* infect the respiratory tract. *C. abortus* is a natural pathogen of the reproductive tract. *C. caviae* infects both the eye and the reproductive tract. *C. trachomatis* also infects the eye and genital tract and can be further divided into biovars that have distinct *in vivo* tissue tropisms. *C. trachomatis* serovars A-C infect the conjunctival epithelium. Serovars D-K are the leading cause of bacterial sexually transmitted infection (STI) and primarily infect epithelial cells of the genitourinary tract. Serovars L1-L3 cause lymphogranuloma venereum (LGV) and can productively infect genital tract macrophages and disseminate to other body sites.

Genomes of diverse chlamydia strains and species have been sequenced (2-10). One of most striking differences between the various species was that the genomes of the environmental chlamydia are much larger than those of the pathogenic isolates. Interestingly, the transition from amoebal to mammalian hosts occurred concomitantly with a reduction in genome size from ~3 Mb (7,8,10) to ~1 Mb (4,9) and a proportional decrease gene number (7). This observation led to the hypothesis that the chlamydia genome size decreased as these pathogens became able to acquire host metabolites (11). Other examples of reductive evolution in chlamydia genomes include the truncation of three putative cytotoxins, which are homologous to large clostridial toxins, in *C. trachomatis* compared to *C. muridarum* (2). The cytotoxins may mediate entry and act as adhesins that dictate tropism (12). Differences in gene content of *C. trachomatis* biovars can also be seen in the inactivation of the *trpBA* operon in the oculotropic serovars, whereas the STI and LGV serovars maintain a functional operon (4). It is hypothesized that tryptophan synthase (TrpAB) utilizes environmental indole produced by the vaginal microflora to synthesize tryptophan (13). In environments lacking indole, such as the eye, TrpAB may produce toxic metabolites, such as ammonia (14). Thus, it may be advantageous for the urogenital and LGV serovars, but not for oculotropic serovars, to maintain *trpBA*.

Comparative genomics has not conclusively identified most of the genes that mediate known differences in chlamydial host and tissue tropism. Genome sequencing revealed a potential pathogenicity island, termed the plasticity zone, that has expanded gene content in *C. muridarum* compared to *C. trachomatis* (2). Another heterogenic region of the genome is the polymorphic membrane protein (Pmp) gene family. The

number of Pmp genes in a given *Chlamydia* spp. varies from just one in *C. felis* to 21 in *C. pneumoniae*, and these proteins are hypothesized to serve as adhesins (5,15). Genomic reduction has led to preservation of a core set of (partial) metabolic pathways and the machinery required for bacterial replication (16). However, up to one-third of the chlamydial genes have no known function or homologs outside of Chlamydiae (16).

Chlamydial pathogenesis

Infections with a number of *Chlamydia* spp. can be modeled in their natural hosts, although experimental human infection with *C. trachomatis* is not permitted due to safety concerns. *C. trachomatis* infection is, however, reportable to the CDC, which estimated that there were 456.1 cases per 100,000 persons in the United States in 2014 (http://www.cdc.gov/std/stats14/chlamydia.htm). A seven-day course of doxycycline or single dose of azithromycin is usually sufficient to treat chlamydia. Despite this, many infections go untreated because an estimated 70% of infected women (17) and 50% of men (18) are asymptomatic. These asymptomatic individuals are a major reservoir for infection and are at high risk for developing complications that impact fertility, especially in women. Discharge and dysuria are the most common symptoms in both men and women. Women may also experience pelvic pain. Left untreated in women, the infection can ascend the reproductive tract and lead to severe sequelae such as pelvic inflammatory disease and fallopian tube scarring, increasing the risk of infertility and/or ectopic pregnancy. In contrast, men rarely experience long term or severe reproductive sequelae.

Much of the pathology elicited by chlamydia infections results from infected epithelial cells attracting T_H1 cells to the site of infection. Once recruited, the T_H1 cells

release inflammatory cytokines such as interleukin (IL)-1 (19-22) and tumor necrosis factor (TNF)-α (20,23). This cytokine storm leads to the recruitment of neutrophils to the site of infection (20). However, because chlamydia are intracellular pathogens, some mechanisms neutrophils use to infiltrate the tissue, such as release of matrix metalloproteases (24,25), are not effective at eliminating these pathogens but lead to damage of the host tissue causing fibrosis and scarring.

The biphasic lifecycle

A chlamydia infection begins when a metabolically inactive, but infectious, elementary body (EB) enters a host cell by pathogen-mediated endocytosis (26). Chlamydia remains inside a non-fusogenic endocytic vacuole within the host cell, termed the inclusion, until the end of the developmental cycle. Approximately 8 hours after entry, the EB completes differentiation into the reticulate body (RB) (27,28). RBs are non-infectious, but are metabolically active and can replicate. As the host cell fills with bacteria, an unknown signal eventually prompts differentiation of RBs back into EBs. Eventually, the heavy chlamydia burden within the host cell leads to release of EBs so that a new round of infection can initiate (29).

The metabolic capacity of EBs has recently been reconsidered (30), but attempts to culture *C. trachomatis* in anexic media by supplying the metabolites that these pathogens cannot synthesize have been unsuccessful for both EBs and RBs (31,32). EBs take up glucose-6-phosphate (glucose-6P), and RBs can take up ATP (31). However, media formulations containing these metabolites were unable to drive differentiation from EB to RB or from RB to EB (31). Multiple signals and steps likely mediate these

transitions, and gaining a better understanding of chlamydial metabolism may be necessary for the development of an anexic culture system.

The chlamydial developmental cycle

Attachment of *C. trachomatis* EBs to host cells is mediated by multiple receptors including the estrogen receptor (33,34), platelet-derived growth factor receptor (PDGFR) (35), apolipoprotein E4 (36), mannose binding proteins (37,38), cystic fibrosis transmembrane receptor (CFTR) (39), and heparin sulfonated proteins (40). After attaching, chlamydia use a type III secretion system (T3SS) to translocate several effectors into host cells that induce their endocytosis. TarP is secreted within five minutes of attachment and is tyrosine phosphorylated by host Src-family kinases to induce actin polymerization beneath the EB (35,41,42). Type III secreted effectors that are delivered later, including CT694, are also phosphorylated by the host and direct actin polymerization near the inclusion (43). This enhanced actin polymerizing environment generates an "actin pedestal" that drives endocytosis of the EB (44). The nascent inclusion is then trafficked along microtubules to the perinuclear space by 6-8 hours post infection (hpi) (45). Other early effectors have functions unrelated to attachment and entry. For example, TepP modulates the host cell innate immune response (46). Additional secreted effectors that decorate the inclusion, termed Inc proteins, prevent recognition of the nascent inclusion by cell-autonomous immune effectors and fusion with lysosomes (47). Pulse chase experiments showed that *de novo* Inc expression begins by 2 hpi (48).

After entry, the EB begins differentiation into an RB. Key differences between EBs and RBs include their sizes and outer membrane protein arrangements (49). EBs are

0.3 μm in diameter, have condensed genomes, and have highly disulfide-linked outer membrane proteins. EBs only contain trace amounts of peptidoglycan (50), but gain additional structural integrity from a cysteine-rich outer membrane complex (COMC), which is constructed from several cysteine-rich proteins including OmpA, OmcA, and OmcB (reviewed in (51)). RB differentiation may be driven by the reduction of disulfide bonds between different proteins in the COMC, which results in a more spacious (~1 μm diameter) RB, and release of the chlamydial genome from the histone-like Hc1 protein (52). The signal that drives this process is unknown.

After differentiation into RBs, chlamydiae must obtain nutrients from the host cell. Chlamydiae incorporate host-derived sphingolipids that they obtain by intersecting lipid droplets from the endoplasmic reticulum (ER) in a ceramide transport protein (CERT)-dependent manner (53-56). Chlamydiae cannot make nucleotides or amino acids *de novo*, so they utilize various transporters to siphon these building blocks from the host cell (2,4,57,58). Chlamydiae derive their energy by importing of ATP from their host and generating ATP using a truncated tricarboxylic acid (TCA) cycle (2,4,59).

De novo transcription of chlamydial genes is developmentally regulated (27,60,61). Transcription of the three known chlamydia sigma-factors occurs in sequential waves during development (61). Housekeeping genes, such as *dnaE* and *groEL*, are expressed early in infection, followed by metabolic genes, such as *eno*, during mid-cycle, and primarily structural proteins, such as *omcB*, at the end of development (27,28,60). Chlamydia encode few known transcription factors, and gene expression—especially for early genes—is thought to be regulated by supercoiling (62). Expression of early chlamydia genes may be supercoiling-independent or these genes may have a

distinct secondary structure that allows them to be transcribed early. One early gene, *euo*, is a late gene repressor (63). Other early genes include the anti-σ^{54} factor, whose ligand, σ^{54}, is needed for late gene expression (61). Non-coding RNAs such as *lhtA* inhibit the translation of the chlamydial histone-like proteins Hc1 and Hc2 early in infection (64).

RBs, unlike EBs, can undergo cell division, and, until recently, it was believed that RBs only divided by binary fission. Chlamydiae appear to lack some key cell division proteins that locate the septum in other bacteria (4). Attempts to identify chlamydial homologs of FtsZ and FtsB have been unsuccessful (65,66). Despite this lack of characterized cell division proteins, septum formation does occur, and trace amounts of peptidoglycan localize to the chlamydial division plane (67). Recently, it was shown that chlamydia divide by a budding mechanism rather than by binary fission at least until mid-development (68). How this occurs without classical Fts proteins is unclear.

The end of the chlamydial developmental cycle is marked by de-repression of late genes by Euo, the synthesis of an anti-anti-σ^{54} factor, condensation of genomic DNA, and disulfide bonding in the COMC. It is hypothesized that an RB must remain attached to the interior face of the inclusion membrane via its type III secretion apparatus to prevent its transitioning into an EB (69,70). Therefore, detachment from the membrane would drive RB to EB differentiation. RBs have been observed in the center of inclusions in electron micrographs; however, whether the differentiation process had initiated in these cells is not known. If RBs divided exclusively by polar cell division and inclusion membrane contact is required to maintain the RB state, then, past a certain inclusion

surface area to volume ratio, cell division would exclusively produce EBs in a linear and not exponential manner.

Chlamydiae can exit cells by two different mechanisms, and these are used at similar frequency in cell culture (29). In the first mechanism, the inclusion grows until it takes up the vast majority of the host cell cytosol. The inclusion membrane then bursts in a protease-dependent manner, releasing the inclusion contents into the host cytoplasm. Thirty minutes later, an influx of cytoplasmic calcium causes the host cell plasma membrane to lyse, and EBs release from the host cell. Alternatively, the inclusion can be extruded from the host cell in an actin-dependent manner, leaving both the inclusion and host cell intact (29,71). It is unclear which mechanism is most important *in vivo*.

The developmental cycle is summarized in Figure 1.

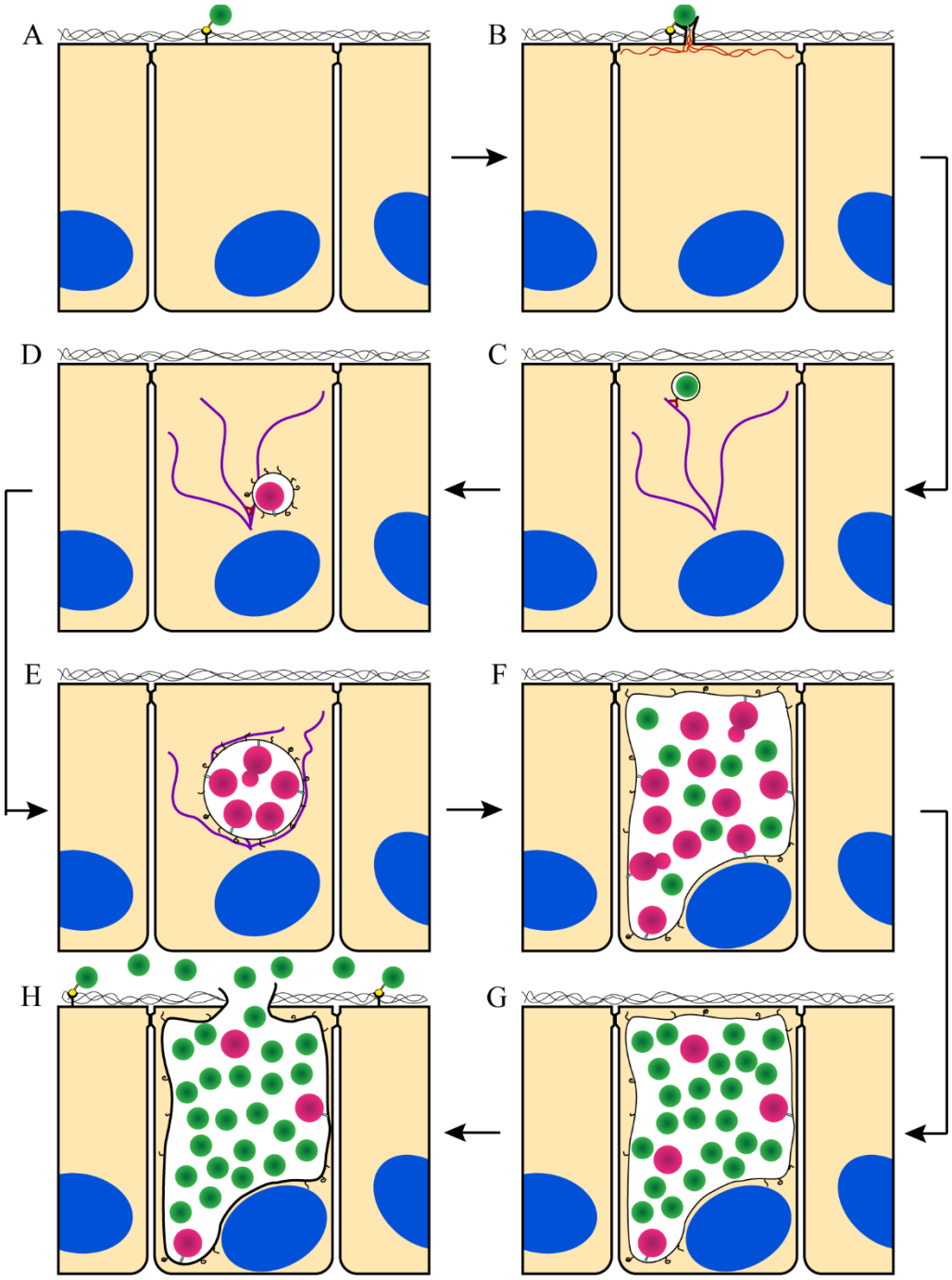

Figure 1 Schematic of the chlamydial developmental cycle. (A) Infection begins when an infectious elementary body (EB) attaches to the host cell via receptor-ligand and electrostatic interactions. (B) Secretion of T3S effectors into the host cell induces actin polymerization that leads to the formation of a "pedestal" and pathogen-mediated endocytosis of the EB. (C) The nascent inclusion is trafficked by dynein motors along microtubules to the perinuclear space. (D) The EB then differentiates into a metabolically active reticulate body (RB), which secretes additional T3S effectors, including Incs. (E) As RBs replicate the inclusion expands. (F) Late in development, the RBs differentiate back into EBs. (G) The inclusion fills the cell cytoplasm near the end of development which can cause rupture of the inclusions and host cell (H) or the entire inclusion can be extruded (not shown). Adapted from (72) and (73).

Section II: Chlamydial Genetics

The dawn of chlamydial genetics

Attempts to use comparative genomics of clinical strains to interrogate the molecular basis of chlamydial pathogenicity and tropism have seen limited success because naturally occurring mutants are rare. Natural mutants that have been identified include a plasmid free variant of *C. trachomatis* serovar L2 (74) and an *incA*$^{-}$ variant (75). The *C. trachomatis* L2 plasmid contains eight ORFs. Four of these ORFs are important for plasmid maintenance, one is a transcription factor, and three appear to encode highly conserved chlamydial hypothetical proteins (76). Loss of the plasmid causes a reduction in EB adherence to host cells in cell culture and a large reduction in virulence in mice (77,78). IncA was the first inclusion membrane protein discovered, and it is required for inclusion fusion when one cell contains two or more inclusions (79,80). Since the mid-2000s, the field of chlamydial genetics has rapidly expanded and new approaches have begun to yield insights into chlamydial pathogenesis and tropism that were not gleaned from naturally occurring chlamydial variants (Figure 2). Some of these advances are discussed below.

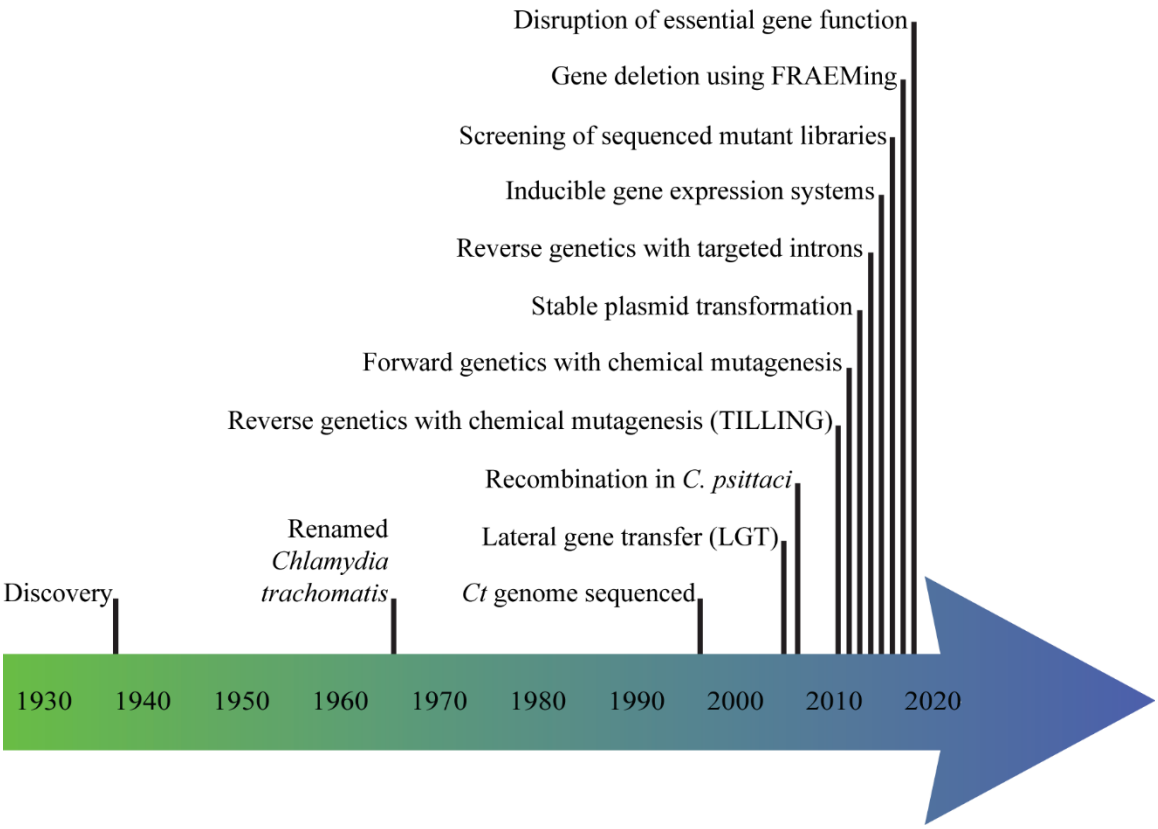

Figure 2 Timeline of genetic advances in *C. trachomatis*. The "psittacosis virus" was found in the 1930s following a severe outbreak of psittacosis that would prompt the formation of the National Institutes of Health (NIH). Moulder *et al.* reclassified *Chlamydia* spp. as bacteria as opposed to viruses given that they can independently make proteins and replicate DNA (81). The advent of whole genome sequencing allowed sequencing of the first chlamydial genome in 1998. From the mid-2000s on, the speed of new advances accelerated dramatically. Figure adapted from (82).

Lateral gene transfer (LGT)

A major advance in chlamydial genetics occurred when DeMars and colleagues determined that they could generate recombinant *C. trachomatis* strains using a technique they termed lateral gene transfer (LGT) (83). This approach uses two parent strains with different endogenously encoded antibiotic resistance alleles. LGT uses co-infection and cultivation in media containing both antibiotics to select for recombinants. LGT has been used to generate interspecies chlamydia chimeras, including *C. muridarum* and *C.*

trachomatis L2 isolates that contain a naturally occurring *C. suis* tetracycline resistance island (84).

Further evidence of chlamydial recombination was observed when a kausagomycin-resistant *C. psittaci* clone was isolated after the parent was transformed with a plasmid containing a kausagomycin resistance allele and neighboring silent mutations (85). The transformant had never been passaged in the presence of antibiotic and contained not only the mutation that rendered it kasugamycin resistant but also the unselected neighboring silent mutation that had been engineered into the donor plasmid (85). This provided the first evidence that chlamydiae could recombine foreign DNA into their genomes. As little as 2000 bp of DNA homology was sufficient to mediate this recombination, although shorter constructs were not tested.

Generation of mutant libraries

Several approaches for random mutagenesis of chlamydia have been developed. For example, N-methyl-N'-nitro-N-nitrosoguanidine (NTG), which causes insertions and deletions (Indels), ethyl methanesulfonate (EMS), which causes G→A transitions, and N-ethyl-N-nitrosourea (ENU), which causes A→T transversions and A→G transitions, have been used to mutagenize various *Chlamydia* spp. (86-88). Cheaper genomic sequencing has made it feasible to identify the chemically induced mutations in chlamydia that induce specific phenotypes.

Several chlamydia mutant libraries have been constructed using EMS mutagenesis (87-90). Mutants that have mutations in specific genes of interest have been isolated from EMS-mutagenized libraries using an approach called Targeting Induced

Local Lesions in Genomes (TILLING) (87). TILLING uses PCR amplification and endonuclease digestion to detect specific mutants in larger pools of mutagenized organisms. Following PCR amplification of an allele of interest from a pool of genomes, the reaction is slowly annealed. If a mutant was present in the pool, wild type and mutant PCR products will generate heterodimers that contain mismatches. These mismatches can be recognized by the endonuclease CelI, which generates cleavage products that can be visualized by gel electrophoresis. The mutant of interest can then be purified from the starting mutant library.

The first use of TILLING in chlamydia targeted *trpB* of *C. trachomatis* serovar D (87). Isolation of a mutant with a nonsense mutation in *trpB*, whose product is the β-subunit of tryptophan synthase, confirmed that tryptophan synthase (encoded by the *trpBA* operon) is required for indole rescue of *C. trachomatis* from persistence. TILLING was also used to test if various *C. muridarum* plasticity zone genes contributed to virulence of this organism in mice (90). Various phospholipase, cytotoxin, and nucleotide transporter mutants were isolated and shown to be equally virulent to wild type C. *muridarum* in cell culture and in the murine genital tract (90).

Another group screened a clonal EMS-mutagenized *C. trachomatis* serovar L2 *rif*^{R} library (88) for mutants that had altered plaque morphologies (88). A granular plaque phenotype was linked to mutations in a glycogen hydrolase (*glgB*) using LGT (88). Genomes of all the isolates in this ~800 clone library were later sequenced (91), which provided insight into which chlamydia genes are essential. Nonsense mutations were identified in some genes that were thought to encode the essential components of the already truncated chlamydial biosynthetic pathways (91). For example, *C. trachomatis*

lacks genes for the first three enzymes of the TCA cycle, but nonsense alleles of another TCA gene, a carbon source transporter gene, and other carbon metabolism genes were isolated, indicating that these pathways may be redundant for growth in cell culture (91).

Functionalizing plasmids

The endogenous chlamydial plasmid has been used as a backbone for development of several shuttle plasmids. The first stably transformable shuttle plasmids spliced the *C. trachomatis* SW2 plasmid with pBR322 or pGFP-N1 (92). This permitted the first introduction of ectopically expressed foreign DNA into *C. trachomatis*. Later shuttle plasmids contained elements that permitted controlled expression of genes using the Tet-On system (93), expression of multiple fluorophores (94), and curing of the shuttle and endogenous plasmids (95).

Unstable plasmids have been used to drive directed recombination events in *C. trachomatis* LGV. The TargeTron® system from Sigma has been successfully adapted for chlamydia (96). TargeTron® was first used to disrupt *incA*, which confirmed that inactivation of this gene led to the same non-fusogenic phenotype observed in some rare, naturally-occurring *incA*$^-$ strains. TargeTron® has important limitations, including the need for a specific proprietary sequence to target the insertion to a particular locus. Additionally, some genes do not contain a suitable Group II intron target sequence or may only contain targets near their 3' ends.

An inducible suicide plasmid was developed to recombine DNA into the *C. trachomatis* genome using a technique termed Fluorescence-Reported Allelic Exchange Mutagenesis (FRAEM) (95). The plasmid gene *pgp6* is required for plasmid

maintenance (97). By placing *pgp6* under the control of a Tet-On promoter in the FRAEM plasmid, it could be downregulated in the absence of tetracycline, leading to loss of the plasmid. FRAEMing was used to knock out *trpA*, whose gene product forms a dimer of dimers with TrpB to form tryptophan synthase. The cargo on the FRAEMing plasmid included a GFP-amp^R cassette flanked by ~3kb of homology in either direction of *trpA* to direct homologous recombination. Ampicillin was used to select for recombinants, and GFP served as a secondary marker for recombinants.

Section III: Genome Replication

DNA replication

Cell division is preceded by genome replication so that each daughter cell inherits a complete set of genetic material. The machinery required to replicate the *Escherichia coli* genome was discovered in 1972 by Arthur Kornberg (98-100). The DNA replication holoenzyme contains 17 unique protein components (101). DNA replication begins by the "melting" of the double helix structure by the ATP-dependent DnaA at the origin of replication (102,103). The DNA replication holoenzyme then assembles on the single-stranded DNA (104-106).

Six monomers of DnaB assemble on the single stranded DNA to form the helicase. Binding of DnaB prompts the attachment of RNA primase, which lays down a single primer for the leading strand, which is polymerized continuously, since the DNA is read in the 3'→5' direction as the helicase unwinds the DNA (107). RNA primase then binds to the tau (τ) protein, which serves to connect it to the polymerase and clamp loader complexes (108). This enhances the efficiency at which RNA primase can synthesize

primers for the lagging strand. This is necessary because DNA can only be synthesized in the 5'→3' direction, but the lagging strand is unwound from 5'→3', so multiple primers are synthesized in the 5'→3' direction approximately every 1 kb as more single stranded DNA becomes available, and DNA polymerase then uses these to polymerize the Okazaki fragments (109).

The helicase is attached via the tau (τ) protein to two independent polymerase subunits that are responsible for either all the leading or lagging strand synthesis (105). DNA polymerase III, also known as DnaE, is required for genome replication (110). The template strand is threaded through this "hand-shaped" protein, and dNTPs are added in an approximately eight nucleotide long channel (111). DNA synthesis by DnaE is template-dependent and proceeds by addition of dNTPs to the free 3'-OH of the newly synthesized strand. The initial 3'-OH belongs to the last nucleotide that the RNA primase synthesized, and DNA synthesis by DnaE continues until double stranded DNA is encountered.

There are five known DNA polymerases, but only DNA polymerase III can replicate entire genomes. DnaE also has the highest degree of processivity (112). DnaE in the context of the holoenzyme can replicate up to 100,000 bp before falling off the template *in vitro*, but DnaE alone can only replicate approximately 100 bp before falling off the template. The high processivity of the holoenzyme is conferred by the β-clamp (DnaN) (113,114). Two subunits of DnaN are loaded around the single stranded template by the clamp loader complex (τγδ'δ), which transfers the β-clamp from the interaction motifs on the clamp loader complex to a similar motif on DnaE using ATP hydrolysis to fuel the transfer (105).

In addition to being highly processive, DnaE is highly accurate because it has exonuclease proofreading activity. Mismatched residues are detected inside the channel by the polymerase and histidinol phosphatase (PHP) domain of DnaE (111,115). Proofreading is more accurate when DnaE is bound to the ε and θ proteins, although how these proteins improve the accuracy is not known, and they do not appear to have any catalytic domains (116,117).

DNA replication ends in the genomic terminator sequence. The speed of DNA polymerization typically slows as genome replication nears completion because the polymerases encounter *ter* sequences near the terminator (115). Thus, DNA replication ends in a similar location each replication cycle even though the replisomes on each side encounter different obstacles (e.g., highly transcribed genes, DNA damage, etc.) (112). In addition, each replisome must complete replication of both the leading and lagging strands before dissociating, and synthesis rates of the two strands differ *in vitro* (118). The consistent location of the terminator is important, since bacteria can initiate a new round of replication before the previous round is complete.

Genome replication is completed after DNA polymerase I (PolA) replaces the RNA primers in the leading and lagging strands with dNTPs, since DnaE cannot remove these, and DNA ligase seals the nicks between the PolA and DnaE synthesized strands (112).

Chlamydial genome replication

Chlamydia contain all the homologs of the *E. coli* DNA replication machinery. The EB is assumed to be metabolically inactive, since it does not replicate its genome or

synthesize proteins (119), although it may transport glucose-6P (30,31). This may be due to special constraints inside the EB including a high degree of DNA supercoiling and/or a complication of chlamydial DNA being wrapped around histone-like proteins (120,121). Interestingly, transcripts for *dnaE* are detectable by 2 hpi, although the first round of DNA replication is not completed until approximately 6 hpi (27). The speed of chlamydial genome replication has been calculated to be either 1.45 hours (27) or nearly 3 hours (61). Whether the increased rate of genome replication after the first round is due to the absence of histones in mid-development or a more nutrient-rich environment in mid-development is unclear.

Chlamydia initiate genome replication approximately every 4.5 hours and divide approximately every 2-3 hours in normal conditions (61). How stressful stimuli affect DNA replication is not well described. A viable but non-cultivatable state (i.e., persistence) has been described in which chlamydial DNA replication proceeds in the absence of cell division (122,123). Stress imposed by interferon (IFN)-γ and penicillin can inhibit chlamydial cell division, but does not block genome replication, resulting in the production of large, aberrant RB that contain many copies of the genome. Removal of the stress allows persistent chlamydiae to resume cell division. This observation suggests that there is a certain degree of independence between the chlamydial DNA replication and the cytokinesis machinery (124).

The effects of an inhibitor (KSK120) of UhpC, a glucose-6P transporter, on inclusion size led the authors to conclude that chlamydial DNA replication is independent of inclusion expansion (125,126). An alternative explanation for why KSK120 inhibits *C. trachomatis* genome replication is that lack of a glucose-6P inhibits DNA replication,

but does not inhibit inclusion expansion. The effect of DNA replication on chlamydial morphology and development is investigated in Chapter IV.

Section IV: Protein Synthesis

Translation

Protein production is tightly regulated by several feedback loops and involves many proteins and RNA species. Proteins are synthesized from genes through an RNA intermediate called messenger RNA (mRNA). mRNA production of a given gene is dictated by the epigenetic landscape, the presence (or absence) of specific repressors and/or activators, supercoiling of the genome, and, in bacteria, the availability of specific sigma (σ) factors (127). The level of mRNA in a cell is not only the product of active transcription, but also degradation. mRNAs are degraded by ribonucleases when they are not protected by actively translating ribosomes, resistant secondary RNA structures, or RNA modifications (128).

Levels of a given protein do not necessarily reflect numbers of correlating transcripts (127). For example, small non-coding RNAs and secondary structural elements can prevent ribosomal binding, and thus act as post-transcriptional regulators of protein synthesis.

In prokaryotes, mRNAs are translated by the 70S ribosome as they are simultaneously transcribed. Loading of mRNA onto the 30S ribosome begins when initiation factor (IF)-3 binds to the 30S ribosome, preventing binding of the 50S ribosomal subunit as the mRNA is loaded (129). IF-1 then binds to block the A-site as

the 5' end of the mRNA begins to interact with the 16S rRNA of the 30S ribosomal subunit (130,131). The reading frame is determined by interaction of the Shine-Delgarno sequence with the 16S rRNA contained in the 30S ribosomal subunit (132). Met-$tRNA^{fMet}$-IF-2-GTP binds to the mRNA in the P-site of the ribosome (133), and the 50S ribosomal subunit can then bind the mRNA-30S ribosomal complex. The GTP bound to IF-2 is then hydrolyzed, and IF-2-GDP is released (134). Aminoacyl-tRNAs bound to EF-Tu-GTP can then enter the ribosome and interact with the mRNA through complementary basepairing of the three nucleotide (nt) anticodon of the tRNA with the 3 nt codon in the mRNA residing in the A site of the ribosome (135,136). Next, the amino acid in the A-site initiates nucleophilic attack of the amino acid in the P-site, allowing transfer of the growing polypeptide chain (137). The 30S subunit then shifts relative to the 50S subunit from GTP hydrolysis of elongation factor (EF)-G-GTP. This shift moves the tRNA originally in the P-site to the E-site and the tRNA originally in the A-site to the P-site (138). This process continues for the length of the mRNA until a stop codon is encountered. Release factors (RF) bind to stop codons and potentiate the disassembly of the ribosomal complex and release of the transcript (139).

Regulation of translation

Protein synthesis is an energy intensive process, so it is highly regulated in many bacteria (140). Model bacterial organisms like *E. coli* and *Bacillus subtilis* have organized the majority their translational machinery into operons consisting of up to 21 genes (141,142). This allows coordinate regulation of a variety of rRNAs, ribosomal proteins, and tRNAs at the transcriptional level (143). A rapid response to nutrient deprivation via the stringent response, an increase in the ADP:ATP ratio, or the lack of

amino acids via the general amino acid stress response is key to cellular survival. This is important, since the inability to complete translation of transcripts not only wastes energy reserves, but also leads to stalled ribosomes and the eventual release and accumulation of incomplete polypeptides (144), which can be detrimental (145).

To downregulate translation of mRNA, ribonucleases such as MazF (146-148) and RelE (147) degrade mRNA that is either free or ribosome-bound, respectively. mRNAs that are important for the stress response are not immune to this and are processed for leaderless protein synthesis. This is performed on "stress" ribosomes containing 16S rRNA that has been cleaved to remove the Shine-Delgarno recognition sequence (148).

Several ribosomal accessory proteins help regulate ribosome function and efficiency during the canonical stringent response. Ribosomes can sense amino acid deprivation through the ratio of uncharged to charged tRNA in the cell (149). While lack of any aminoacyl-tRNA can cause translational pausing, lack of aminoacylated tRNAs that already cause translational pausing, such as Pro-tRNA^{Pro}, can be especially detrimental to maintaining translation (150). If the ratio of aminoacylated to non-aminoacylated tRNA is too low, then lack of a donor for the growing peptide chain will be terminated by tmRNA, which uses a protein template to simulate a stop codon. Subsequent interaction of tmRNA with RFs causes peptide release from the ribosome and allows the ribosome to be recycled (150). Another accessory protein, EttA, is responsive to ATP:ADP levels and binds to and inhibits ribosomes when ADP levels are high, allowing the cell to tune protein synthesis to the amount of available cellular energy (151). Free ribosomes also are increased when guanosine pentaphosphate [(p)ppGpp]

stimulates ObgE, which has been shown to be essential (152) except in a r*elA*$^-$ background (153). Lack of ObgE shifts the equilibrium of ribosomes to favor the 30S and 50S forms rather than the 70S form, which decreases the amount of translation (154,155). ObgE also has a role in rRNA processing, since pre-16S and pre-23S rRNA levels increase in its absence (154).

Rapid regulation of translation extends from the transcriptional level to the post-translational level. Ribosomes contain at least 27 proteins and 3 large rRNAs. Ribosome assembly is regulated by the availability of mature rRNA transcripts. For example, RNase J is required to trim the 16S rRNA transcript to the proper length from the 5' end (156). The endonuclease YbeY trims the 3' end of the 16S rRNA transcript (157,158). Ribosomes cannot assemble without mature rRNA transcripts, so absence of these ribonucleases inhibits translation. Ribosome activity can also be modulated post-translationally. Transcription of *rmf* increases in the presence of ppGpp, and Rmf physically holds 50S ribosomes together to form the 100S ribosome—an inactive ribosome dimer—which is used to reversibly inactivate mature ribosomes (159).

Another way to regulate translation is through the substrates—namely the tRNAs (160). Decreased levels of individual tRNAs have been shown to induce accumulation of immature 16S rRNA transcripts, which decreases the number of functional ribosomes in the cell (161). Furthermore, control of translation efficiency and accuracy is perhaps most closely linked to tRNA number (162-165) and modification (166-171). Immature tRNA transcripts are trimmed to their mature size of 74-91 nt (depending on species and isoform) by RNase P at the 5' end (172) and RNase D at the 3' end (173). Most tRNAs then require the addition of the –CCA sequence on the 3' end by the –CCA-adding

enzyme to be able to accept an amino acid (174). The aminoacyl moiety is added to the final adenine.

Over 90 different tRNA modifications have been described (175). The two most common are methylguanosine (mG) 18 and pseudouridine (ψ) 55, which are found in virtually all tRNAs from prokaryotes to eukaryotes (169). These modifications enhance the base-pairing interactions between G18 in the D arm and U55 in the T arm of the tRNA and allow the cloverleaf-like secondary structure of the tRNA to adopt a stable "L"-shaped tertiary structure. These modifications are required for optimal aminoacylation and translational efficiency (176). Other common modifications aiding in translational efficiency include threonylation of A37 (tA^{37}) for tRNAs using ANN codons and ψ34, which both create more rigid anticodon loops that enhance the rate of proper base pairing with codon sequences during translation and reduce the risk of frameshifting (177).

The majority of known tRNA modifications have no known function. Up to 17% of bases in tRNAs are modified—the highest percentage of any RNA species (178). Until the mid-1990s, tRNA research focused primarily on quantifying the number of isoacceptors, molecular sizes, and quantities of tRNA under different stimuli. The advent of tRNA sequencing by mass spectrometry revealed a high number of modified bases and posed new questions about the roles of tRNAs and their associated enzymes in stress responses and disease. Modifications are normally added to various tRNAs, and additional modifications may be added in response to stress. The list of modifications continues to grow as new enzymes are found and more tRNA sequencing studies are performed. Linking why a particular modification exists is complicated by not knowing

which enzyme(s) placed it there and why (166,168). Thus, bioinformatic searches for tRNA interacting proteins as well as data sets from tRNA sequencing studies spur discovery of new modifications. Another challenge is determining the *in vivo* significance of tRNA modifications (179,180). Lack of essential tRNA modifications can cause degradation of the tRNA which suggests that these enzymes help maintain optimal cell health (181-183).

Other tRNA modifications have been found using mass spectrometry (184-186), but the enzymes performing these modifications have not yet been identified. Investigating the role of tRNA modifications has often been hindered by a lack of obvious phenotypes. As more information is gained regarding the regulation of the modification enzymes, some of the unobvious biochemical purposes of the modifications in response to stress are beginning to be elucidated (183). For example, certain tRNA modifications are important for heat shock survival (182,187), antibiotic resistance (188,189), immune activation (190), and, in higher eukaryotes, cancer progression (191).

tRNAs function as translators between the nucleic acid message and the functional protein. This is accomplished by the addition of an amino acid to the terminal 3' adenosine residue of the –CCA motif by aminoacyl-tRNA synthetases (aaRSs). These proteins recognize key features of mature tRNAs to decrease the chance of mis-aminoacylation. The features used by the aaRS to identify the appropriate tRNA vary from enzyme to enzyme. For example, the *E. coli* alanyl-tRNA synthetase only recognizes the amino acid stem of the tRNA (192). This is a rare case though, and most aaRSs recognize a certain primary sequence in the tRNA, specific combinations of tRNA modifications, and the anticodon (193).

aaRSs catalyze two enzymatic reactions using the same catalytic site (112). The first is the adenylation of the incoming amino acid. The adenylated amino acid can then attack the 3'-adenosine of the tRNA, which ultimately results in a labile ester bond between the 3'-OH of the tRNA and the carboxyl group of the amino acid. The proportion of mis-aminoacylated tRNA in bacteria is typically higher than in eukaryotes because bacterial aaRSs typically have less stringent editing capabilities.

Interestingly, several organisms only encode 19 or 18 aaRSs, which is less than what would be required to aminoacylate tRNAs for the 20 amino acids found in proteins. *Chlamydia* spp. were the first bacteria to be shown to have only 18 aaRSs (194). In organisms with fewer than 20 aaRSs, AspS adds aspartate to both $tRNA^{Asp}$ and $tRNA^{Asn}$ and GltX adds glutamate to both $tRNA^{Glu}$ and $tRNA^{Gln}$. These mis-acylations are subsequently corrected by the transamidase complex GatCAB (195). GatCAB docks onto the N-terminal domain of both AspS and GltX while in complex with the mis-aminoacylated tRNA (196). GatC is the catalytic subunit in the complex and transamidates the carboxyl group of the aspartate or glutamate using the amine group from glutamine (195).

Expression of translation-related genes in *Chlamydia* spp.

Translation regulation in *Chlamydia* spp. has not been directly investigated. Belland *et al*. conducted a time course study of *C. trachomatis* serovar D RNA throughout the development (28). Transcription of putative tRNA modification enzymes and aaRSs primarily begins early in infection (3-8 hpi) (28). Putative *C. trachomatis* homologs of known tRNA modifying enzymes are listed in Table 1. While this expression pattern makes sense in terms of the order in which the genes are used, it is

particularly remarkable given that these genes are scattered throughout the *C. trachomatis* genome, unlike in *E. coli* and *B. subtilis* where these genes are more organized into multicistronic operons (Figure 3).

Table 1 Predicted tRNA modifying enzymes in *C. trachomatis*

Enzyme	Function and Modification(s)	First Transcribed [a]
Pseudouridinases		
TruA	U-55 isomerase	8 hpi
TruB	U-38, 39, & 40 isomerase	3 hpi
RluA	U-32 isomerase	8 hpi
Methyltransferases		
TrmB	Guanine-N7 methyltransferase	8 hpi
TrmD	Guanine-N1 methyltransferase + DUF	3 hpi
TrmL	C-34 2'-O-methyltransferase	3 hpi
TrmU	5'-methylaminomethyl-2-thiouridate methyltransferase	8 hpi
Others		
TilS	$tRNA^{Ile}$ lysine synthase	8 hpi
YrdC	N6-A^{37}-threonylcarbomoyal transferase	8 hpi
Tgt	Quenine tRNA-ribosyl transferase	8 hpi
GidA	Uridine 5-carboxymethylaminomethyl modifying enzyme	16 hpi
MiaA	δ2-isopenylpyrophosphate transferase	8 hpi

[a] From Belland *et al*. 2003 transcriptome of *C. trachomatis* serovar D/UW-3

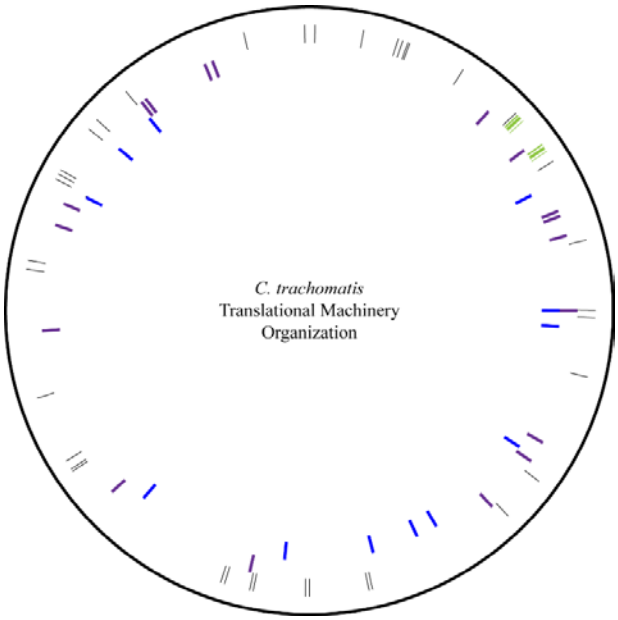

Figure 3 Organization of tRNA modifying enzymes. The location of genes encoding the 37 tRNAs (outer circle, black lines), 2 rRNA loci (outer circle, green lines), the 18 aminoacyl-tRNA synthetases (middle circle, purple lines), and the putative tRNA modifying enzymes (inner circle, blue lines) is shown on the *C. trachomatis* L2 434/Bu chromosome. Notice the highly dispersed nature of these genes around the chromosome. Most genes would not be predicted to fall into operons.

De novo translation of *C. trachomatis* proteins begins ~2 hpi, so pre-existing translational machinery must be present (48). Another transcriptomics study used RNAseq to compare the transcripts in EBs and RBs isolated at 24 hpi (197). Notably, the majority of EB transcripts were tRNAs. If these tRNAs are functional is unknown.

Multiple studies of chlamydial proteomes have identified peptides that correspond to various aaRSs (198-200). Although no study has shown the complete set of aaRSs, given that *Chlamydia* spp. only possess the most minimal set of aaRSs, they must all be expressed, albeit at a low level. A recent study of the *C. caviae* phosphoproteome detected phosphopeptides from two different aaRSs: ProS in EBs and ThrS in RBs (201). Because EBs quickly differentiate into RBs, the authors hypothesized that phosphorylation might be used to post-translationally regulate chlamydial proteins,

including the aaRSs, since Pkn kinases are active early in infection (201). Phosphorylation of several eukaryotic aaRSs by casein kinase reduced their enzymatic activities (202). Thus, the discovery of chlamydial aaRS phosphopeptides suggests the tantalizing hypothesis that RB-EB transition may involve inactivation of translation by phosphorylation of aaRSs.

The behavior of tRNAs and aaRSs during times of stress is ill-defined. *E. coli* and other gram-negative bacteria can enter the stringent response, which generally downregulates both transcription and translation of most proteins, but increases expression of proteins that aid in acquiring or synthesizing the "missing" amino acid(s) (145). *Chlamydia* spp. appear to lack the genes required for the synthesis of the second messenger (p)ppGpp (4), which initializes the stringent response. Cyclic di-AMP has been suggested to act as a secondary messenger to trigger stress responses in *Chlamydia* spp. similar to (p)ppGpp for other bacteria, although the targets of cyclic di-AMP in chlamydia have not been described (203). The transcriptome of *C. trachomatis* serovar D grown in the presence of IFN-γ showed an approximately 50% increase in the number transcripts for all of the aaRSs transcripts (204), suggesting that the chlamydia may be trying to capture all available amino acids and that, despite the apparent lack of gene organization, this response is highly coordinated.

Antibiotics targeting either transcription (e.g., rifampicin) or translation (e.g., chloramphenicol) have been used to show that chlamydial entry into host cells does not require *de novo* bacterial transcription or translation. Inclusions still form and are trafficked to the perinuclear space in the presence of these drugs but do not expand (205). These inclusions also resist lysosomal fusion, indicating that the effectors that uncouple

the inclusion from endocytic progression are not synthesized *de novo*. What signals EB-RB differentiation and, concomitantly, the switch to active metabolism is unknown. Whether differentiation is dependent on *de novo* protein synthesis is also unknown.

Research goal

To be viable, chlamydia must metabolize and replicate; however, how the genes that drive these core processes are regulated in the context of the chlamydial biphasic lifecycle is unknown. The small genome and obligate intracellular nature of *Chlamydia* spp. suggests that many chlamydial genes are essential. One approach for genetic analysis of functions of essential genes is to generate conditional alleles. We hypothesized that temperature sensitive *C. trachomatis* mutants could be identified, and the contribution of individual essential genes to the developmental cycle could then be characterized. We also hypothesized that mutants with temperature sensitive alleles of genes that mediate chlamydial metabolism and cell division would exhibit defects early in the developmental cycle. DNA replication and protein synthesis are essential, and chlamydia mutants with defects in either of these processes have not been identified previously. Here, we describe the phenotypes of heat sensitive mutants of *dnaE* and *gltX*.

CHAPTER II: Materials and Methods

Chlamydial strains and cultivation

McCoy and HeLa 229 (HeLa) cells were obtained from the American Type Culture Collection and were maintained in high glucose DMEM (HyClone) supplemented with nonessential amino acids, HEPES, and 10% fetal bovine serum (DMEM-10; Atlanta biologicals). *C. trachomatis* L2 434/Bu was stably transformed with pGFP::SW2 (a kind gift from Dr. Ian Clarke), which expresses green fluorescent protein (GFP) under the control of a *Neisseria meningitidis* promoter and is β-lacatamase resistant due to the presence of *bla* on the plasmid (92). The transformed strain (L2-GFP) was plaque-purified twice prior to being mutagenized for library construction (206). Cell culture was performed in a 5% CO_2 humidified incubator at 37°C unless stated otherwise.

Mutant library construction

McCoy cell monolayers were infected with L2-GFP in sucrose phosphate glutamic acid buffer (SPG) at a multiplicity of infection (MOI) of 2 as described previously (207). The inoculum was then replaced with DMEM-10 containing 1 µg/ml cycloheximide to inhibit host cell protein synthesis. The medium was replaced at 18 hours post infection (hpi) with 10 mL of DMEM-10 containing 4 mg/mL EMS. Cells were rocked for 1 h at 37°C, washed extensively with PBS to remove excess mutagen, and fresh DMEM-10 + 1 µg/ml cycloheximide was added. The medium was aspirated at 34 hpi and mutagenized EB were harvested from the cells by mechanical disruption of the cell monolayer with 3 mm glass beads in SPG. Mutants were isolated from EB stocks by plaque cloning and were arrayed in SPG in 96-well cell culture plates. A portion of

each plaque was then expanded in McCoy cells in a 96-well cell culture plate for 70 h, which corresponds to approximately 2 developmental cycles. The medium was then aspirated, SPG was added to each well, and the expanded library plates were stored at -80°C.

Temperature sensitivity screen

HeLa cells in 96-well cell culture plates were infected with equal volumes of expanded library isolates by centrifugation at 1600 x g for 1 h in a swinging bucket rotor followed by rocking at 37°C for 30 min. Inocula were replaced with pre-warmed DMEM-10 + 1 µg/ml cycloheximide, and replicate plates were incubated at 32°C, 37°C, or 40°C. Infected monolayers were fixed at 34 hpi (for 37°C or 40°C plates) or at 58 hpi (for 32°C plates) with 3.7% formaldehyde to preserve GFP fluorescence. Chlamydial inclusions were imaged at 4X using an EVOS automated fluorescent microscope and inclusions were enumerated using a custom macro in FIJI (208). Ratios of inclusion formation were calculated for individual library isolates incubated at permissive versus non-permissive temperatures (37°C vs. 32°C or 37°C vs. 40°C). Isolates which had fold-changes equal to or greater than 15 were re-screened to confirm their phenotypes. Mutants were plaque cloned twice and expanded prior to further characterization.

Whole genome sequencing

Genomes were sequenced using two strategies. For some isolates, 1 µg of genomic DNA from MD-76R purified and DNase treated EB (209) was fragmented using NEBNext dsDNA Fragmentase (NEB) treatment to generate dsDNA fragments for multiplex Illumina sequencing using the TruSeq Nano DNA sample preparation kit

according to the manufacturer's protocols (Illumina). Samples were multiplexed using TruSeq Single Index Sequencing primers. Equimolar concentrations of indexed libraries were combined into a single pool and submitted for sequencing at Tufts University Genomics Core Facility in Boston, MA. Paired-end 100 bp sequencing was performed on an Illumina HiSeq 2500.

For other isolates, whole genome amplification was performed on crude EB preparations using REPLI-g (Qiagen) as described in (210), excluding the immuno-magnetic cell-separation step. Sequencing libraries were prepared using the NexteraXT DNA Library Preparation kit according to the manufacturer's instructions (lllumina). Samples were multiplexed using the NexteraXT Dual Index primer kit, combined in equimolar concentrations, and sequenced at the Oregon State University Center for Genomic Research and Biocomputing Core Sequencing Facility in Corvallis, OR for single-end 100 bp reads on an Illumina HiSeq 2000 or at the Tufts University Genomics Core Facility in Boston, MA for paired-end 100 bp sequencing on an Illumina HiSeq 2500.

Whole genome sequence data generated from the TruSeq Nano library was analyzed as described (90). Ambiguous sequences from the dataset and mutation calls with low quality scores were resolved by PCR and Sanger sequencing using primers in Table 2. Genome assemblies for the NexteraXT generated sample libraries were performed using an alternate workflow as described in (210) adding the use of *ad hoc* Python scripts and Geneious sequence manipulation software suite (version 7, http://www.geneious.com) (211). Genotypes of TS isolates and recombinants are listed in Chapter III and Appendix II.

Table 2 Primers used to map recombinants

Genome Position	ROI[a]	Forward	Reverse
14452-15184	CTL0009	gcgtatctatttcctattgtagcag	acgccttaacctctaccacc
46598-47549	CTL0039	ggcagttgcttcatcaattac	caattactactaggctctgctgc
63464-64192	CTL0052	cgagtagggttagatcgtgagc	gaccgctttattgtatagaccttgag
105701-106865	gpsA	agatagttcactagcttgctactc	catgaaagagactatagcctacctag
130701-133997	FtsK	ctattagtaatttacatgaccttgttcc	caatctgaaccaagatcaaattctc
155555-161373	AlaS-16S rRNA	caagaaggaatatactagtggatc	gcattcctggatgacctgaag
180132-181241	CTL0136	gtaaatcctcatctagctaaagagagc	aattggtagtcaaagtttgctctgg
182244-183011	CTL0137	ccgtttggctgctacttcc	gctcttcacctttgactacttg
188801-189574	CTL0144	cgtagactgtatgaggtgtgttatac	gctgtattcctattatctcgcatctc
214840-215464	pgsA	catggctgatagtgtataccg	ccgttagtaagagctacaggag
224443-225235	ptr	atagggacgcgatatacggcactgc	atggacaaccaccttcctgttatcaatgaccctacc
233317-233936	pmpD	gcagaaagtaaagttcctcaatgtattc	gttccatcttgaattttagcctcag
244620-245780	sucC	tgcatcttcatgagtatcaagc	gctaacgacttaattgcacagc
254809-255545	nrdA	tgataacagagaagaggacggg	cttgtacagtggaaagatagcaag
267894-268667	CTL0211	ctcgttgggattagatgtgcg	cgggttatcatagcatcgttc
309407-310397	pmpF	gcgtgatggtataggttgttg	gctattgactgtggttacattgac
312764-313595	pmpG	gaatctggagagctcagtttatc	gaccattatttgctgtattaggatcc
318735-319675	pmpI	gaactagaacctgtaagtggtcc	atgtgcctcatccagaacg
322831-323659	CTL0255	tgttgtaaaggatcgacgcatc	cctaaacttcttgaaatgctgc
394198-394950	tyrS	gaacaggatagataagatgttgctag	gatccagccagatagttccag
400847-401446	CTL0322	gaacaagcagaagggtccac	taccatctgtagaactagactacc
402105-403085	CTL0323	cagaggactcttgtgtttagcagg	cacaaagatcctctacggacc
427765-428935	sctU	ctactgacaaagttgagtagcttg	aacatttatatacggtaacttgcgaag
430894-431474	truB	gataatcaatgccgcagccag	caagtccctcctatgttctctgc
442009-442666	fabI	aacagcacgcatggaagc	gatccagccagtgaatctactc
451922-452741	pepF	gatatcattctgaaatagtgctgcttc	catgaccactgctactacttc

Genome Position	ROI[a]	Forward	Reverse
459820-460557	IncA-CTL0375	ctgtagaacgctcagcatg	gtagagatgacgcacgtac
466694-467383	CTL0384	cttgtgatactaatgacaggatagg	ctttaacttcaacagtcatgcag
472937-473695	CTL0388	ggagatccattcttccatactatc	cgatccgaaacgacttatggtg
490049-490964	CTL0402	gagtttaagcagttgatggaagagc	gtaattctgcaacaccatccagc
504404-505210	CTL0413	catagagtttagattcccgatccc	caaccgacacctagccag
526566-527387	devB	gcaagaggttatatacatggctac	cgacaacagatggctattcg
535794-536425	tgt	cttacggccatctcggtag	cttctggtccgattgttacagctc
539504-540168	CTL0448	caacaacagttaatcctaattactctcttc	gtttacaccgatagatagggctcc
546972-548627	CTL0456	aagtcttctcctccacagatc	gagctttaaaccttatgtcttctgttaatag
578274-578909	incC	atgacgtactctatgtccgatatagc	caaggctcgcaacgatcc
602415-603281	lgt	cgctttcagatgtggacgc	acgtgatacattgggaccagtc
619233-619926	murE	cagctatacctttctctggc	atgcatttagaccaacttcttcgg
625234-626060	dnaA	cgtttcgataatttcattgaaggtcc	tacatggcaacttgtcgagc
626662-627339	CTL0529	caaggatatgtcaaagccaatatagaac	ggcggcgatgtagtaaacg
627322-627924	nqrB	gtttactacatcgccgcc	cttcgcaagttcctcctacag
652497-653126	pknD	caactgccggtggattagg	gctatctatgacccagccagtg
661930-662628	atpB	gttaactttatttgtgaagacatgctttagg	cggttgaatgtgtattgataccag
664673-665504	CTL0561	caaatggcattaacgtattcgcctcttc	cgtttaacgcatttctcagagttagttag
674953-675975	rpoB	agctccagaatctttggcag	gctcgatccacaattatgc
677187-678281	rplL	ctgttaagacgtaccgggaac	ggatactagggagttgattgcg
687036-687731	trpC	ggttgccccattcttgtctc	gttttagccccttttgttgtatgaag
694629-695486	uvrA	ctatgatccggttacactacac	ctgagtccagtcttgttacatc
703257-704213	ptsH-CTL0592	cattacaactctccgaatccag	gtttatccgctccttatgatgtg
709892-710559	CTL0597	cacatgacaacatcccttatctaaac	gtgcatctaacacgagaaagtatagc
714841-715866	xerC	cctagttagcgcatatactgttg	cggtgtagttactcctctaagttg
724156-724918	CTL0609	tctgcaagaagtttagttattgtagc	ctatgtggcctgtggttctg
738215-738988	aroC	aacaatgctctcttagtcttactcg	acctgttgtattagcgagtcgg

Genome Position	ROI[a]	Forward	Reverse
752372-753277	phnP	cttgttctaaggttaaatgcgaagg	gccatctatcgctcaagttgtc
735386-736155	CTL0619	cttgtacagcaggcaatccc	gaccgtagttgctccgag
754878-755606	CTL0638-CTL0639	gatgctattctgatccgttagac	gagagatgctatcaaagtgctg
806908-807570	obgE	cctggaatatctgccatgatcc	aggacgagtcatgtttgttgatc
809833-810688	CTL0681	ttgttcctcaaattggttaattattagag	cgataatagccagcagaatatatagc
826951-827660	rpsL-CTL0699	cgaacccaagcaaccttacg	ggtctgtgagatagccagttcttc
833115-834723	gltX	ctcaagcagtatttgaaatgaccttc	ggttagtagcgaatgactgtcc
858379-858952	CTL0724	ttgcatacactctaaaaccg	gaggtttggcgattgtctg
893816-895248	dnaB	cctctaactatggcgaccc	cttgtttatccagggaactcac
897112-897663	lplA	cgcttctttggagatggagatc	cttttgaagatggagatggagtagg
907739-908788	rplF & rpsH	tgtctttacaacggataatctggg	gagcatttgtacattgatatcgagcatag
916258-916882	fmt	catatagcagccatattcacctacc	ctttagccgcctctggtg
924066-924874	tRNAleu-trxA	catcctgaatcgactacatgctatc	gtctttgagtccaacgctgc
927406-928190	aspS	aataccgatccaaacctccaac	gatgctgccgatcaacaagtc
929021-929760	hisS-uhpC	ccaacaatgcacgaacaactg	gattcataggtgttagctcgattc
929737-930808	uhpC	gaatcgagctaacacctatgaatc	cgagtaccccataatcccaag
933403-934098	dnaE	gaacagatggtcaaggaacg	ctccttaggagagcgttgg
940437-941632	CTL0815	aggtttctgaacttaccgatatactc	cctcgtcctatagtacctgc
952870-953831	sctR	cctatagcttcgccagtac	aaatgatcagaattaataagagggc
962022-962805	gspD	gttcggtaatctcgctgacag	ggctatgggtttctagggac
969410-970314	copB	caagccattaagcaagctg	gtcataatcagtcccatgagc
1006911-1007649	uvrD	gccgctcttatgaactatgcc	gcatctgtagcatatccagtcc
1007634-1008456	rpoN	gatatgctacagatgccagttg	ggatgagaactcgaaggatagc
1009600-1010293	CTL0875	cataaaacgtgtgttctagcatatg	gattgtgagtttatgtgaaggcg
1027396-1027970	CTL0886-CTL0887	ggcatcacgaagagagattaatg	gaagctttagcgattccagaaattg

[a] ROI = region of interest

Negative selection lateral gene transfer (LGT)

For same species crosses, HeLa cells were co-infected with different pairs of heat sensitive (HS) or cold sensitive (CS) mutants, with each parent at an MOI of 2, incubated at 37°C, and then harvested at 34 hpi by freezing and bead agitation. Portions of the harvests were passed in HeLa cells grown at the appropriate non-permissive temperature (32°C or 40°C) to select against the parent strains and were harvested at 34 hpi. An additional passage and harvest cycle was then performed. Recombinants were isolated by limiting dilution, re-screened to confirm their temperature resistant phenotypes, plaque-cloned, and expanded in cell culture.

Interspecies crosses between L2-GFP and *C. muridarum* use a similar procedure with the exceptions that McCoy cells were used throughout and two rounds of plaque cloning were performed *in lieu* of a round of limiting dilution and a round of plaque cloning.

Genomic DNA was isolated from recombinant EBs by alkaline lysis. Sanger sequencing of PCR products using the primers listed in Table 2 was used to determine which SNPs present in the parents were retained in the recombinants (Appendix II). Genomes of select recombinants were sequenced as described above.

Immunofluorescence microscopy

HeLa cells in 96-well plates (BD Falcon) or on glass coverslips were infected with TS mutants and control strains at MOI of 0.1 as described above. Where indicated, cells were treated with either 12.5 μg/mL chloramphenicol or 0.2 μg/mL rifampicin. At the indicated time post infection, cells were fixed with 3.7% formaldehyde. Cells were

subsequently blocked and permeabilized with blocking buffer (1% BSA and 0.1% saponin in PBS) and labeled with conditioned EVI-H1 hybridoma supernatant, which contains a chlamydial LPS-specific monoclonal antibody, and a secondary DyLight 594-conjugated goat anti-mouse IgG secondary antibody (Thermo Scientific) in blocking buffer. Images at 10X were acquired on an EVOS FL Auto Microscope (Thermo Scientific), whereas images at 40X or 63X were acquired on a Leica inverted DMI6000B microscope. Inclusion cross-sectional areas for temperature shift assays were measured in CellProfiler (212) using a modified pipeline (213). Inclusion cross-sectional areas for antibiotic treatment experiments were measured using ImageJ. Presented images were equally adjusted for brightness and contrast in Adobe Photoshop.

Temperature shift assays

For HS mutants, replicate experimental plates were initially incubated at 40°C then moved to 37°C at either 8, 12, 18, or 24 hpi. Control plates were incubated at 37°C or 40°C throughout. For CS mutants, plates were initially incubated at 37°C (with the exception of the 32°C only control) and then moved to 32°C at 8, 12, 18, or 24 hpi. The cells were fixed at 34 hpi (TS) or 58 hpi (CS) with 3.7% formaldehyde. Inclusions were stained as described above with anti-LPS antibody and imaged at 10X on an EVOS automated fluorescent microscope (Thermo Scientific). Four images per well were used to calculate the inclusion cross sectional areas, which corresponds to ~500 inclusions at an MOI of 0.2 grown at 37°C. Inclusion cross sectional areas were used to sort the mutants into developmental cycle classes based on the first time interval where their mean normalized inclusion area was ≤80% of L2-GFP.

Progeny formation assays

HeLa cells were infected at an MOI of 0.1 with 30% MD-76R purified (214) EBs or clarified harvests in SPG by centrifugation and rocking. The SPG was then aspirated and DMEM-10 + 1 µg/ml cycloheximide was added. The infections were incubated at 32°C, 37°C, or 40°C. The media was aspirated at 34 hpi (37°C and 40°C plates) or 58 hpi (32°C plates) and replaced with SPG. The infected plates were frozen at -80°C. EBs were harvested upon thawing the plates and titered on fresh HeLa cell monolayers as described previously (90). A parallel 96-well plate was infected to titer the inoculum, incubated at 37°C, and fixed with 3.7% formaldehyde to normalize fold change differences between strains.

Genome copy number

Genomic DNA was extracted from aliquots of samples generated for progeny formation assays using a gMax kit according to the manufacturer's instructions (IBI Scientific). FastStart TaqMan Probe Master mix (Roche) was used to quantitate the number of genome copies in 1 uL of purified genomic DNA (gDNA) using the primers 5'-GTAGCGGTGAAATGCGTAGA-3' and 5'-CGCCTTAGCGTCAGGTATAAA-3' with a corresponding TaqMan probe specific to the 16S rRNA gene of Chlamydia (5'-/56-FAM/ATGTGGAAG/ZEN/ACCACCAGT-3'). Genome copy numbers were determined using a standard curve generated from serial dilutions of a plasmid containing a cloned copy of a chlamydial 16S rRNA gene run in parallel. Reactions underwent 40 cycles of amplification on an Eppendorf Realplex4 using the following conditions: 20 sec at 95°C, 1 min at 60°C, and 20 sec at 68°C. Copy number analysis was performed using Realplex software.

Transmission electron microscopy

HeLa cells were infected at an MOI of 0.5 as described above. Infections were fixed at 32 hpi for 1 hour on ice using 4% paraformaldehyde/2.5% gluteraldehyde. Sample processing was performed essentially as described in (215). Briefly, the cells were washed with sodium cacodylate, embedded in resin, and stained with osmium tetroxide. Ultrathin sections were further stained with uranyl acetate and lead citrate. Images were captured using a JEOL JEM 1011 microscope with a Gatan 890 4k x 4k digital camera at the Indiana University Microscopy Center, Bloomington, IN.

DnaE suppressor screen

HeLa cell monolayers of 15 T-175 flasks were infected at an MOI of 30 by rocking for 2 hours at 37°C. The inoculum was then replaced with fresh DMEM-10 + 1 µg/ml cycloheximide, and the infections were incubated at 40°C for 34 hpi. The monolayers were harvested using glass beads. Host cell debris was removed by centrifugation at 500 x g for 5 minutes. Each supernatant was passaged immediately onto fresh HeLa cell monolayers in 2 wells of a 6 well plate and centrifuged to enhance infection. Selection at 40°C for 34 hours was repeated five times. A portion of the resulting progeny was scaled up at 37°C to generate a stock and to isolate genomic DNA by alkaline lysis for Sanger sequencing of *dnaE* using the primers in Table 3.

Table 3 Primers used for *dnaE* Sanger sequencing

Position	Direction	Primer
-200 bp	Forward	cggctttacaggatggttcg
312 bp	Forward	ctctcctctcttgcttacacag
843 bp	Forward	ctatttgcagcacatccagagac
1379 bp	Forward	cagagagcgcgttattaactatgc
1894 bp	Forward	ccacgattcctctagatgacc
2265 bp	Forward	gaacagatggtcaaggaacg
2808 bp	Forward	gctatccttaatgacctttacgacac
+297 bp	Reverse	gttcgtgttgagtatattaatgctattacagg

Statistics

Statistical analyses were performed using GraphPad Prism version 6.0. For statistical analysis, data were analyzed either by one- or two-way ANOVA followed by the *post hoc* tests indicated in the figure legends to correct for multiple comparisons.

CHAPTER III: A Genetic Screen for Conditional Alleles of Essential Genes

Portions of this chapter were published in Brothwell JA, Muramatsu MK, Toh E, Rockey DD, Putman TE, Barta ML, Hefty PS, Suchland RJ, and Nelson DE. 2016. Interrogating Genes That Mediate *Chlamydia trachomatis* Survival in Cell Culture Using Conditional Mutants and Recombination. *J bacteriol*. **198**, 2131-2139.

Generation of a mutant *C. trachomatis* library

C. trachomatis serovar L2 434/Bu transformed with pGFP::SW2 (L2-GFP) was used as the parent for the mutant library. This strain was used because it infects humans and has the highest availability of reagents among the *C. trachomatis* serovars. Ethyl methanesulfonate (EMS), which causes G→A transitions, was used to generate random point mutations. EMS has been used previously in other *C. trachomatis* and *C. muridarum* libraries (87,88,90).

Higher mutation levels of *C. trachomatis* serovar L2 can be achieved in Vero cells (monkey kidney cell line), since these cells can withstand 20 mg/mL of EMS (88). Attempts to use high levels of EMS with L2-GFP failed to produce progeny, as evidenced by lack of fluorescent inclusions at 34 hpi. Titration of EMS down to 10 mg/mL also failed to produce fluorescent inclusions.

Mutagenesis was then attempted in McCoy cells (murine fibroblast cell line), which could withstand up to 8 mg/mL EMS (90). Although GFP^+ inclusions were

evident at 8 mg/mL, the progeny failed to plaque efficiently (data not shown). A parallel culture mutagenized with 4 mg/mL EMS, however, could be plaqued efficiently, and the high yield of progeny after mutagenesis suggested a diverse population of mutants was present in the stock.

The mutant population was isolated by plaque cloning in McCoy cells and these isolates were arrayed into 96-well plates in SPG for ease of screening. A library of 4,184 arrayed plaques was generated from the cells mutagenized with 4 mg/mL EMS.

Temperature sensitivity (TS) screen

Because the natural host of *C. trachomatis* is humans, genetic screens were performed in HeLa cells (human cervical epithelial cell line). Three replica plates of HeLa cells were infected with equi-volume inoculums of mutants from the library (Figure 4). The infected monolayers were then incubated at 32°C, 37°C, or 40°C. These temperatures were chosen since large inclusions fail to form in a timely manner below 32°C and chlamydial death has been seen at higher temperatures (data not shown and (216)). After 34 hpi, monolayers incubated at 37°C and 40°C were fixed with formaldehyde; monolayers incubated at 32°C were fixed at 58 hpi, since development and inclusion fusion are slower at 32°C (217).

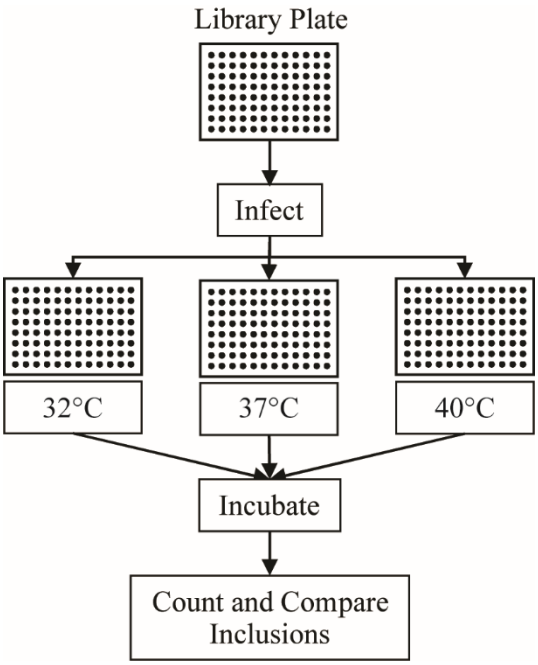

Figure 4 Temperature (TS) screen scheme. Replica plates of HeLa cells were infected with equal volumes of EMS-mutagenized *C. trachomatis* plaque isolates in 96-well plates. Plates were incubated at either the permissive temperature (37°C), or 32°C or 40°C to identify cold (CS) and heat (HS) mutants, respectively.

Monolayers were imaged, and the number of inclusions was determined. The number of inclusions that the isolates formed at 32°C or 40°C compared to 37°C revealed isolates with a range of thermal sensitivities. A threshold of a 15-fold difference between 37°C and the non-permissive temperature was used to define a TS mutant. These primary screen candidates were re-screened in duplicate alongside the L2-GFP parent. A total of 26 heat sensitive (HS) mutants and 2 cold sensitive (CS) mutants were isolated. 4 mutants that had produced at least a 15-fold decrease in the number of inclusions at both 32°C and 40°C relative to at 37°C, but failed to meet this cutoff in the secondary screen were also pursued. Fold change values for the mutants meeting this cutoff are listed in Table 4.

Table 4 Isolates with a ≥15-fold reduction of inclusion number at the non-permissive temperature

Isolate	Fold Difference	
	Primary Screen	Secondary Screen
Heat Sensitive		
HS 1	30.16	29.84
HS 2	16.86	33.36
HS 3	20.46	22.12
HS 4	16.24	17.13
HS 5	152.68	19.04
HS 6	26.49	19.29
HS 7	15.38	35.39
HS 8	16.24	52.73
HS 9	23.40	18.95
HS 10	17.96	63.02
HS 11	31.67	38.58
HS 12	58.28	41.46
HS 13	28.74	58.56
HS 15	17.40	15.12
HS 16	98.00	86.25
HS 17	118.32	56.49
HS 21	39.59	44.82
HS 22	30.58	16.57
HS 23	53.67	27.27
HS 24	102.48	64.48
HS 25	19.79	61.62
HS 26	56.03	23.52
HS 27	46.31	71.88
HS 28	37.07	19.84
HS 29	67.29	153.81
HS 29b[a]	86.51	24.99
Cold Sensitive		
CS 1	16.72	23.76
CS 2	15.21	66.09

[a] Genome sequence of this isolate matches that of HS 29

Variation in the fold change of these isolates in the primary and secondary screens may have been caused by to the inability to account for varying multiplicity of infection (MOI) of different isolates. Later experiments use identical MOI to avoid this variable.

The temperature sensitivity displayed by these isolates is highlighted in the statistical summary of the screen in Table 5.

Table 5 Statistical summary of temperature sensitivity in a mutagenized library

	Cold Sensitive (Inclusion number at 37°/32°)	**Heat Sensitive (Inclusion number at 37°/40°)**
Median	0.961	2.012
Interquartile Range	0.763-1.272	1.275-3.099
95th percentile	2.34	12.21

Mutant phenotypes emerge at different times in the developmental cycle

Because a single pool of mutagenized L2-GFP was used to generate the library and a high proportion of TS mutants were identified, we next wanted to determine the diversity of phenotypes in the population and whether or not the mutants had different genotypes. Temperature shift assays were performed to sort the mutants into classes based on when they became temperature sensitive during the developmental cycle. We reasoned that if a gene's function was not required until a certain point during the developmental cycle, then incubation at 40°C would have no effect if the culture was shifted to 37°C prior to this time. Temporal gene expression patterns have been described in the literature (28), so we chose an 8 hpi timepoint to distinguish if a gene was needed for EB-RB transition, a 12 hpi timepoint to define defects during early development, a 18 hpi timepoint for early-mid-development defects, and a 24 hpi timepoint for late-mid-development. Mutants exhibiting a late defect would appear between 24 hpi and the time at which all of the infections were fixed—34 hpi. The inclusion areas of L2-GFP and the HS mutants were determined and plotted for the 40°C

to 37°C shifts (Figure 5). The inclusion area of CS mutants was assayed using the same timepoints, however the plates were shifted from 37°C to 32°C because of the longer developmental time at 32°C (58 h v. 34 h) (Figure 6). Mutants displaying both HS and CS phenotypes, but not meeting the 15-fold cut off were also characterized (Figure 7).

The time of the onset of temperature sensitivity was determined by normalizing the inclusion area in each condition to its size at 37°C, thus differences in the sizes of mutants at 37°C could be accounted for. When this value was <80% of the inclusion size of L2-GFP, the mutant was considered to have passed the point at which it could be rescued. This time is denoted by arrows in Figures 5-7 for each mutant. The number of TS mutants in each temperature sensitive class is in Table 6. Defects in the majority of the mutants manifested during mid-development (i.e., 12-24 hpi) which was expected because *de novo* expression of most chlamydial genes initiates in mid-development (28).

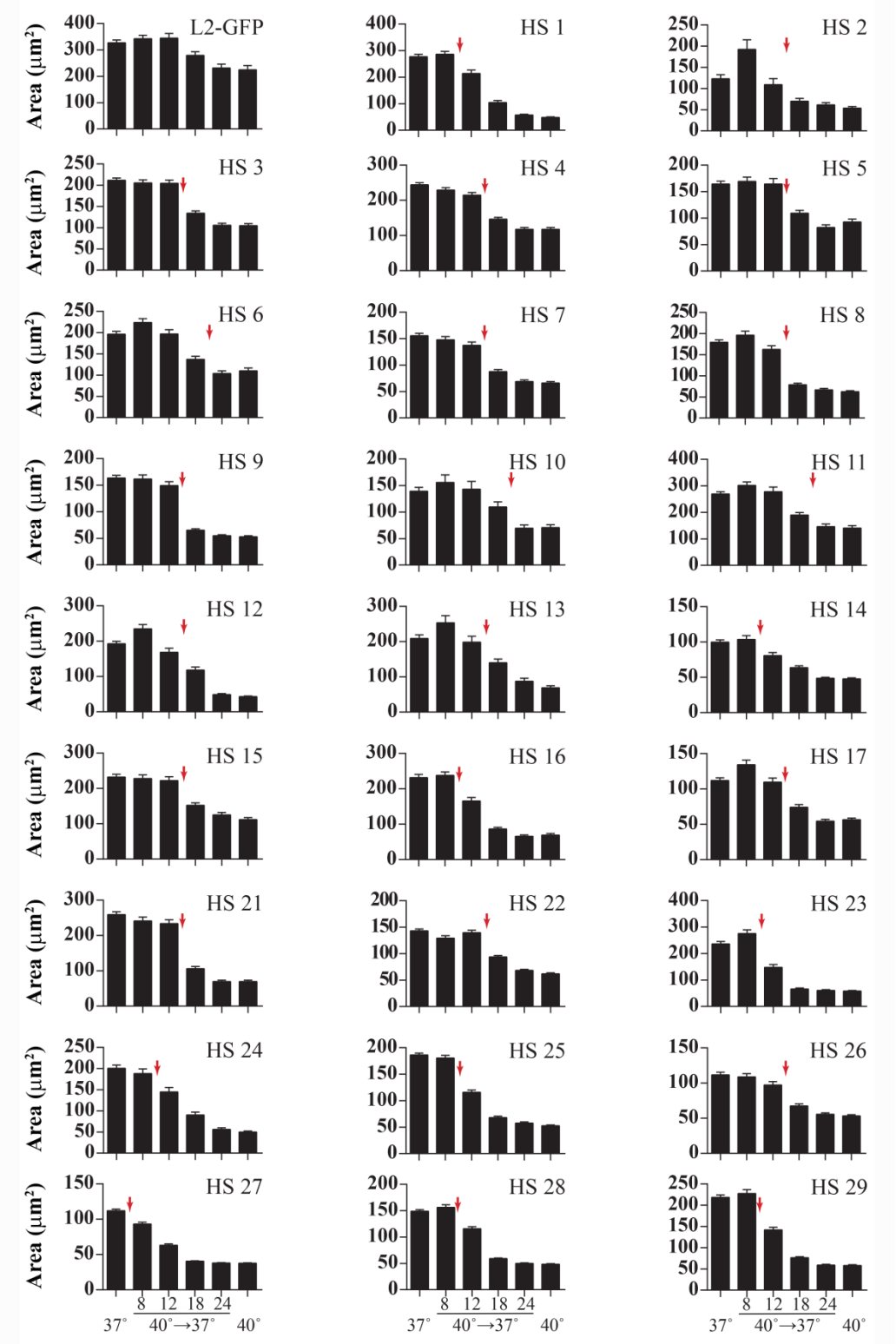
L2-GFP
HS 1
HS 2
HS 3
HS 4
HS 5
HS 6
HS 7
HS 8
HS 9
HS 10
HS 11
HS 12
HS 13
HS 14
HS 15
HS 16
HS 17
HS 21
HS 22
HS 23
HS 24
HS 25
HS 26
HS 27
HS 28
HS 29
Area (μm²)
8 12 18 24
37° 40°→37° 40°

Figure 6 Inclusion area of HS mutants. HeLa cells were infected with HS mutants at an MOI of ~0.1. The infections were incubated at 37°C, 40°C, or were transferred at the times indicated above from 40°C to 37°C until 34 hpi, when they were fixed. LPS was stained, and inclusions were imaged at 10X. Cross-sectional areas (μm^2) of the inclusions were determined using CellProfiler. Red arrows indicate the time of temperature sensitivity, which was defined as when the area was <80% of L2-GFP.

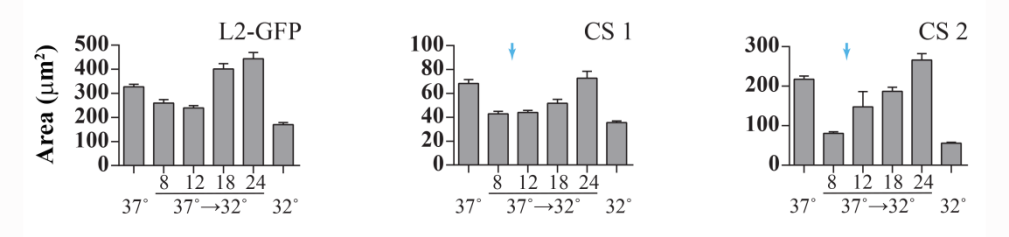

Figure 5 Inclusion area of CS mutants. HeLa cells were infected with each CS mutant at an MOI of ~0.1. Infections were incubated at 37°C, 32°C, or were transferred at indicated times from 37°C to 32°C, until 58 hpi, when they were fixed. LPS was stained, and inclusions were imaged at 10X. Cross-sectional areas (μm^2) were determined in CellProfiler. Blue arrows indicate the time of temperature sensitivity, defined as when the area was <80% of L2-GFP.

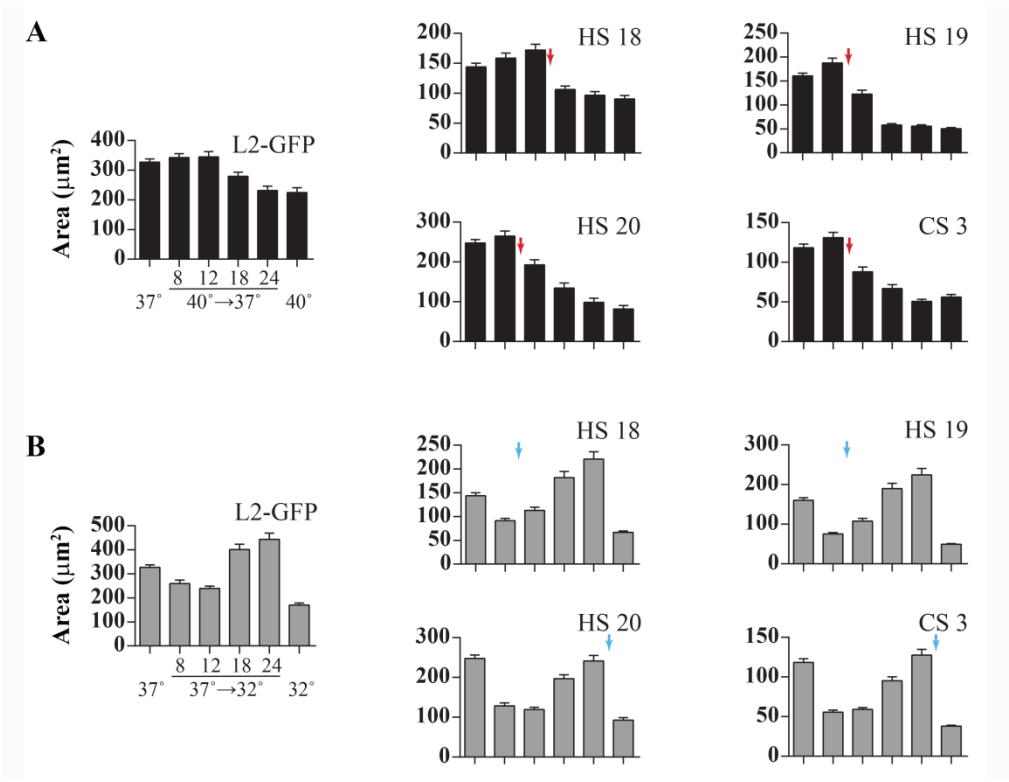

Figure 7 **Inclusion areas of dual HS/CS mutants.** HeLa cells were infected with each HS/CS mutant at an MOI of ~0.1 and incubated as described in Figures 5 (A) and 6 (B). LPS was stained, and inclusions were imaged at 10X. Cross-sectional areas (μm^2) were determined in CellProfiler. Red and blue arrows indicate the time of heat and cold sensitivity, respectively, which was defined as when the area was <80% of L2-GFP.

Table 6 Distribution of mutants in phenotypic classes

TS type	Point in Developmental cycle				
	Very Early (0-8 hpi)	Early (8-12 hpi)	Early-mid (12-18 hpi)	Mid-late (18-24 hpi)	Late (24-34 hpi)
HS	1	9	19	3	0
CS	2	1	0	2	1

TS mutants represent a diversity of genotypes

Since the temperature shift experiments indicated the TS mutants had diverse phenotypes, the genomes of all 26 HS, 2 CS, and 4 dual HS/CS mutants were sequenced (Table 7). One duplicate isolate was identified. Two isolates differed from each other by only two mutations, indicating that they were likely siblings. All of the other mutants were unique, indicating that the screen did not reach saturation.

The mutants had between 1 and 11 (average: 6) mutations per genome. One isolate had a single mutation (HS 17; *rspH*). Different nonsynonymous mutations were detected in the same genes in 22 cases (2-4 occurrences). No genes known to be involved with the heat shock response in chlamydia (*groEL*, *groES*, or *dnaK*) or in other bacteria contained mutations (216). Two TS mutants (HS 15 and HS 27) contained mutations in genes involved in the stringent response in other bacteria. HS 15 encodes $DksA^{E61K}$. DksA has been shown to be responsive to (p)ppGpp in *E. coli* and downregulate transcription of rRNA transcripts during stress (218). HS 27 encodes $ObgE^{G92E}$. ObgE interacts with the 50S subunit of the *E. coli* ribosome to inhibit translation in the presence of ppGpp (219). Whether ObgE functions similarly in *Chlamydia* spp. is unknown, as *C. abortus obgE* is unable to complement an *E. coli* *ΔobgE* mutant (220).

Table 7 Mutations in temperature sensitive mutants

Genome Coord.	Nuc. Sub.	Amino Acid Sub.	Codon	Gene	Gene Locus	Product & Function	TS	hpi of TS [a]
HS 1							HS	8-12
319,045	C → T	R → K	777	*pmpI*	CTL0254	outer membrane protein		
402,693	G → A		209		CTL0323	ABC transporter substrate binding protein		
466,895	G → A	V → M	58		CTL0384	ABC transporter permease		
547,235	C → T	P → L	51	*sodTi*	CTL0456	sodium:sulfate symporter		
687,326	G → A		129	*trpC*	CTL0581	N-(5'-phosphoribosyl)anthranilate isomerase		
833,253	G → A	Q → *	487	*gltX*	CTL0705	glutamyl-tRNA synthetase		
894,118	C → T		98	*dnaB*	CTL0759	helicase		
941,515	G → A	V → M	345		CTL0815	putative methyltransferase		
962,561	C → T	S → N	87	*gspD*	CTL0835	general secretion pathway protein D		
1,007,275	G → A	S → N	539	*uvrD*	CTL0872	DNA helicase for repair		
HS 2							HS	12-18
323,177	C → T	P → L	510		CTL0255	hypothetical protein		
625,575	C → T		232	*dnaA*	CTL0527	chromosomal replication initiation protein		
724,595	G → A	R → W	198		CTL0609	hypothetical protein		
752,659	G → A	P → L	127	*phnP*	CTL0635	metal-dependent hydrolase		
897,396	C → T		13	*lplA*	CTL0761	lipoate-protein ligase A		
927,802	C → T	G → R	84	*aspS*	CTL0804	aspartyl-tRNA synthetase		
HS 3							HS	12-18
60,444	G → A	R → H	6	*pbpB*	CTL0051	penicillin-binding protein		
488,901	G → A	G → E	263		CTL0402	putative integral membrane protein		
597,658	C → T	A → T	42	*glgP*	CTL0500	glycogen phosphorylase		
674,019	C → T	V → I	971	*rpoB*	CTL0567	DNA-directed RNA polymerase subunit beta		
1,029,700	C → T	G → E	376	*mviN*	CTL0888	putative virulence protein		
HS 4							HS	12-18
644,042	C → T	A → T	128	*ptsN_2*	CTL0543	PTS family membrane transport protein IIA subunit		
883,313	G → A	P → L	16		CTL0749	putative phosphohydrolase		
907,588	C → T	G → R	88	*rplR*	CTL0775	50S ribosomal protein L18		
982,227	G → A	G → S	139	*rbsU*	CTL0851	sigma regulatory family protein-PP2C phosphatase		
1,004,010	C → T	Intergen				between CTL0868 & CTL0689		
1,028,279	G → A	P → S	241		CTL0887	hypothetical protein		

Genome Coord.	Nuc. Sub.	Amino Acid Sub.	Codon	Gene	Gene Locus	Product & Function	TS	hpi of TS [a]
HS 5							HS	12-18
141,878	G → A		219		CTL0111	rRNA SAM-dep. methyltransferase; TrmA family		
404,846	G → A	E → K	343		CTL0325	ABC transporter permease		
875,332	G → A	S → F	270	*oppA4*	CTL0741	oligopeptide transport binding protein		
HS 6							HS	18-24
27,569	G → A		382		CTL0019	putative exported lipoprotein		
55,081	G → A	Intergen				between tRNAlys & tRNAglu		
147,818	G → A	S → F	261	*hemN*	CTL0115	coproporphyrinogen III oxidase		
150,235	G → A	A → V	867	*mfd*	CTL0117	transcription-repair coupling factor		
244,456	C → T	G → R	32	*ftsY*	CTL0192	cell division protein		
460,138	C → T	Intergen				between IncA & CTL0375		
622,529	C → T		280	*mraW*	CTL0524	S-adenosyl-methyltransferase		
891,978	C → T	G → S	206		CTL0756	putative nucleotide transport protein		
892,219	C → T		125		CTL0756	putative nucleotide transport protein		
899,269	C → T	D → N	13	*ruvA*	CTL0763	Holliday junction DNA helicase		
HS 7							HS	12-18
41,392	G → A	E → K	274		CTL0033	phosphopeptide binding protein (to be a TTSS protein)		
179,699	G → A	R → Q	195	*miaA*	CTL0135	tRNA delta(2)-isopentenylpyrophosphate transferase		
365,543	G → A	L → F	146	*dcd*	CTL0294	deoxycytidine triphosphate deaminase		
490,565	G → A	V → I	818		CTL0402	putative integral membrane protein		
555,911	C → T	G → E	251	*leuS*	CTL0461	leucyl-tRNA synthetase		
729,656	C → T	Intergen				between CTL0614 & CTL0613		
803,532	C → T	P → S	1,728	*pmpC*	CTL0671	polymorphic outer membrane protein		
874,299	C → T		614	*oppA4*	CTL0741	oligopeptide transport system binding protein		
888,894	C → T	G → E	309	*polA*	CTL0754	DNA polymerase I		
939,415	C → T		261	*dacC*	CTL0813	D-alanyl-D-alanine carboxypeptidase		

Genome Coord.	Nuc. Sub.	Amino Acid Sub.	Codon	Gene	Gene Locus	Product & Function	TS	hpi of TS [a]
HS 8							HS	12-18
49,730	C → T	Intergen				between sctQ & pkn5		
317,497	G → A		962	*pmpH*	CTL0251	outer membrane protein		
399,058	C → T	A → T	508		CTL0321	ADP/ATP carrier protein		
663,660	G → A	P → S	458	*atpA*	CTL0560	V-type ATPase subunit A		
887,743	C → T	E → K	693	*polA*	CTL0754	DNA polymerase I		
931,309	G → A	A → T	58	*dnaE*	CTL0807	DNA polymerase III subunit alpha		
952,657	G → A	G → E	174	*sctL*	CTL0824	type III secretion system protein		
992,991	C → T	R → Q	46		CTL0858	hydrolase		
HS 9							HS	12-18
48,347	G → A	G → E	277	*sctQ*	CTL0041	type III secretion system protein		
69,385	C → T	L → F	300	*sufS*	CTL0056	cysteine desulfurase		
172,972	G → A	G → R	103	*ftsW*	CTL0129	cell division protein		
273,112	C → T	G → E	572	*pnp*	CTL0214	polynucleotide phosphorylase/polyadenylase		
797,655	C → T	P → S	1,577	*pmpB*	CTL0670	polymorphic outer membrane protein		
HS 10							HS	18-24
436,408	C → T	D → N	539	*rpsA*	CTL0353	30S ribosomal protein S1		
484,238	G → A		23	*pkn1*	CTL0400	serine-threonine-protein kinase		
517,348	G → A	R → C	228	*dsbG*	CTL0429	disulfide bond chaperone		
908,097	C → T	G → E	109	*rplF*	CTL0776	50S ribosomal protein L6		
916,562	C → T	D → N	276	*fmt*	CTL0792	methionyl-tRNA formyltransferase		
924,519	C → T	Intergen				between tRNAleu & trxA		
HS 11							HS	18-24
130,997	G → A	P → L	730	*ftsK*	CTL0108	DNA segregation ATPase		
155,775	G → A	Intergen				between AlaS & 16S rRNA		
401,254	C → T	M → I	51		CTL0322	hypothetical protein		
HS 12							HS	12-18
150,596	C → T	V → I	747	*mfd*	CTL0117	transcription-repair coupling factor		
216,881	T → C	Intergen				between glgA & tRNAgln		
545,762	C → T		171	*oppF*	CTL0454	oligopeptide transport system ATP-binding protein		
593,969	C → T	P → S	314	*pdhB*	CTL0498	pyruvate dehydrogenase E1 component beta subunit		

Genome Coord.	Nuc. Sub.	Amino Acid Sub.	Codon	Gene	Gene Locus	Product & Function	TS	hpi of TS [a]
HS 13							HS	12-18
106,075	G → A		264	*gpsA*	CTL0083	NADPH- G3P dehydrogenase		
428,014	C → T	V → I	288	*sctU*	CTL0346	type III secretion system protein		
452,424	G → A	S → F	106	*pepF*	CTL0367	oligoendopeptidase F		
578,442	C → T	P → S	57	*incC*	CTL0485	inclusion membrane protein C		
677,584	G → A		33	*rplL*	CTL0568	50S ribosome L7/L12		
810,518	C → T	P → L	159		CTL0681	metal dependent hydrolase		
HS 14							HS	8-12
284,726	C → T	*P → L*	*134*	*fumC*		*pseudogene: fumerate hydratase*		
337,254	G → A	V → I	15	*cydB*	CTL0269	cytochrome d ubiquinol oxidase subunit II		
525,571	C → T	L → F	180	*zwf*	CTL0437	glucose-6-phosphate 1-dehydrogenase		
605,142	C → T	Intergen				between CTL0506 & CTL0507		
624,545	C → T		109		CTL0526	hypothetical protein		
640,060	C → T	Intergen				between mnmA & CTL0540		
HS 15							HS	12-18
310,806	G → A		191	*pmpF*	CTL0249	polymorphic outer membrane protein		
760,537	C → T	S → L	473		CTL0643	hypothetical protein		
784,211	G → A	E → K	61	*dksA*	CTL0664	dnaK suppressor protein		
1,013,676	C → T		213	*rpoD*	CTL0879	RNA polymerase sigma factor		
HS 16							HS	8-12
141,403	C → T	D → N	378		CTL0111	rRNA methyltransferase		
199,418	C → T	L → F	17		CTL0152	hypothetical protein		
411,812	G → A		320	*dnaN*	CTL0331	DNA polymerase III subunit beta		
485,047	C → T	T → I	293	*pkn1*	CTL0400	serine-threonine-protein kinase		
518,215	G → A	R → H	14		CTL0430	putative integral membrane protein		
533,764	G → A		8	*gyrB*	CTL0442	DNA gyrase subunit B		
654,541	G → A	P → L	321	*pknD*	CTL0553	serine/threonine-protein kinase		
723,243	G → A	Intergen				between def & ksgA		
753,018	C → T		7	*phnP*	CTL0635	metal-dependent hydrolase		
765,491	G → A	S → F	307		CTL0648	hypothetical protein		
932,237	C → T	P → L	367	*dnaE*	CTL0807	DNA polymerase III subunit alpha		
HS 17							HS	12-18
908,496	G → A	A → V	119	*rpsH*	CTL0777	30S ribosomal protein S8		

Genome Coord.	Nuc. Sub.	Amino Acid Sub.	Codon	Gene	Gene Locus	Product & Function	TS	hpi of TS [a]
HS 18[b]							HS/	8-12
47,344	G → A	V → I	264		CTL0040	hypothetical protein	CS	
180,826	G → A	P → S	123		CTL0136	hypothetical protein		
233,540	C → T	A → V	1061	*pmpD*	CTL0183	outer membrane protein		
268,424	C → T	A → T	46		CTL0211	putative membrane transporter		
473,407	G → A	P → S	79		CTL0388	putative methyltransferase		
603,056	C → T	R → K	75	*lgt*	CTL0504	prolipoprotein DAG transferase		
827,208	G → A	Intergen				between rpsL & CTL0699		
HS 19[a]							HS/	8-12
309,983	C → T	D → N	466	*pmpF*	CTL0249	outer membrane protein	CS	
627,630	C → T	P → S	39	*nqrB*	CTL0530	NADHubiquinone oxidoreductase, subunit 2		
662,238	C → T	G → D	339	*atpB*	CTL0559	V-type ATPase subunit B		
695,055	G → A		261	*uvrA*	CTL0587	DNA damage recognition		
703,673	C → T	Intergen				between ptsH & CTL0592		
953,331	G → A	D → N	171	*sctR*	CTL0825	type III secretion system protein		
1,009,794	C → T	V → I	206		CTL0875	gamma-glutamyl ligase		
HS 20[b]							HS	8-12
14,768	G → A	G → E	369		CTL0009	putative membrane efflux protein	CS	>24
224,695	G → A	H → Y	181	*ptr*	CTL0175	exported insulinase/protease		
536,147	G → A	R → W	20	*tgt*	CTL0445	queuine tRNA-ribosyltransferase		
547,516	G → A	G → R	145	*sodTi*	CTL0456	sodium:sulfate symporter		
665,123	G → A	R → W	235		CTL0561	hypothetical protein		
1,027,647	C → T	Intergen				between CTL0886 & CTL0887		
HS 21							HS	12-18
73,202	G → A		196		CTL0060	hypothetical protein		
141,232	G → A	S → L	3	*yajC*	CTL0110	preprotein translocase subunit YajC		
200,637	G → A	H → Y	75	*rnpA*	CTL0153	ribonuclease P		
337,791	C → T		194	*cydB*	CTL0269	cytochrome d ubiquinol oxidase subunit II		
443,923	G → A	C → Y	350		CTL0360	conserved chlamydial hypothetical protein		
445,731	G → A	R → C	47	*truA*	CTL0361	tRNA pseudouridine synthase A		

Genome Coord.	Nuc. Sub.	Amino Acid Sub.	Codon	Gene	Gene Locus	Product & Function	TS	hpi of TS [a]
HS 22							HS	12-18
73,000	C → T	S → F	129		CTL0060	hypothetical protein		
117,829	G → A	Intergen				between CTL0095 & CTL0096		
298,065	G → A	Intergen				between tRNAleu & xerD		
396,999	C → T		603	*lepA*	CTL0320	GTP-binding protein LepA		
451,917	G → A	T → I	275	*pepF*	CTL0367	oligoendopeptidase F		
472,424	G → A		112		CTL0387	hypothetical protein		
778,217	G → A	Intergen				between sucB & gltT		
913,763	G → A		168	*rplD*	CTL0789	50S ribosomal protein L4		
1,020,129	C → T	D → N	29		CTL0883	hypothetical protein		
HS 23							HS	8-12
245,221	G → A		201	*sucC*	CTL0193	site-specific tyrosine recombinase		
313,171	G → A	M → I	543	*pmpG*	CTL0250	polymorphic outer membrane protein		
933,691	C → T	P → S	852	*dnaE*	CTL0807	DNA polymerase III subunit alpha		
969,663	G → A	G → E	428	*copB*	CTL0841	type III secretion system translocator CopB		
HS 24							HS	8-12
255,178	T → C		342	*nrdA*	CTL0199	ribonucleotide-diphosphate reductase subunit alpha		
442,329	C → T	D → N	79	*fabI*	CTL0359	enoyl-(acyl carrier protein) reductase		
539,803	C → T	H → Y	102		CTL0448	hypothetical protein		
HS 25							HS	8-12
457,262	G → A	Intergen				between CTL0369 & IncD		
865,032	C → T	S → L	38	*yagE*	CTL0733	conserved hypothetical		
882,286	C → T	D → N	115		CTL0748	N6-adenosine methyltransferase		
931,402	C → T	L → F	89	*dnaE*	CTL0807	DNA polymerase III subunit alpha		
1,038,007	G → A	P → L	180		CTL0897	hypothetical protein		
HS 26							HS	12-18
63,837	C → T	S → F	35		CTL0052	hypothetical protein		
189,152	C → T	R → C	124		CTL0144	1-acyl-sn-glycerol-3-phosphate acyltransferase		
215,125	G → A		169	*pgsA*	CTL0166	CDP-diacylglycerol--glycerol-3-phosphate 3-phosphatidyltransferase		
431,207	C → T	D → N	208	*truB*	CTL0349	tRNA pseudouridine synthase B		
490,357	G → A		748		CTL0402	putative integral membrane protein		
626,971	C → T	A → T	182		CTL0529	hypothetical protein		
710,152	C → T	G → R	69		CTL0597	O-sialoglycoprotein endopeptidase		
876,051	C → T		30	*oppA4*	CTL0741	oligopeptide transport system binding protein		

Genome Coord.	Nuc. Sub.	Amino Acid Sub.	Codon	Gene	Gene Locus	Product & Function	TS	hpi of TS [a]
HS 27							HS	0-8
652,817	C → T	E → K	896	*pknD*	CTL0553	serine/threonine-protein kinase		
735,802	G → A	A → V	227		CTL0619	putative integral membrane protein		
738,520	C → T	P → L	20	*aroC*	CTL0622	chorismate synthase		
807,286	C → T	G → E	92	*obgE*	CTL0675	GTPase ObgE		
HS 28							HS	8-12
136,669	A → G	Intergen				23S rRNA		
538,957	G → A		106		CTL0447	putative integral membrane protein		
804,601	G → A	S → N	125		CTL0672	metal ABC transporter substrate-binding protein		
900,088	C → T	D → N	103		CTL0765	hypothetical protein; acetyl coenzyme A carboxylase carboxyltransferase		
919,922	C → T		452	*lnt*	CTL0796	apolipoprotein N-acyltransferase		
HS 29							HS	8-12
27,098	G → T	M → I	225		CTL0019	putative exported lipoprotein		
136,669	A → G	Intergen				23S rRNA		
538,957	G → A		106		CTL0447	putative integral membrane protein		
804,601	G → A	S → N	125		CTL0672	metal ABC transporter substrate-binding protein		
900,088	C → T	D → N	103		CTL0765	hypothetical protein; acetyl coenzyme A carboxylase carboxyltransferase		
919,922	C → T		452	*lnt*	CTL0796	apolipoprotein N-acyltransferase		
CS 1							CS	8-12
46,820	G → A	R → K	55		CTL0040	hypothetical protein		
548,046	G → A	W → *	321	*sodTi*	CTL0456	sodium:sulfate symporter		
CS 2							CS	8-12
182,608	C → T	Q → *	443		CTL0137	hypothetical protein		
619,657	C → T		90	*murE*	CTL0521	UDP-N-acetylmuramoylalanyl-D-glutamate-2, 6-diaminopimelate ligase		
675,514	C → T		472	*rpoB*	CTL0567	DNA-directed RNA polymerase subunit beta		
715,353	G → A	G → E	148	*xerC*	CTL0601	site-specific tyrosine recombinase (interacts with FtsK)		
858,744	C → T	D → N	14		CTL0724	HAD superfam hydrolase; phosphoglycolate phosphatase		

Genome Coord.	Nuc. Sub.	Amino Acid Sub.	Codon	Gene	Gene Locus	Product & Function	TS	hpi of TS [a]
CS 3 [b]							HS	8-12
394,511	G → A		88	*tyrS*	CTL0318	tyrosyl tRNA synthetase	CS	>24
460,134	G → A	Intergen				between IncA & CTL0375		
527,030	C → T	T → M	150	*devB*	CTL0438	6-phosphogluconolactonase		
548,409	G → A	W → *	442	*sodTi*	CTL0456	sodium:sulfate symporter		
755,200	C → T	Intergen				between CTL0638 & CTL0639		
929,330	G → A	Intergen				between hisS & uhpC		
1,008,128	C → T		187	*rpoN*	CTL0873	sigma 54		

Abbreviations used: nuc..: nucleic acid; sub.: substitution; hpi: hours post infection; Intergen: intergenic mutation

[a] time at which the normalized cross-sectional area falls to <80% of L2-GFP in the same condition

[b] dual heat/cold sensitive mutants

The fitness of some TS mutants is compromised

The ability of the mutants in which the TS allele was mapped (discussed in the section below) to produce viable progeny was assayed (Figure 8). Approximately half of the mutants generated progeny at 37°C comparable to that of the L2-GFP parent (within ~2-fold) (Figures 8A and B). Notably, all of the dual HS/CS isolates produced approximately 50-fold fewer infectious progeny compared to L2-GFP (Figures 8A and 8B). Two other isolates, HS 10 and HS 27 produced far fewer progeny at 37°C compared to L2-GFP (Figure 8B).

TS mutants produced fewer EBs at 32°C or 40°C compared to 37°C than did L2-GFP (Figures 8C-E). The difference in the ratios formed by L2-GFP versus mutants ranged from ~10-1000-fold. Since the burst size of *C. trachomatis* is 500 inclusion forming units (IFU)/inclusion (27,60), we consider mutants with a defect of 1000-fold to be lethal. The phenotypes seen in the progeny assays were also generally reflected by cross-sectional inclusion area (Figures 5-7), suggesting that inclusion size and progeny production are linked (221,222).

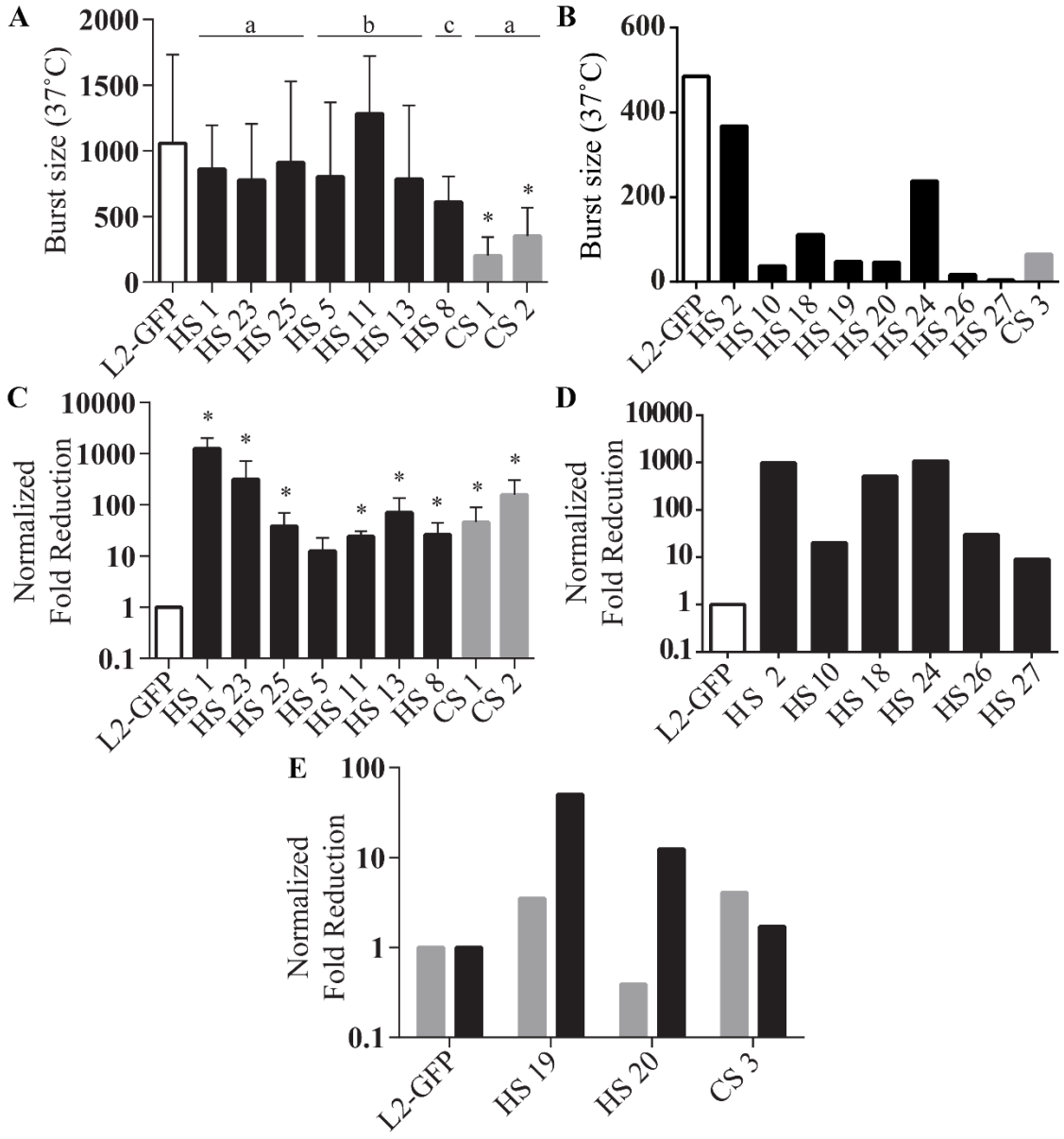

Figure 8 Progeny production of select TS mutants. HeLa cells were infected at an MOI of 0.2 and incubated at either 37°C or 40°C for 34 hpi or at 32°C for 58 hours. Infections were stopped by freezing in SPG. EBs were titered on fresh HeLa cell monolayers to count progeny. Normalization to input EBs allowed determination of the burst sizes of (A) prepped and (B) clarified stocks of different mutants. The differences in the number of progeny produced at 37°C/40°C or 37°C/32°C by these strains were normalized to L2-GFP (C-E). Black bars, ratio for 37°C/40°C. Gray bars, ratio for 37°C/32°C. a, early mutants; b, mid-development mutants; c, late mutants. *, $p<0.05$, ANOVA with Dunnett's post hoc test.

Negative selection lateral gene transfer (LGT) maps 14 TS mutants

We attempted to identify the temperature sensitive alleles in the TS mutants. An antibiotic-driven LGT mapping approach was initially attempted but was abandoned because the antibiotic resistance alleles altered phenotypes of some parents and recombinants (data not shown). We next reasoned that since the TS alleles decreased the fitness of the mutants, we could select against these alleles to enrich for recombinant progeny.

To become non-temperature sensitive, a TS allele would have to be replaced by recombination, revert, or be suppressed. In the case of recombination, the recombined region could be as small as a single base or could be a substantial portion of the entire genome. This could be differentiated by linkage analysis of other genetic markers that transferred from the donor parent, although this could be complicated by multiple recombination events. HS 1, HS 13, and HS 23 were chosen as parents for the first crosses. These strains were chosen because they had strong phenotypes in progeny assays (Figure 8A) and could not be rescued after 18 h at 40°C (Figure 5). Whole genome sequencing identified the mutations in these strains (Table 7). HS 1 had 10 mutations, HS 13 had 6, and HS 23 had 4.

We reasoned that HS 1 would be the most useful for determining how much DNA was exchanged since it had the most mutations, which could be used as silent markers throughout different regions of the genome. Alternatively, if large fragments of DNA were transferred and recombined, HS 23 would have the best chance of donating wild type sequence since it had the fewest mutations. Passaging of the progeny from the

above TS mutant crosses twice at 40°C was sufficient to eliminate most of the parents and temperature sensitive recombinants (~10-1000X enrichment/well) (Figure 9).

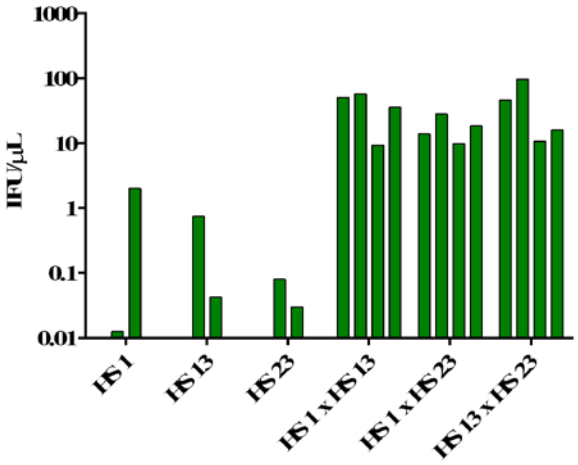

Figure 9 Selection at 40°C enriches for temperature resistant progeny. HeLa cells were infected at a total MOI of 4 with either one or two temperature sensitive strains and were grown until 34 hpi at 37°C. EBs were released by freeze-thaw and bead agitation. Temperature resistant progeny were enriched for by two rounds of growth (34 hours each) at 40°C. The number of infectious progeny in each well was determined at 37°C. Single strain infections were performed in 2 independent wells and double strain infections were performed in 4 independent wells. Each bar represents a well.

Recombinants were isolated from wells that contained high numbers of progeny by limiting dilution followed by plaque cloning. Alleles that differed in the parents were Sanger sequenced in the recombinants (i.e., all mutations in both parents). Negative selection LGT generated some recombinants that lacked the TS allele but which were otherwise isogenic to one parent used in the cross (Figures 10B and 33). Genome sequencing confirmed that one recombinant from an HS 1 x HS 13 crosses was isogenic to HS 1. The HS 1 recombinant identified *gltX*^{C1459T} (encoding GltX^{Q487*}) as the TS allele, and this recombinant rescued both inclusion size (Figure 10C) and the number of progeny (Figure 10D) compared to either mutant parent.

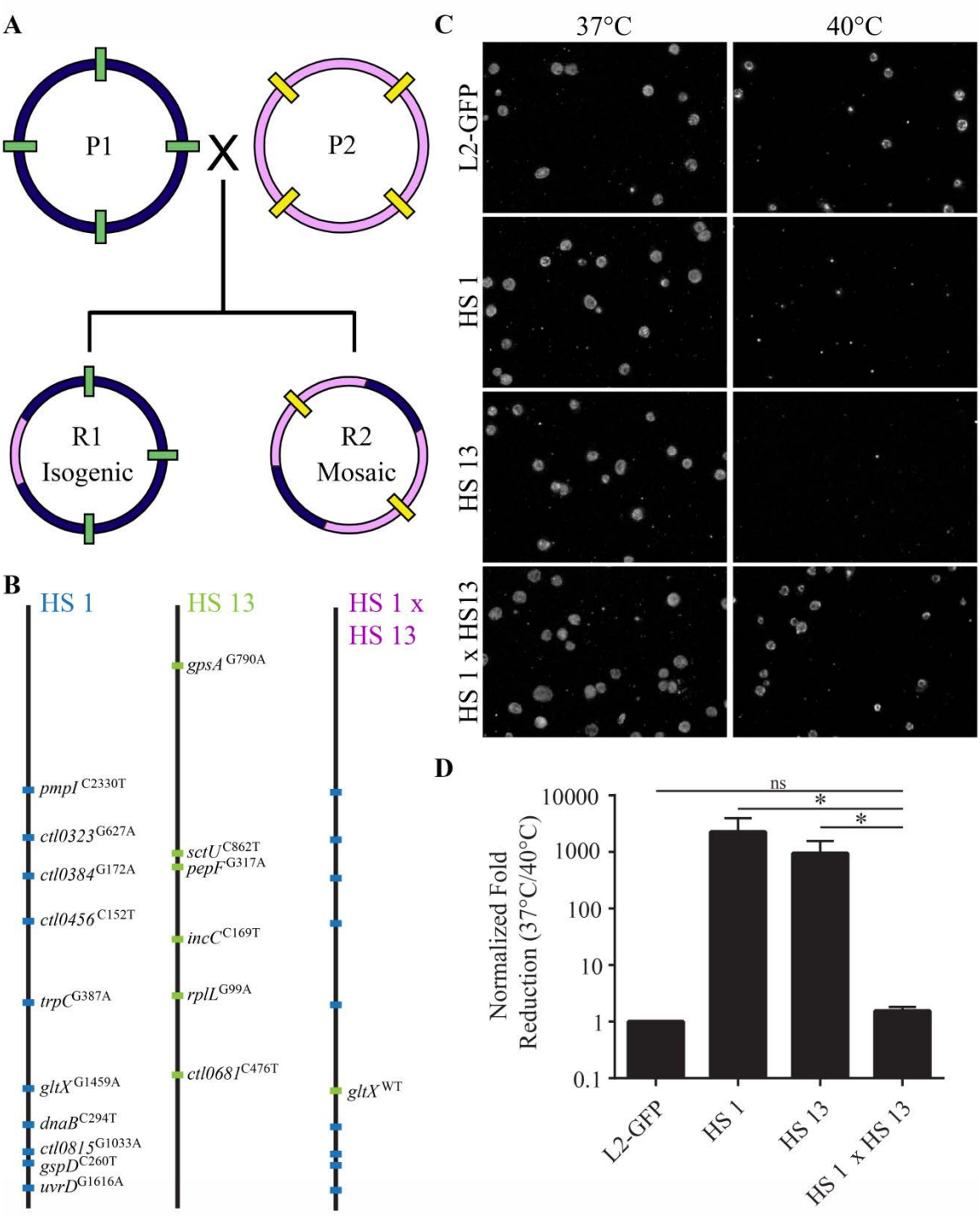

Figure 10 Generation of an isogenic recombinant by negative selection LGT. (A) Co-infections with two different parents can yield recombinants that are isogenic to one parent or that are mosaics, which contain combinations of different alleles from the parents. Sequencing demonstrated that one recombinant from the HS 1 x HS 13 was isogenic to HS 1 (B). Inclusion area (C) and progeny production (D) of this recombinant were similar to L2-GFP.

Analysis of the genomes of the 6 recombinants isolated from these crosses (2 each: HS 1 x HS 13, HS 1 x HS 23, and HS 13 x HS 23) suggested that crosses with HS 1 tended to produce recombinant progeny that contained mostly HS 1 genome (Figures 33, 37, and data not shown). Therefore, progeny from the HS 13 x HS 23 cross helped identify the TS allele in these other mutants. Both *CTL0681*^{ts} (P159L) in HS 13 and *dnaE*^{ts} (P852S) in HS 23 could be identified by Sanger sequencing (Figure 37). Whole genome sequencing confirmed the *ctl0681* recombinant was isogenic to HS 13.

We attempted to map the remaining HS mutants using negative selection LGT. HS 23 served as one of the parents for these crosses because it was reliably eliminated by two passages at 40°C and only contained 4 mutations, which reduced the amount of sequencing reactions required for recombinant mapping.

We attempted to map the TS alleles in all the mutants using the negative selection LGT approach and succeeded in generating temperature resistant phenotypic revertants of HS 2, HS 10, HS 11, HS 19, HS 20, HS 24, and HS 26 (Table 8). Sanger sequencing determined that many of the phenotypic revertants were mosaics, which confirmed that recombination—not reversion—was occurring in these populations. Using phenotypic linkage analysis (88), TS alleles were mapped in some of these strains using as few as 2 different mosaic recombinants (Appendix II).

Unsuccessful HS 23 crosses were re-attempted using HS 27. HS 27 has 4 mutations (Table 7) and cannot be rescued by temperature shift after 12 hpi (Figure 5). A recombinant from a HS 2 x HS 27 cross narrowed down the possible TS alleles in HS 2 to mutations in *CTL0609* or *phnP* (Table 8 and Figure 34). These crosses also

determined that *obgE*^{G275A} was the temperature sensitive allele in HS 27 (Table 8 and Figure 42) (223).

Our TS screen identified two CS mutants and four dual HS/CS mutants with sensitivities below the 15-fold threshold (Table 4). Both of the CS strains were successfully mapped using the negative selection approach. Some dual HS/CS mutants could not be mapped with CS 1, so recombination with CS 2 was performed. This allowed mapping of HS 20 (Figure 39) and CS 3 (Figure 44).

A summary of the mapped strains is in Table 8. Genotypes of recombinants are in Appendix II. Putative roles of the mapped TS alleles are in diverse aspects of chlamydial biology from carbon metabolism, energy usage, lipid synthesis, protein synthesis, cell division, and stress responses. One TS allele was also mapped to a conserved chlamydial hypothetical protein (*ctl0322*).

Table 8 Summary of mapped mutants in this study

Mutant	Gene	Amino Acid Substitution	Function
HS 1	*gltX*	Q487*	Glutamyl-tRNA synthestase
HS 2	*ctl0609*	R198W	Unknown
	phnP	P127L	Phosphonate metabolism
HS 10	*rplF*	G109E	Ribosomal protein
	fmt	D276N	Methionyl-tRNA formyltransferase
HS 11	*ctl0322*	M51I	Unknown
HS 13	*ctl0681*	P159L	rRNA processing
HS 17	*rpsH*	A119V	Ribosomal protein
HS 19	*atpB*	G339D	ATPase
HS 20	*ctl0456*	G145R	Dicarboxylate transport
HS 23	*dnaE*	P852S	DNA replication
HS 24	*fabI*	D79N	Fatty acid biosynthesis
HS 26	*ctl0597*	G69R	t6A37 tRNA modification
HS 27	*obgE*	G92E	Ribosome regulation
CS 1	*ctl0456*	W321*	Dicarboxylate transport
CS 2	*ctl0137*	Q443*	Unknown
CS 3	*ctl0456*	W442*	Dicarboxylate transport

*= stop codon

Caveats of recombination

A caveat of our mapping approach was that TS alleles were inferred from multiple recombinants in cases where we failed to generate isogenic recombinants. It was also not possible to distinguish if the isogenic strains we generated in LGT experiments arose from recombination, reversion, or acquisition of suppressor mutations from just the Sanger sequencing of marker mutations. For example, genome sequencing of a recombinant that Sanger sequencing indicated was nearly isogenic to CS 1 revealed an additional mutation (C656A) in *uhpC* that targeted re-sequencing confirmed was absent in the recombinant's parents. Whether this is a suppressor or a random mutation is unclear. A likely suppressor mutant arose from a cross of HS 18 with HS 23. This isolate acquired a deletion that resulted in a frameshift of the mutant *ctl0211* allele in HS 18. This may have been a viable option to correct the temperature sensitivity because *ctl0211* is a paralog of *ctl0210*.

CHAPTER IV: Characterization of a Temperature Sensitive DnaE Mutant

DNA replication is inhibited in a DnaE^{P851S} mutant

Negative selection LGT determined the TS allele in in HS 23 was *dnaE*^{C2554T}. HS23 had a reduction in inclusion number (Table 4), inclusion area (Figure 5), and burst size (Figure 8C) at 40°C compared to L2-GFP. Genome replication begins after the EB has differentiated into an RB, and *dnaE* transcripts have been observed as early as 2 hpi (27). We tested if *dnaE*^{C2554T} (hereafter referred to as *dnaE*^{ts}) could replicate its genome at 40°C using qPCR. Genome replication of L2-GFP, *dnaE*^{ts}, and its isogenic recombinant (hereafter referred to as *dnaE*^{WT}) were similar at 37°C and started to increase between 8 and 12 hpi (Figure 11). However, *dnaE*^{ts} genomes did not increase at 40°C, whereas L2-GFP and *dnaE*^{WT} genome copies increased similar to what was seen at 37°C (Figure 11).

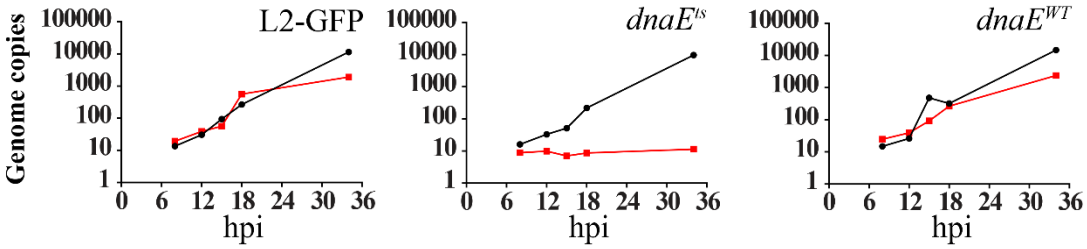

Figure 11 Genome replication in *dnaE*^{ts} is impaired at 40°C. L2-GFP, *dnaE*^{ts}, and *dnaE*^{WT} genome copy number at 37°C (black lines) or 40°C (red lines) was measured by qPCR throughout development. The mean of 2 independent experiments in duplicate is shown.

We tested if genome replication of *dnaE*^{ts} was restored when the mutant was shifted from 40°C to 37°C. The number *dnaE*^{ts} genomes at a total of 34 hpi appeared to

correlate with the proportion of time spent at 37°C versus 40°C (Figure 12). Thus, the DNA replication defect of *dnaE*^{ts} was reversible.

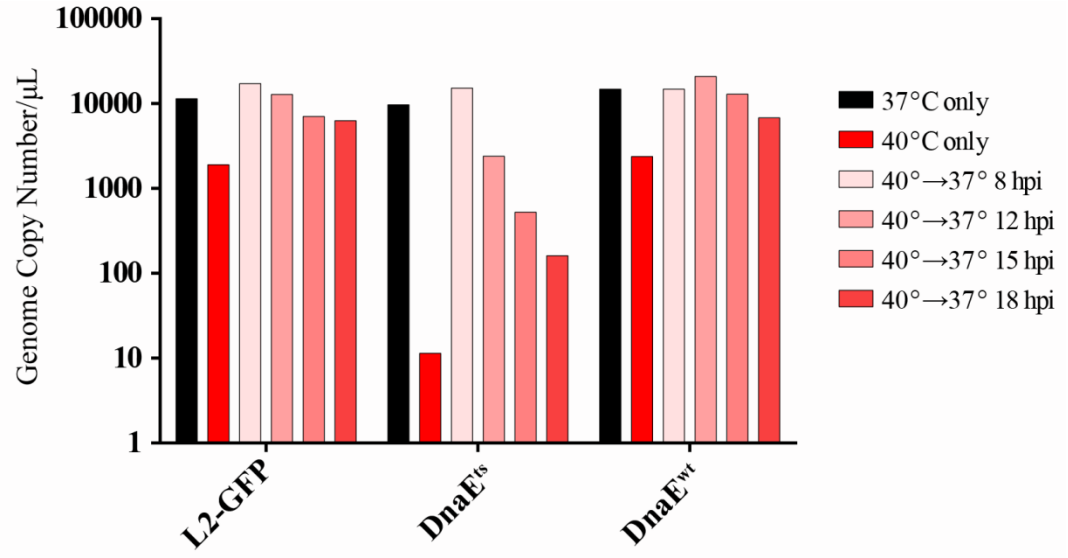

Figure 12 Impaired genome replication of *dnaE*^{ts} at 40°C can be rescued by shifting to 37°C. HeLa cells infected with L2-GFP, *dnaE*^{ts}, and *dnaE*^{WT} were incubated for 34 hpi at 37°C or 40°C only or the infections were initially incubated at 40°C and then moved to 37°C at the times indicated. Genomic DNA was extracted and genomes were counted by qPCR. The mean of two independent experiments in duplicate is shown.

Disruption of DNA replication alters inclusion size

To see if inclusion size is impacted by a lack of DNA replication, infections were shifted between 37°C and 40°C. Chlamydia were labeled with an anti-LPS antibody in these experiments to circumvent the complication of uneven GFP expression in cells. Shifting *dnaE*^{ts} from 37°C to 40°C prior to 18 hpi caused a sharp decrease in inclusion size and number at 34 hpi (Figure 13). Similarly, shifting from 40°C to 37°C caused a decrease in inclusion size and number if the shift occurred after 12 hpi (Figure 13).

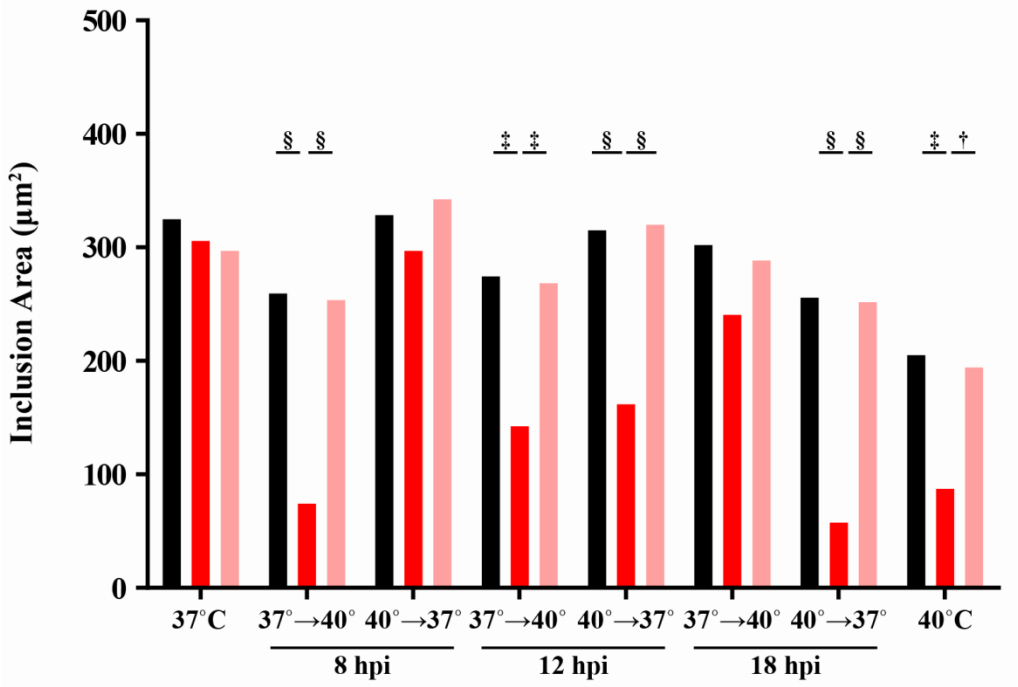

Figure 13 Inclusion size is dependent on functional DnaE. HeLa cells were infected with L2-GFP (black bars), *dnaE*^{ts} (red bars), and *dnaE*^{WT} (pink bars). The cells were either incubated at 37°C, 40°C, or were moved between these temperatures at the times indicated. Inclusions were measured at a total of 34 hpi in all cases. Bars represent the mean of four frames/well of two independent experiments performed in triplicate. Two-way ANOVA and Tukey's *post hoc* test were used to determine statistical significance. †, $p<0.01$; ‡, $p<0.001$; §, $p<0.0001$

Results of a recent study suggested that growth of inclusions was independent of genome replication but not protein synthesis (125). We tested this hypothesis by comparing the sizes of inclusions formed by L2-GFP, *dnaE*^{ts}, or *dnaE*^{WT} at 37°C and 40°C in cells treated with rifampicin or chloramphenicol to inhibit chlamydial transcription or translation, respectively. *dnaE*^{ts} inclusions were smaller than L2-GFP or *dnaE*^{WT} inclusions at 40°C as expected (Figure 14A). The small size of *dnaE*^{ts} inclusions at 40°C indicated that most bacterial metabolism had likely ceased, but further inhibition by either chloramphenicol or rifampicin did have a slight impact on inclusion size, although this was not significant.

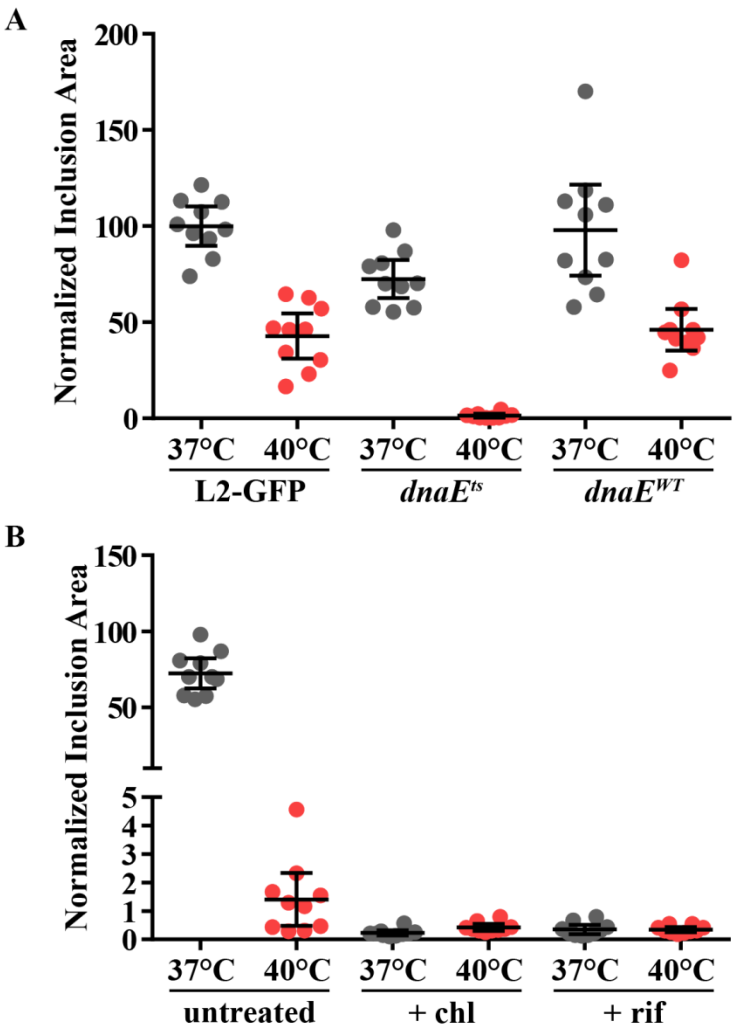

Figure 14 Lack of DNA replication in *dnaE*^{ts} is associated with smaller inclusions. HeLa cells on coverslips were infected with L2-GFP, *dnaE*^{ts}, or *dnaE*^{WT} at MOI of ~ 0.2 and were incubated at 37°C or 40°C (A). Inclusions were fixed at 34 hpi, stained for LPS, and imaged at 40X. In some cases, chloramphenicol or rifampicin were added at the time of infection and again when the inoculum was replaced with media (B). Inclusion sizes are normalized to L2-GFP at 37°C. Ten inclusions per condition were measured and error bars indicate the 95% confidence interval.

Inclusion ultrastructure

dnaE^{ts} does not replicate its genome at 40°C or produce infectious EBs, so we tested if *dnaE*^{ts} EBs could differentiate into RBs at 40°C. No typical EBs were observed in *dnaE*^{ts} inclusions at 32 hpi, indicating that EBs differentiated into RBs, but most of the

apparent RB that were observed had atypical morphologies that suggested that the bacteria were stressed (Figures 15B-H). Many *dnaE*^{ts} inclusions also contained circular membranes that appeared to be extensions of the periplasm (Figures 15D-E). Areas containing numerous vesicles, separated from what may be non-membrane bound inclusion lumen-derived glycogen, were be observed in other *dnaE*^{ts} infected cells (Figure 15F). In some cases, fragmentation of *dnaE*^{ts} inclusions was associated with cytosolic protrusions into the inclusion lumen (Figures 15G and 15H).

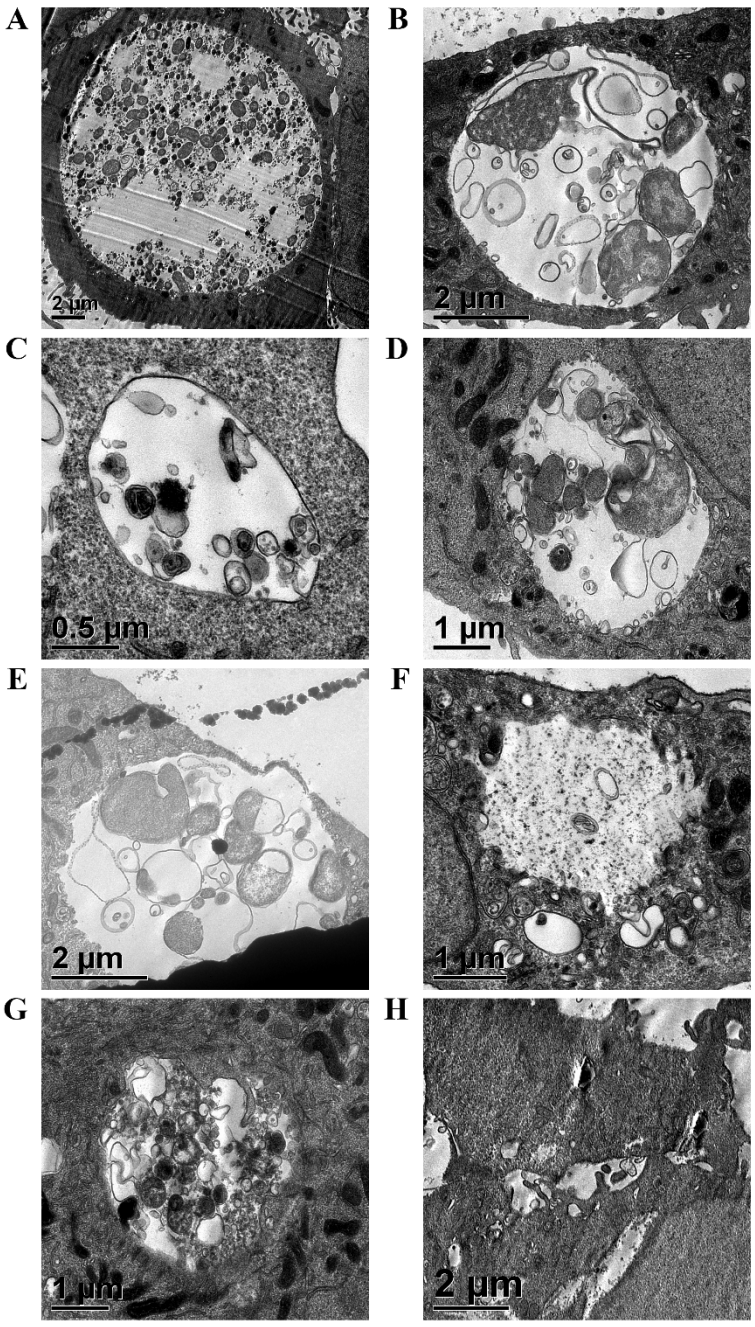

Figure 15 Inclusion Ultrastructure of *dnaE*^{ts}. HeLa cells were infected with *dnaE*^{ts} at either 37°C (A) or 40°C (B-H) for 32 hpi and fixed. Growth at 37°C produced normal inclusions; however, growth at 40°C produced comparably smaller inclusions that contained aberrant RB forms (B-D), enlarged periplasms (D and E), destroyed inclusion membranes (F), and potential inclusion fragmentation (F-H).

A screen identifies *dnaE*^{ts} suppressors

DNA replication is essential, so we hypothesized that incubation of *dnaE*^{ts} at 40°C would select for revertants that restored DnaE function. Attempts to isolate revertants from ~6x10^{7} EBs failed (data not shown), so we tried a larger inoculum. We infected fifteen T-175 flasks at an MOI of 30 (~1x10^{10} EBs total) and incubated them at 40°C for 34 hours. EBs harvested from these flasks were used to infect new plates of fresh cells. The entire process was repeated 5 times. GFP^{+} inclusions became visible in some of the lineages as early as the second round of passage and were evident in 12/15 lineages by the fifth passage (Table 9). Sanger sequencing revealed that the C2554T mutation was retained in all 12 of these populations.

Table 9 Summary of *dnaE*^{ts} Suppressor Screen

Flask	Passage when Positive	Suppressors Present
1	None	
2	3	E1061K
3	2	D828Y and E1061K
4	2	D828Y and E1061K
5	2	E1061K
6	None	
7	4	D828Y and E1061K
8	3	E1061K
9	4	E1061K
10	3	E1061K
11	4	E1061K
12	4	E1061K
13	None	
14	4	E1061K
15	2	E1061K

Suppressors are intragenic

Isolates were plaque-cloned from each of the 12 populations. Sequencing of *dnaE* revealed that the isolates all contained one of two different mutations that caused either E1061K or D828Y amino acid substitutions in DnaE and confirmed that the mutants all retained $dnaE^{C2254T}$, which indicated that they were suppressor mutants (Table 9).

COBALT was used to perform a primary sequence alignment of *C. trachomatis* serovar L2 DnaE (*Ct*DnaE), *E. coli* DnaE (*Ec*DnaE), and *T. aquaticus* DnaE (*Ta*DnaE) to gain insight into how the suppressor mutations might restore the function of mutant DnaE (Figure 16). P852 is the second proline in an LPPD motif that is conserved in all three DnaE sequences. E1061 and D828 are located in less conserved regions of DnaE. D828 aligns with an aspartate in *Ec*DnaE and a glutamate in *Ta*DnaE, suggesting that a negatively charged residue is important at this location. The substitution in the suppressor mutant introduces a polar aromatic residue in place of this negatively charged residue. E1061 is preceded by an aspartate that is conserved in all three homologs. Like *Ct*DnaE, *Ta*DnaE codes for a glutamate, however *Ec*DnaE codes for an arginine at the analogous position, indicating that a charged residue is important in this position.

Figure 16 Alignment of DnaE from C. *trachomatis*, *E. coli*, and *T. aquaticus*. *C. trachomatis* (*Ctr*), *E. coli* (*Eco*), and *T. aquaticus* (*Taq*) DnaE were aligned using COBALT software. The C-terminal portion of DnaE is shown. Identical residues are in red. *Ct*DnaE^{P852} is shown in the blue box. Two independent suppressors are also shown and are in either the magenta (*Ct*DnaE^{D828}) or yellow (*Ct*DnaE^{E1061}) boxes.

We next interrogated the possible effects of the amino acid changes in the suppressor mutants on the tertiary structure of DnaE by generating a model using Phyre2. *Ct*DnaE was modeled with >90% confidence due to the high similarity of the *Ec*DnaE and *Ta*DnaE crystal structures (PDB accession codes 2HQA and 3E0D, respectively) (Figure 17). P852 is in the β-clamp binding subdomain (224); however, the β-clamp binds distal to this site (225,226). The mutation is predicted to be located in a three-stranded β-sheet that is a conserved structural feature in both *Ec*DnaE and *Ta*DnaE.

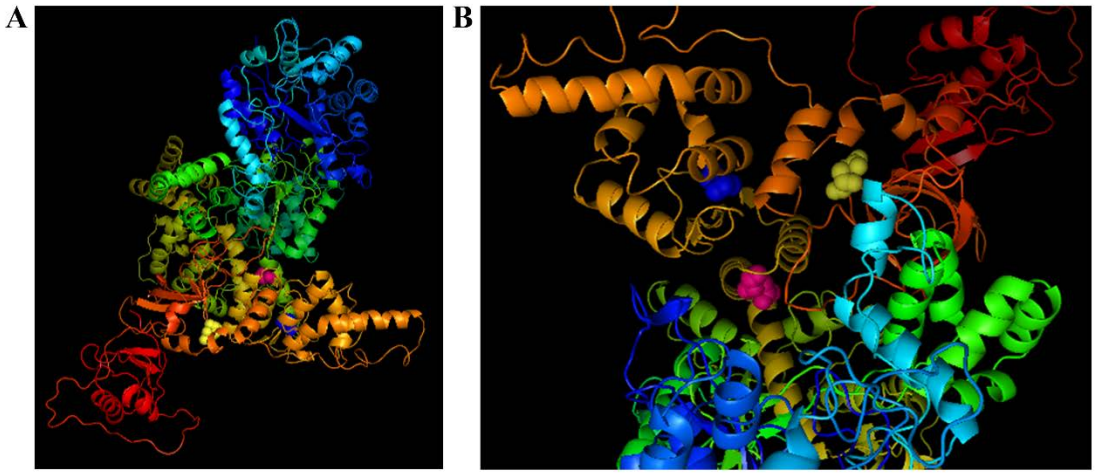

Figure 17 Modeling predicts that *dnaE*^{ts} DnaE-DNA interaction is altered. Relevant amino acids are shown in spacefill on the ribbon diagram of a *Ct*DnaE model. P852, blue; D828, magenta; E1061, yellow. (A) Forward view of DnaE. The PHP domain is mostly blue, the β-clamp binding domain is mostly orange, the OB-fold domain is mostly red, and the catalytic core is yellow and green. (B) View looking down through the channel where the DNA template passes through. The structure of *C. trachomatis* L2 434/Bu was modeled using Phyre2 software and manipulated in PyMol.

Our model predicts that P852S does not a directly interact with amino acids that are altered in the DnaE suppressor mutants. D828 falls in another well conserved structural feature—the helix-hairpin-helix (HhH) motif—at the edge of the helix-hairpin transition. E1061 is proximal to the oligonucleotide-binding (OB)-fold domain. Both of these motifs could interact with the DNA template during DNA polymerization (111). Interaction of DnaE with the DNA template is in part mediated by residues in the HhH motif. The positively charged residues in the HhH sequence interact with the sugar-phosphate backbone of the DNA template and have evolved to balance polymerization speed and accuracy (227). The OB-fold may interact with the single stranded template, and this subdomain moves 30° upon binding DNA template (111).

Suppressor phenotypes

We compared phenotypes of the suppressor mutants, *dnaE*^{ts}, and various controls (Figure 18). L2-GFP, *dnaE*^{ts}, *dnaE*^{WT}, and the two suppressor mutants (DnaE$^{D828Y\ P852S}$ and DnaE$^{P852S\ E1061K}$) formed similar sized inclusions at 37°C. However, *dnaE*^{ts} inclusions were much smaller than those of L2-GFP at 40°C. At 40°C, DnaE$^{P852S\ E1061K}$ inclusions were similar in size to those of L2-GFP and *dnaE*^{WT}, whereas DnaE$^{D828Y\ P852S}$ inclusions were smaller, but still larger than *dnaE*^{ts} inclusions (Figure 18A). Both of the suppressor mutants produced far fewer progeny than did L2-GFP at 40°C (Figure 18B). Chlamydial genomes were counted in the same samples using qPCR. Interestingly, the 37°C/40°C genome copy ratios of both the suppressor mutants were indistinguishable from L2-GFP or *dnaE*^{WT}, but differed from *dnaE*^{ts} by ~100-fold (Figure 18C), indicating that DNA replication was restored in the suppressors.

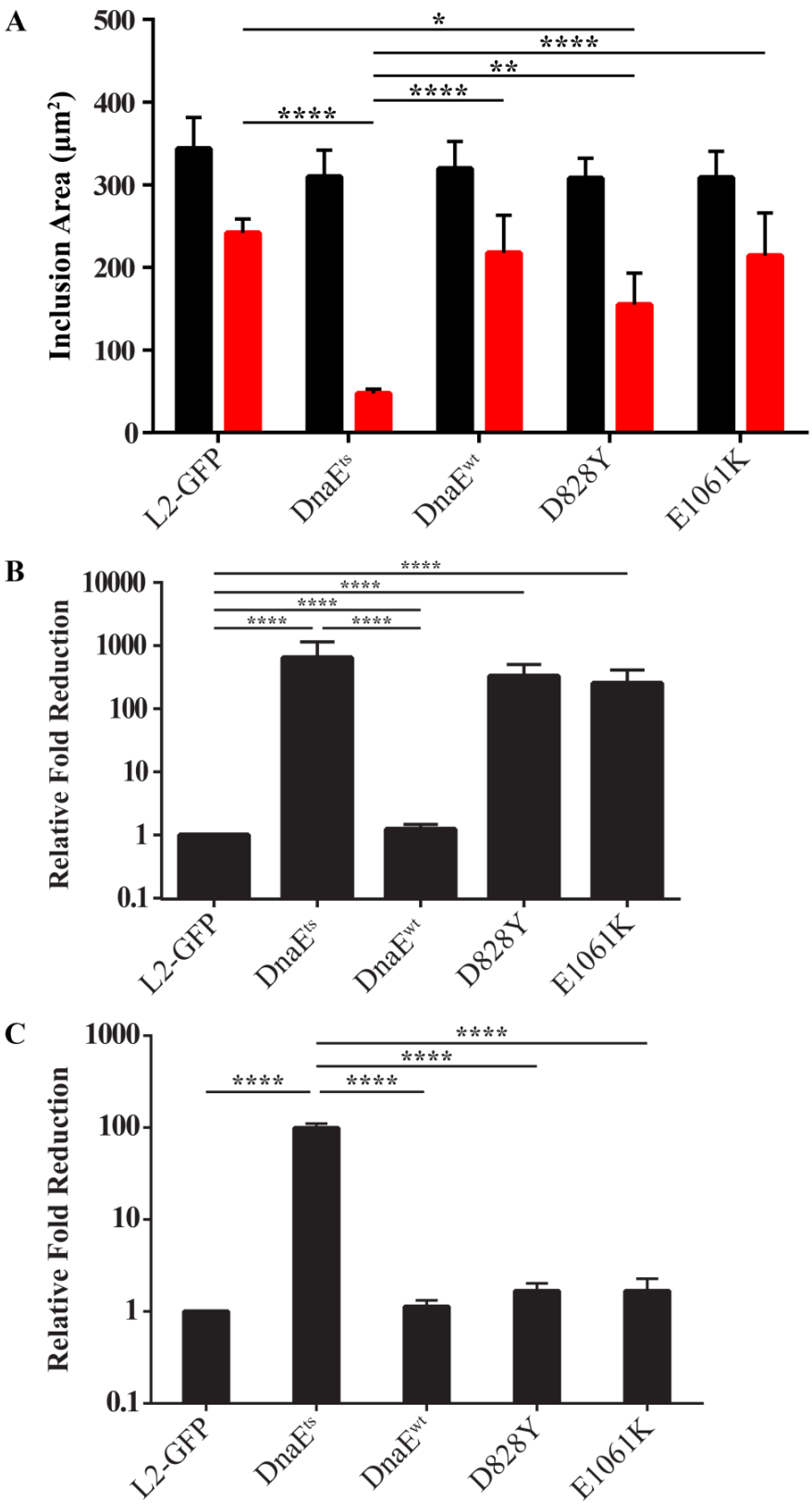
A
Inclusion Area (μm²)
500
400
300
200
100
0
*
****
**
****
****
L2-GFP
DnaE^ts
DnaE^wt
D828Y
E1061K
B
Relative Fold Reduction
10000
1000
100
10
1
0.1
****
****
****
****
****
L2-GFP
DnaE^ts
DnaE^wt
D828Y
E1061K
C
Relative Fold Reduction
1000
100
10
1
0.1
****
****
****
****
L2-GFP
DnaE^ts
DnaE^wt
D828Y
E1061K

Figure 18 *dnaE*^{ts} suppressors partially rescue growth. The sizes of inclusions strains formed at 37°C (black bars) or 40°C (red bars) was measured (A). The ratio of progeny formed at 37°C/40°C was normalized to L2-GFP at the same temperatures (B), and genome copy numbers were measured by qPCR (C). Results are means of 3 independent experiments ± SD. Statistical significance was assessed by one- (B and C) or two-way (A) ANOVA followed by Tukey's *post hoc* test. *, $p<0.05$; **, $p<0.01$; ****, $p<0.0001$

CHAPTER V: Characterization of a Temperature Sensitive GltX Mutant

Sequence analysis predicts a truncation in the glutamyl-tRNA synthetase GltX

We isolated a *C. trachomatis* L2-GFP mutant by EMS mutagenesis (HS 1 in Chapter III) whose temperature sensitive allele was $gltX^{C1459T}$ (hereafter referred to as $gltX^{ts}$). This mutation generates a stop codon in codon 487 that truncates GltX 20 amino acids from the C-terminus (Table 6). To better understand why fitness of $gltX^{ts}$ was normal at 37°C (Figures 8 and 9), we generated a *Ct*GltX model using Phyre2 software. X-ray crystal structures of GltX from *Mycobacterium tuberculosis* (*Mt*GltX) and *Thermotoga maritima* (*Tm*GltX) are available (PDB accession numbers 2O5R and 3AKZ, respectively). The high similarity of these proteins permitted construction of >90% confidence model of *Ct*GltX (Figure 19).

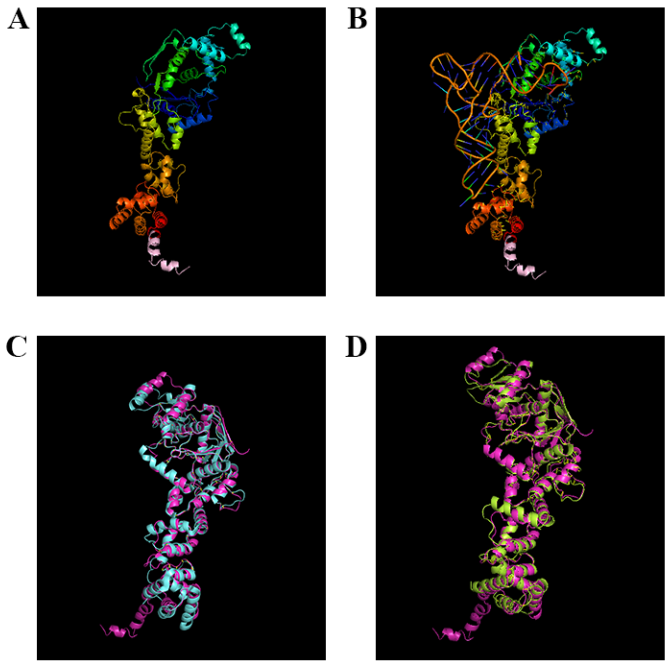

Figure 19 A model of *Ct*GltX predicts that the structure of GltX^{ts} is not altered. A model of *C. trachomatis* serovar L2 GltX was generated using Phyre2. (A) The 20 residue truncation (shown in pink) in *Ct*GltX deletes two alpha-helices that do not interact with the rest of the structure. (B) Modeling of *Ct*GltX with a bound tRNA suggests that the truncation does not disrupt the catalytic or the anticodon recognition sites. *Ct*GltX (magenta) aligned with *Mt*GltX (cyan; PDB: 2O5R) (C) and *Tm*GltX (yellow; PDB: 3AKZ) (D).

The *Ct*GltX model suggested that the last 20 amino acids form two small alpha-helices that are not present in either *Mt*GltX or *Tm*GltX. A general search for GltX homologs using the basic search alignment tool for proteins (BLASTp) algorithm showed that the longer GltX sequence is rare, but not unique to *Chlamydia* spp. For example, *Bacteroides fragilis* GltX is approximately the same length as CtGltX, although tertiary structural information of this protein is not available.

The core GltX enzyme is highly conserved in *Chlamydia* spp., and GltX sequences are nearly identical in *C. trachomatis* serovars. However, alignment of

chlamydial GltX proteins determined that the C-terminal amino acids of these proteins are more variable than any other part of the protein (Figure 20).

```
         450       460       470       480       490       500
L2         KQGLPLFDSMELLGKARTRARLTYAQNLLGGVSKKVQ**QQVDKALQDQPLEDIRFLDF**
D          KQGLPLFDSMELLGKARTRARLTYAQNLLGGVSKKVQQQVDKALQDQPLEDIRFLDF
MoPn       KQGLPLFDSMELLGKARTRARLTHAQNLLGGVPKKLQQQIDKALQDQPLEEIRFLDF
CPn        KQGLPLFDSIEILGKPRARARLVYAEKLLGGVPKKLAATVDKFMQREDFEEATFDL-
GPIC       KQGLPLFDSMELLGKPRTRMRMVHAQNLLGGVPKKIQTAIDKVLKEENFENK-ILEF
           *********:*:*** *:* *:.:*::***** **:   :** :: : :*:  :
```

Figure 20 Conservation of the GltX C-terminus in *Chlamydia* spp. GltX from *C. trachomatis* serovars L2 and D, *C. muridarum* (MoPn), *C. pneumoniae* (CPn), and *C. caviae* (GPIC) were aligned using ClustalO. Residues predicted to be absent in $GltX^{ts}$ are shown in bold.

Growth characteristics of an aminoacyl-tRNA synthetase mutant

We characterized $gltx^{ts}$ using progeny forming assays and qPCR. The mutant produced significantly fewer EB than did L2-GFP or $gltX^{WT}$ by 24 hpi, and this trend continued to 34 hpi (Figure 21A). While $gltx^{ts}$ formed a few EBs at the 18 hpi and 24 hpi timepoints, fewer EBs were formed than were used for the initial infection, indicating that these were either carry over EBs from the infection or the result of non-productive infections.

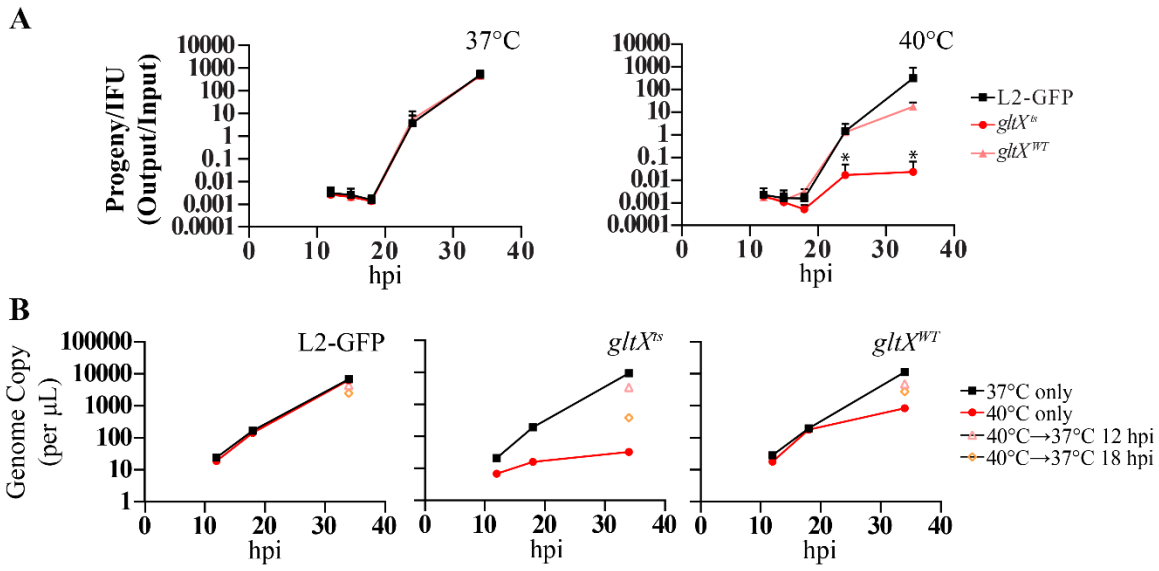

Figure 21 *gltX*^{ts} progeny production is impaired at 40°C. HeLa cells were infected with L2-GFP, *gltX*^{ts}, or gltX^{WT} and grown at 37°C, 40°C, or were shifted from 40°C to 37°C. Infections were stopped at the indicated times by freezing the infected cells in SPG. Part of each sample was used to count infectious EBs (A). The other part was used to count genome copies using qPCR (B). Values are normalized to the number of inclusion forming units of the inoculum. Progeny assays were performed four times in triplicate; genome copy number experiments were performed two times in duplicate. Error bars in (A) represent standard deviation. Values were log transformed and analyzed by two-way ANOVA followed by Tukey's *post hoc* test to correct for multiple comparisons. *gltX*^{ts} produced fewer progeny at 24 and 34 hpi compared to L2-GFP or gltx^{WT} at 40°C, but not at 37°C. *, $p<0.0001$

A lack of charged tRNAs can induce the general amino acid stress response in eukaryotes and the stringent response in bacteria. Tryptophan-limiting conditions cause some *Chlamydia* spp. to enter a viable but non-cultivatable state termed persistence that is characterized by aberrant RBs that fail to divide but continue to replicate their genomes (122). We measured the numbers of genomes *gltX*^{ts} formed at 37°C and 40°C to test if this mutant continued to replicate its genome at the non-permissive temperature. Differences in the number of genomes produced by the *gltX* mutant were evident early in infection (i.e., 12 hpi), and genome copies increased only slightly by the end of the

infection (34 hpi), culminating in an ~3 log decrease in the at 40°C/ 37°C ratio compared to L2-GFP or ~2 log decrease when compared to *gltX*^{WT} (Figure 21B).

The lack of progeny production and genome replication suggested that the mutant was likely dead after extended incubation at 40°C. We tested whether *gltX*^{ts} growth could be rescued by determining the number of infectious progeny and genome copies from infections that were shifted from 40°C to 37°C during the course of infection. Shifting the *gltX* mutant at 12 hpi to 37°C rescued genome production, while shifting at 18 hpi only partially rescued the defect. Since inclusions could be seen and genome replication could be detected if shifted to 37°C by mid-development, we hypothesize that *gltX*^{ts} is still alive early in development and that it enters a stress response from which it can be rescued by returning to the permissive temperature by mid-cycle.

Temperature shifting identifies when the growth defect occurs

Extended incubation in stressful conditions (i.e., incubation at the non-permissive temperature) is lethal. Therefore, we wondered if shifting between 37°C and 40°C during the course of infection could either rescue or inhibit inclusion growth. Because we had shown that *gltX*^{ts} (HS 1) had a decrease in inclusion size between 12-18 hpi (Figure 7), we concentrated on these early/early-mid timepoints. *gltX*^{ts} inclusion size could not be rescued after 18 hours of incubation at 40°C (Figure 22). The reverse conditions—incubation at 37°C followed by a shift to 40°C—indicated that growth at the permissive temperature for early and early-mid development could not overcome the small inclusion phenotype. Inclusion size decreased more dramatically at 8 hpi compared to 12 hpi, indicating that a longer amount of time at 37°C increased inclusion growth. L2-GFP and

gltX^{WT} inclusion areas were minimally affected and nearly identical in all tested conditions.

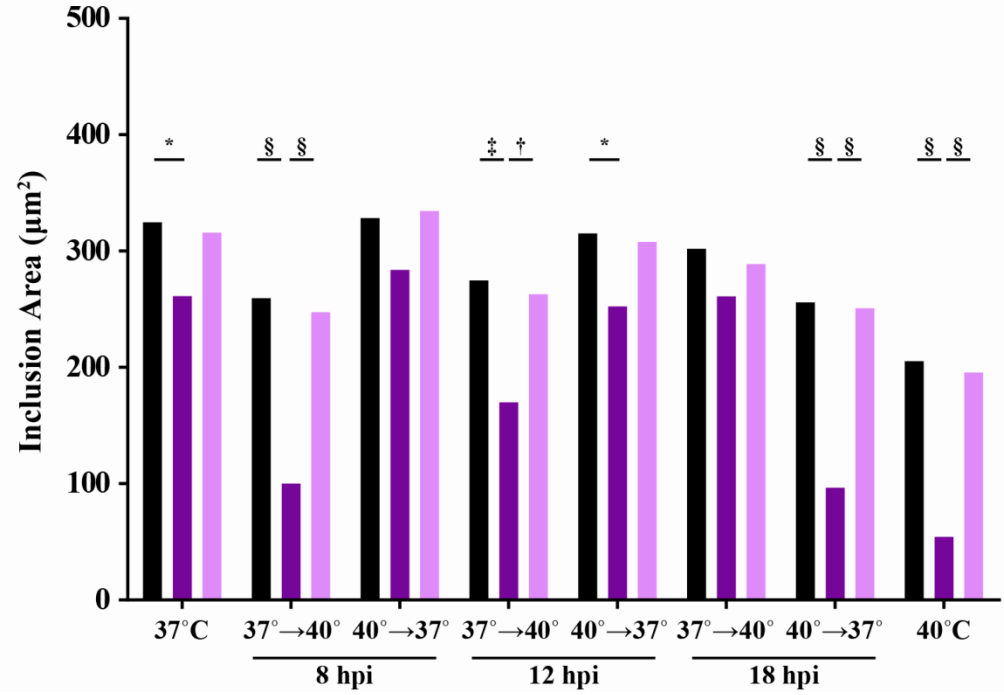

Figure 22 *gltX*^{ts} inclusions are smaller at 40°C. HeLa cell monolayers were infected with L2-GFP (black bars), *gltX*^{ts} (purple bars), or its isogenic recombinant (lavender bars). Infections were incubated either continually at 37°C or 40°C, or were transferred between these temperatures at the times indicated. All infections were fixed at 34 hpi, and inclusions were stained for chlamydial LPS. Bars represent the mean of two independent experiments. A two-way ANOVA and Tukey's *post hoc* test were used to determine statistical significance. *,p<0.05; †, p<0.01; ‡, p<0.001; §, p<0.0001

gltX^{ts} EBs differentiate into RBs at 40°C

Higher magnification (≥10X) and staining with anti-chlamydial LPS antibody showed the presence of numerous small *gltX*^{ts} inclusions compared to L2-GFP or *gltX*^{WT} at 40°C that were not detected during our initial screen, which was performed at 4X magnification (Figure 22). The presence of inclusions, reduction in recovered progeny

and number of genomes, and our knowledge of the IFN-γ persistence model prompted us to examine what chlamydial developmental forms were present in the *gltX*^{ts} inclusions at 40°C. Transmission electron microscopy of *gltX*^{ts} inclusions revealed that *gltX*^{ts} could still differentiate into RBs, indicating that GltX function is not required for the EB to RB transition. Inclusions grown continuously at 40°C for 32 hours contained aberrant RBs as well as intermediate bodies (IBs) (Figure 23). This was not observed with either L2-GFP or *gltX*^{WT} (data not shown). Inclusions shifted from 40°C to 37°C at 12 hpi, and to a lesser extent at 18 hpi, contained normal RB by 32 hpi, confirming that the growth inhibition at the mutant at 40°C is reversible (data not shown).

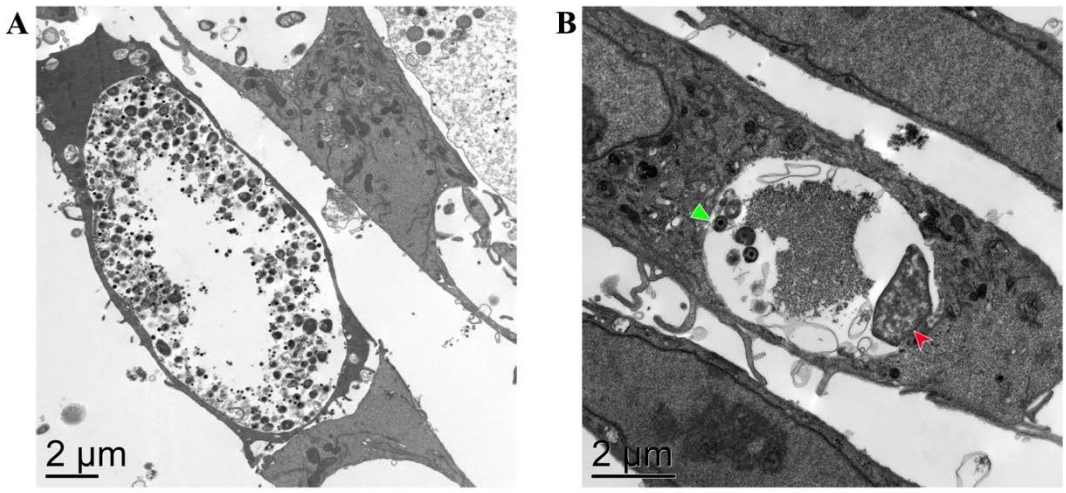

Figure 23 Ultrastructure of the *gltX*^{ts} inclusion. Transmission electron microscopy was used to examine the inclusion content of HeLa cells infected with *gltX*^{ts} at 37°C (A) or 40°C (B) for 32 hpi. While normal EBs and RBs were present at 37°C, the presence of intermediate bodies (green arrowhead) and aberrant bodies (red arrowhead) could be seen at 40°C.

CHAPTER VI: Conclusions

Summary

Our study generated important new tools for future *Chlamydia* research. First, we generated a large *C. trachomatis* library for future genetic screens. Second, we developed the first unmarked LGT mapping approach in *Chlamydia* spp. Unlike earlier LGT mapping approaches, negative selection LGT does not require the introduction of genetic markers and can be used, theoretically, in any *Chlamydia* strain or species capable of LGT. Finally, we developed a suite of conditional mutants that permit interrogation of the order of critical developmental processes in *Chlamydia* spp.

Section I: Chlamydial Genetics

Development of conditional mutants

Results of the temperature sensitive screen in Chapter III indicate that a larger screen might identify additional TS mutants. 183 unique mutations were identified in the 33 sequenced isolates. Nonsynonymous mutations were detected in the same gene in different mutants in 22 cases (2-4 occurrences). Identical alleles were identified in three of the HS mutants identified in that screen; one strain was a duplicate and another was a sibling. Because we did not identify the same alleles in strains with other background mutations, the screen was not saturated.

The TS mutants differed from the parent by 6 mutations on average (range 1-11) (Table 7). Mutants isolated from the same library in other screens had similar numbers of mutations, indicating that the number of mutations in the TS mutants generally reflects

the mutation load of the library (228). The number of mutations per genome has generally not proven to be too challenging for mapping mutations and allows for good coverage of the genome while condensing the number of isolates that need to be screened.

The TS mutants we isolated have defects in diverse processes including carbon acquisition, energy utilization, protein synthesis, cell replication, and lipid synthesis (Table 8) and are summarized in Figure 24. *gltX*, *dnaE*, and *atpB* are essential in other organisms. *fabI* is essential in *C. trachomatis*, since chemical inhibition of FabI reduced inclusion size and prevented progeny production (229). *ctl0322* may encode a histone-like protein (230) and this gene is regulated by a non-coding RNA—*lhtA*—that regulates a known chlamydia histone, HctA (64). We predict that CTL0322 plays a similar role to HctA in the RB-EB transition. TS alleles in 13 TS mutants were identified in total, and the TS allele of two additional TS mutants was narrowed down to two possible mutations (Table 8). These strains are further discussed in Chapter VII.

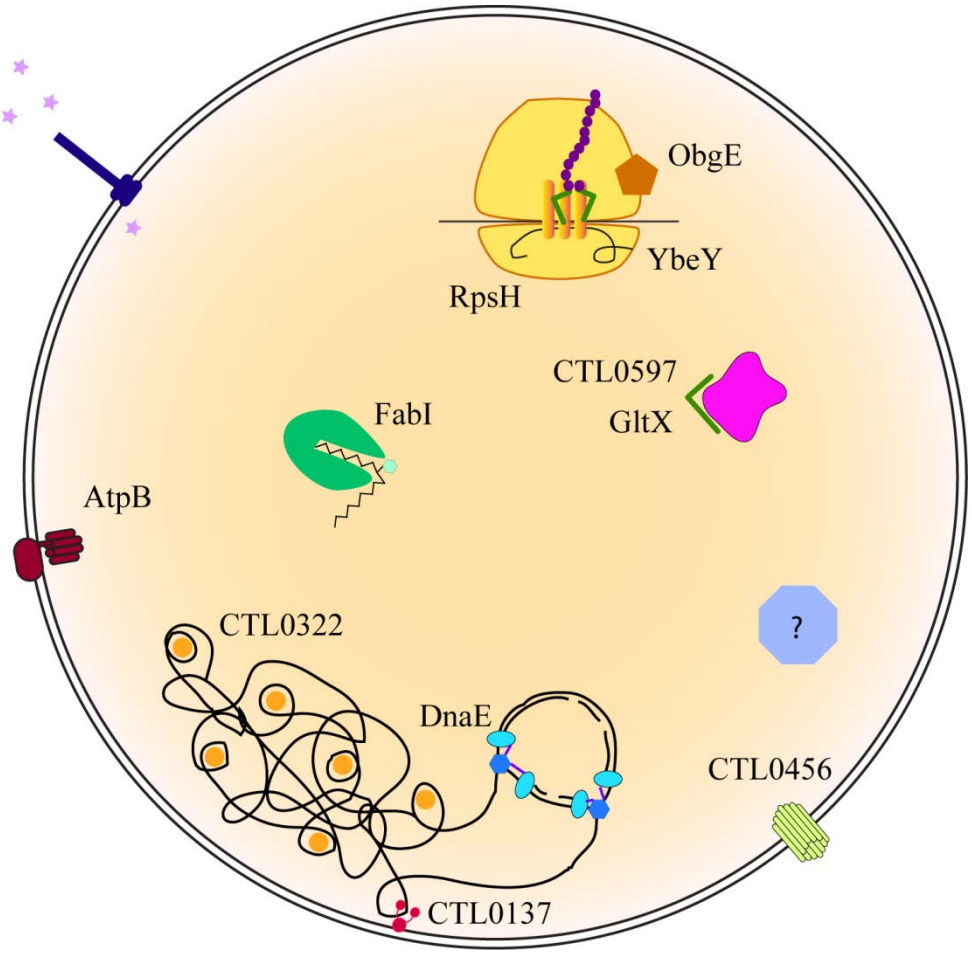

Figure 24 TS mutant provide insights into essential chlamydial processes. Genes of which we identified TS alleles in this study may mediate multiple aspects of chlamydial growth and development and are expressed at different developmental stages (Figures 5-7). Multiple TS alleles of genes involved in protein synthesis at either the ribosomal level (ObgE, RpsH, and YbeY) or tRNA level (GltX and CTL0597) were identified. Other mapped TS alleles relate to genome replication (DnaE) and chromosome management (CTL0137 and CTL0322). Mutants in energy acquisition (AtpB), fatty acid metabolism (FabI), and carbohydrate acquisition (CTL0456) were also identified.

Temperature shift assays showed that while the majority of genes need to function in mid-development, there are genes that are needed earlier and later in infection (Figures 5-7). Because few chlamydial protein antibodies are available to detect when specific proteins are expressed and because of developmental asynchrony, these temperature shift assays inform us as to when these genes function in the developmental cycle, which has

not been previously possible. The temperature shift timepoints used in this study were broad, but finer time intervals can be considered in further characterization studies of individual mutants to examine time of function more carefully. When comparing multiple TS mutants simultaneously, the order in which processes such as DNA replication and protein synthesis, for example, are needed can be determined.

The number of progeny produced by TS strains also helps to define how critical a gene is to the developmental cycle. A reduction of 10-fold in progeny production compared to the L2-GFP parent does not suggest essentiality. The TS allele in these mutants may result in a partially inactive protein at 40°C or the presence of an alternative, redundant pathway to circumvent the mutation. Progeny reductions of ~1000-fold or more suggest lethality and essentiality of a gene product to complete the developmental cycle, since a reduction of this size would require fewer infectious progeny to be produced than were originally used in the infection. While some of these mutants produced a number of progeny comparable to that of L2-GFP at 37°C (e.g., $gltX^{C1459T}$), others produced far fewer progeny (e.g., $obgE^{G275A}$) (Figure 8). Mutants with severely decreased fitness at 37°C speak to the general essentiality of these genes to normal cell growth. These mutants are still valuable tools for investigating gene function.

A caveat to our TS screening strategy and interpretation of the phenotypes of the mutants is that host and bacterial physiology differ at 32°C, 37°C, and 40°C. For example, our results suggest that more glycogen accumulates in the inclusions when *C. trachomatis* is grown at 40°C (Figure 23). It is also intriguing that three different TS alleles were identified in the dicarboxylate transporter *ctl0456*. While these all displayed growth defects at 37°C (Figure 8), decreased survival of the mutants that contained

nonsense alleles (W321* and W442* in CS 1 and CS 3, respectively) at 32°C (Figures 6, 7, 8C, and 8E) suggests that the host cell cytosol may contain less free glutamate and more 2-oxogluterate at lower temperatures compared to 37°C. Thus, although redundant carbon acquisition transporters (e.g., GltT) may be sufficient to allow these *ctl0456* mutants to grow at 37°C, they are not sufficient at 32°C.

Extending the chlamydial genetic toolbox

We used negative selection LGT to map multiple TS alleles. There are advantages and disadvantages to using negative selection over antibiotic selection to generate recombinants. Negative selection uses inherent phenotypes (e.g., temperature sensitivity) of mutants to enrich for recombinants. Enrichment can be sufficient after only a few rounds for mutants with robust phenotypes, but mutants with weaker phenotypes represent a challenge. In contrast, selection is consistently robust in antibiotic driven lateral gene transfer, which requires the generation of drug resistant mutants. Positive selection LGT is time intensive and may generate strains with altered phenotypes (231,232). Positive selection LGT in *C. trachomatis* is also limited to antibiotics for which either spontaneous mutation causes resistance or that a resistance cassette can be moved onto the chromosome. Rifampicin, ofloxacin, lincomycin, and spectinomycin have been used in positive selection LGT for *C. trachomatis*. The spontaneous resistance in these genes restrains and biases recombination events to include the genomic regions near *rpoB*, *gyrA*, *23S rRNA*, or *16S rRNA*, respectively. In addition, these genes are not evenly dispersed throughout the genome. Finally, because the positive selection marker (i.e., antibiotic resistance) must be present, no isogenic strain can be generated without backcrossing (Figure 25).

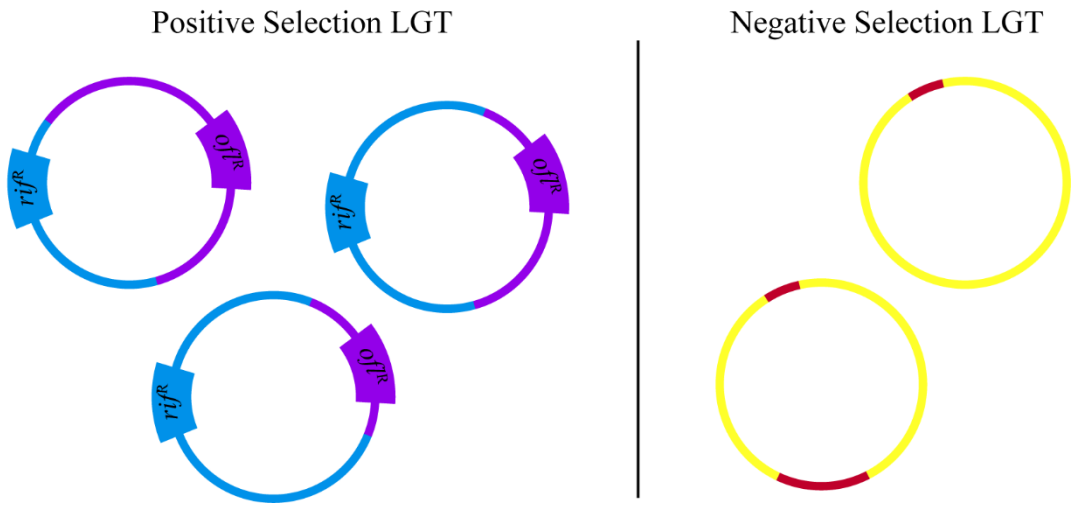

Figure 25 Comparison of recombinants from LGT crosses. Positive selection LGT relies on two different antibiotic markers to select for recombined progeny. The antibiotic resistance marker results from spontaneous mutation of the wild type allele, so the location of the selection markers is fixed. The proportion of DNA acquired each parent varies and is determined by unknown factors (blue v. purple). Phenotypic analysis of recombinants allows deduction of the mutation. Negative selection LGT relies on a loss-of-function mutation (e.g., temperature sensitivity) being replaced during recombination (red regions).

While negative selection LGT is a valuable strategy for generating isogenic recombinants, the recombinants will contain other background mutations unique to the parent used. This means that comparisons cannot be made to a common wild-type parent and that phenotypes of recombinants must be considered in the context of the parent's genotype. Negative selection LGT also prevents associating the presence of an allele with a given phenotype, since the mutant allele is replaced with a wild type copy during recombination. In contrast, positive selection LGT generates new recombinant strains that express the mutant phenotype when the mutant allele is present on the chromosome, and these can be compared to a common parent strain.

Negative selection LGT is not restricted to use in temperature sensitive crosses. It has also been used to map mutants that could not survive IFN-γ induced persistence by enriching for recombinants using the same conditions used to identify the mutants (228).

Furthermore, the lack of a second mutant with the same phenotype does not preclude the use of negative selection. An IFN-γ sensitive *C. muridarum* mutant was crossed with a temperature sensitive *C. muridarum* isolate (Amanda M. Giebel, *et al*., unpublished data). Selection at 40°C and IFN-γ resulted in recombinants. One of these isolates contained all of the alleles of the IFN-γ sensitive parent except for one allele, and this recombinant was IFN-γ resistant.

Negative selection LGT is applicable to at least two chlamydial species and can harness a variety of selection conditions. We also used the technique to generate *C. trachomatis* serovar L2 x *C. muridarum* crosses (see Appendix I). These chimeric strains could facilitate investigation of the molecular bases of chlamydial tropism. For instance, using these strains, we could investigate why *C. trachomatis* serovars cannot ascend the murine genital tract. Identifying a gene or locus from *C. muridarum* that led to a gain-of-function for a primarily *C. trachomatis* derived genome could facilitate murine modeling studies for urogenital and/or LGV *C. trachomatis* studies. These genes would also be potential vaccine targets, since they would relate to spread of disease and disease severity.

Mapping of TS alleles of some HS mutants with HS 23 failed. Many recombinants from these crosses were isogenic or nearly isogenic to HS 23 ($dnaE^{ts}$). There are a few possible explanations for these results. The use of mis-matched phenotype strengths (i.e., the other parent has a weaker TS phenotype) may allow the parent to produce enough progeny at 40°C to overwhelm the smaller population of recombinants. Additional rounds of enrichment might rectify this issue. Another possibility is that several mutants that could not be mapped had mutations in known type

III secretion system genes or hypothetical genes whose products could be secreted. Here, we speculate that cross-complementation of secreted effectors could have mitigated selection if the enrichment infections were performed at an MOI ≥2.

Some mutants failed to produce diverse recombinant populations when crossed with HS 23, and this may provide insight into the mechanism of gDNA transfer. It is unknown whether recombinants are the products of natural transformation or conjugation. Crosses between two purified strains or two crudely harvested strains tended to yield more diverse recombinants than crosses of crudely harvested strains with purified strains. For example, when purified HS 23 was crossed with other crudely prepared strains, isogenic *dnaE* recombinants predominated (data not shown). This suggests that the source of gDNA in some recombination events may be extracellular gDNA. This hypothesis could be tested by co-infecting a purified TS mutant with a different crudely harvested TS mutant that had or had not been treated with DNase to remove any extracellular gDNA. If the hypothesis is correct, then more genomic diversity of the recombinants should result from the cross with DNase, since this should be analogous to crossing two purified strains. In contrast, the cross that did not use DNase should have a backbone that is predominately derived from the first, purified parent. The observation that bias is created based on how strains were harvested also suggests that a strain is more likely to be the donor if it is dominant in the co-infection inoculum. This could be tested by varying the ratio of recombinant parents to each other in the initial co-infection.

The chlamydial genome encodes homologs of several genes that mediate conjugation in other bacteria (4). Recent work from the Hefty group suggests that *C.*

trachomatis has a functional conjugation system. Disruption of the *comEC* homolog by transposon insertion precludes the ability to act as a recipient in LGT crosses (P. Scott Hefty, unpublished).

Regardless of the mechanism governing DNA transfer and recombination, *Chlamydia* spp. can exchange DNA. The molecular mechanism for how the Tet island transferred *in vivo* into *C. suis* (233) and *in vitro* from *C. suis* to *C. muridarum* (84) is not known. Numerous examples of transformation with shuttle plasmids now exist (92,93,95), which supports competency of DNA uptake *in vitro,* although the molecular mechanism for how and when the plasmid enters the bacterium is not known. Linearized plasmids have been taken up by electroporated *C. psittaci* (85), although these were no longer than ~4 kb.

Our work suggests that some recombinants incorporated up to ~500 kb of DNA based on Sanger sequencing of divergent allele loci between the two parents (see Appendix II). The recombinants produced in this study were not biased for higher frequencies of DNA transfer from one part of the chromosome compared to others, as would be expected for Hfr conjugation in *E. coli* (234). Rather, the sometimes small areas of recombination and mosaicism is more reminiscent of the horizontal gene transfer seen in *Mycobacterium* spp. (235).

Section II: Chlamydial Genome Replication

A TS DnaE mutant fails to replicate its genome

Our data indicates that DNA replication is inhibited in *dnaE*^{ts}, but not L2-GFP or *dnaE*^{WT}, at the non-permissive temperature of 40°C (Figure 11). DNA replication resumes upon shifting from 40°C to 37°C (Figure 12). However, temperature shift assays indicate that *dnaE*^{ts} inclusion size is not rescued after 18 hpi (Figure 13). This may reflect of how the assay was performed, since all infections were stopped at 34 hpi, and therefore the longer an infection spent at 40°C, the shorter amount of time it spent at 37°C.

The DnaE suppressors display an intermediate growth phenotype. While there is only a slight defect for genome replication of either the D828Y or E1061K suppressor compared to L2-GFP or *dnaE*^{WT}, inclusions formed by the suppressors are noticeably smaller and still produce fewer progeny at 40°C (Figure 18). In all cases, the suppressors grow better than *dnaE*^{ts}. This suggests that even a small advantage in the ability to replicate the genome increases the chances of completing the developmental cycle and expanding the inclusion. Since an equal number of genome copies are seen in the suppressors compared to strains with *dnaE*, we hypothesize that the suppressors rescue DNA replication, but not to the wild-type kinetics. The probe used to assay genome copies by qPCR anneals approximately 200,000 bp from the origin of replication. It is possible that genome replication appears to be completely restored in the suppressors if genome replication has passed this point but that progeny are not produced because genome replication is not complete (approximate genome size 1 Mb). Extended

incubation of the suppressors at 40°C may allow them to complete RB-EB differentiation so that progeny production is rescued.

Nature of the DnaE^{P852S} mutation

The HS 23 genome contained four mutations (Table 7). The temperature sensitive allele was mapped using negative selection LGT to *dnaE*^{ts}, which is predicted to code for DnaE^{P852S}. Primary sequence alignment of *Ct*DnaE with *Ec*DnaE and *Ta*DnaE suggested that the mutation falls in the β-clamp binding domain (Figure 16). Phyre2 modeling of *Ct*DnaE places P852 in a loop of a three-stranded β-sheet (Figure 17). Structural modeling of this mutation failed to suggest an obvious mechanism for DNA replication inhibition. Both *Ec*DnaE and *Ta*DnaE have analogous prolines in their sequence that are part of a conserved (V/I)LP**P**D(I/V)N motif found in all three DnaE homologs (Figure 16). The analogous proline residue in the *Ec*DnaE and *Ta*DnaE crystal structures falls into the same three-stranded β-sheet as in the *Ct*DnaE model. Structure-function studies have analyzed this region of DnaE. The presence of two prolines in a loop between two β-strands is a hallmark of a tight hairpin turn, since proline allows tighter turns that are not favorable conformations for the other 19 amino acids. Thus, the P852S mutation may result in a protein with looser local structure that becomes further denatured at 40°C. A TS screen of EMS-mutagenized *E. coli* that could synthesize protein but could not replicate their DNA (236) identified a TS *E. coli dnaE* allele (*dnaE486*) that encodes *Ec*DnaE^{S885P} (237). The residue in *Ct*DnaE at the analogous position is A922 (Figure 17). Interestingly, when modeled on the tertiary structural model of *Ct*DnaE, A922 is predicted to directly contact P852—the location of our TS mutation.

To better understand how DnaE^{P852S} would be defective, a suppressor screen was performed. Two intragenic suppressors were isolated that conferred temperature resistance in the presence of the *dnaE*^{ts} mutation. Fifteen independent cultures containing a total of 1x10^{10} EB were passaged five times at 40°C. Sanger sequencing of *dnaE* from the twelve positive cultures revealed that the original mutation was still present, confirming that reversion did not occur. All twelve cultures contained a suppressor that would be predicted to encode DnaE$^{P852S\ E1061K}$ (*dnaE* $^{C2554T\ G3181A}$). However, this suppressor did not become evident in the infected wells at the same time and was absent in three of the fifteen original cultures (Table 9), suggesting that this suppressor arises independently and frequently. The other suppressor that encodes DnaE$^{D828Y\ P852S}$ (*dnaE* $^{G2482T\ C2554T}$) was found in three independent cultures. It was dominant in one population, but was a sub-population in two other DnaE^{E1061K}-dominant populations in the other two cases. Sequencing of *dnaE* from clonal isolates from these mixed populations confirmed that these were independent suppressors and that no *dnaE* $^{G2482T\ C2554T\ G3181A}$ strain was present. Due to the high frequency of recovering duplicate suppressor alleles in *dnaE*^{ts}, it is unlikely that other intergenic suppressors are present in these strains, although this must be confirmed with whole genome sequencing. Whole genome sequencing is especially important, since *E. coli dnaE486* is predicted to increase the mutation frequency by ~6-fold (237) and may have a similar TS mechanism to *dnaE*^{ts}.

How either DnaE suppressor permits DNA replication at 40°C is not obvious from modeling. The D828Y mutation falls in the conserved hairpin of the HhH motif of the β-clamp binding domain. Extrapolating from the *Ta*DnaE DNA-ligand bound structure (111), D828 is proximal to the DNA template strand. The HhH motif mediates

processivity in response to *in vitro* salt concentration in other polymerases (227). The D828Y mutation raises several possibilities as to how this could support DNA replication. The charged polar to polar aromatic amino acid change may reduce charge repulsion of the incoming DNA template through the channel, slowing polymerization speed. Tyrosine may be preferred to either serine or threonine because the hydroxyl group extends further into the channel. Alternatively, the aromaticity of tyrosine may allow more extensive interaction with DNA, since the phenyl group could participate in hydrophobic base stacking interactions with bases of the DNA template. This may be important, since no other hydrophobic residues are in the immediate vicinity of position 828 and the tyrosine residue is otherwise solvent exposed (Figure 17).

The E1061K suppressor is proximal to the characteristic β-barrel of the OB-fold domain. During polymerization, this domain is hypothesized to show substantial rotation compared to the apoenzyme form of *Ta*DnaE (111). E1061 is preceded by an aspartic acid residue (Figure 17). The mutation thus suggests that a salt bridge would form, that the local pI would be lowered further, and that less electrostatic repulsion would be present, which should produce more rigid local structure. *Ec*DnaE has an asparagine at this location, while *Ta*DnaE has a glutamate like *Ct*DnaE (Figure 17). Both are preceded by an aspartate. This suppressor mutation is thus surprising in that to become more temperature resistant, *Ct*DnaE became more like the mesophilic *Ec*DnaE and less like the thermophilic *Ta*DnaE.

Inclusion expansion is dependent on genome replication

No EBs were observed in our TEM samples of *dnaE*^{ts} at 40°C (Figures 14B-H), suggesting that genome replication is not required for EB-RB differentiation. However,

the inclusion ultrastructure for these cells requires further investigation. Few bacteria were observed in these inclusions, indicating that cell division is severely impaired. This is expected, since cell division requires partitioning of the replicated chromosome into daughter cells. We did not observe enlarged RB forms, which have been associated with chlamydial stress responses to IFN-γ and penicillin; however, the presence of multiple empty vacuoles and an enlarged RB periplasm suggests that the bacteria were stressed (Figure 15). The multi-vesicular nature of these rare, nearly empty, and small inclusions may indicate that the inclusion is susceptible to host immune clearance mechanisms, such as autophagy (Figures 15B-H). Since our microscopy data indicated that *dnaE*^{ts} inclusions are rare, DNA replication may be required to produce secreted, protective effectors.

Interestingly, the surviving population of *dnaE*^{ts} cells can reactivate DNA replication up until ~18 hpi (Figure 12). We hypothesize that *dnaE*^{ts} denatures at 40°C, inhibiting its polymerase activity, but can be renatured when returned to 37°C. Renaturation of TS proteins involved in DNA replication has been seen previously with TS *E. coli dnaA* and *dnaC* mutants—two proteins that are required for replication fork initiation (238).

Inclusion size at 40°C correlated with the number of genomes, and changes in inclusion size during temperature shifts were reflected in the number of genomes (Figures 12 and 13). In contrast, the UhpC inhibitor KSK120, which was previously shown to inhibit DNA replication (125), did not inhibit inclusion expansion. Inhibition of protein synthesis with chloramphenicol inhibited both genome replication and inclusion

expansion, indicating that carbohydrate transport and protein synthesis differentially impact genome replication capacity (125).

Genome replication and inclusion expansion are impaired in *dnaE*^{ts} at 40°C (Figures 11, 13 and 14). Because inclusion size is severely reduced for *dnaE*^{ts} at 40°C alone, inhibitors of transcription and translation had a negligible effect on inclusion size at 40°C (Figure 14). Treatment of *dnaE*^{ts} with rifampicin or chloramphenicol at 37°C resulted in inclusions of similar size to what is observed at 40°C (Figure 14B). Therefore, the inhibition of DNA replication by KSK120 (125) is likely a side-effect of decreased glucose-6P levels that is independent of inclusion expansion. One possible reason that inhibition of UhpC has an effect on DNA replication is that *uhpC* lies directly upstream of *dnaE* in the same direction on the chromosome (9). Although transcription of *dnaE* begins earlier than *uhpC* (28), which suggests that these genes are not part of an operon, we cannot exclude that KSK120 may effect transcription of the *uhpC-dnaE* locus.

Section III: Chlamydial Protein Synthesis

Protein synthesis substrates are required mid-development

C. trachomatis begins *de novo* protein synthesis within the first few hours after invasion of a host cell (48); however, *gltX*^{ts} does not display a noticeable phenotype until mid-development (i.e., 15-18 hpi) (Figure 21). Transcriptome analysis of *C. trachomatis* serovar D developmental cycle, which is slightly longer than that of serovar L2, showed that transcription of all 18 aaRSs has begun by 8 hpi and increases to a steady state by 16

hpi (28). Several proteomics studies have identified individual aaRSs in EB (198-201). Although the whole set of 18 aaRS has not been found in any one study, this is likely due to the low peptide count. Whether the chlamydial aaRSs are functional throughout the developmental cycle or if they can be inactivated by post-translational modifications is unknown.

A lack of charged tRNA activates stress responses in other organisms. In bacteria, amino acid deprivation activates the stringent response. The ribosome interprets the ratio of aminoacylated to non-aminoacylated tRNA that enters the A-site rather than detecting lowered cytoplasmic concentrations of an amino acid (149). Induction of the stringent response causes the upregulation of amino acid biosynthesis genes in a (p)ppGpp-dependent manner (239). In high-persistence (*hip*) *E. coli* mutants, GltX is inactivated by phosphorylation as part of the stringent response (240,241). In eukaryotes, the general amino acid stress response is induced and upregulation of amino acid biosynthetic genes occurs in conjunction with eIF-2α phosphorylation (242,243). This halts translation since phospho-eIF-2α cannot interact with $tRNA^{Met}$. Additionally, in response to heat shock, yeast develop heat-activated granules, which precipitate several initiation and elongation factors, multiple aaRSs, as well as other cytoplasmic proteins, which refold upon stress termination (244). The goal of these responses is to halt translation until the appropriate levels of protein precursors are available. If translation is not stopped, cellular energy will be wasted on unusable aminoacylated-tRNAs and stalled ribosomes. Stalled ribosomes eventually disassemble and release their partial polypeptides, which ultimately results in the cytoplasm filling with aggregates of protein

fragments and subsequent death. Pathways involved in amino acid starvation have not been described in chlamydia, so how amino acid stress is mitigated is not known.

In actively replicating *E. coli*, the aminoacylated tRNA pool turnover is complete within one *E. coli* generation (245). Furthermore, the ester bond linking the amino acid to the tRNA is extremely labile (at least *in vitro*) and is highly sensitive to high temperature and basic pH. Given these facts, how chlamydiae differentiate and survive until mid-development seems quite unusual. However, it remains possible that truncated *Ct*GltX experiences either a great reduction in catalytic rate or mischarges tRNAs rather than completely ablating aminoacylation activity. Future experiments will be needed to address if translation is active in *gltX*^{ts} at 40°C, and, if so, whether tRNA^{Glu} and tRNA^{Gln} are properly charged (discussed in Chapter VII).

gltX^{ts} was able to differentiate and replicate at a low level at the non-permissive temperature (Figure 21A). However, replication was not robust, the RBs present had aberrant morphology (Figure 23), and genome copy numbers stayed low (Figure 21B). Growth could be rescued up until 15 hpi by shifting from 40°C to 37°C (Figure 21). The presence of IBs and large aberrant RBs argues against this mutant dying by 32 hpi post infection when grown at 40°C (Figure 23). Rather, this suggests that despite typically residing in a very consistent and predictable environment inside the host cell, chlamydia evolved a way to persist in the absence of ideal aminoacyl-tRNA conditions for several hours post infection. Taken together, our data suggests that chlamydial EB must contain sufficient pools of aminoacylated tRNA for early *de novo* protein synthesis, since a morphological phenotype is not observed until mid-development.

CHAPTER VII: Future Directions

Section I: Investigation into Essential Biological Processes with TS Mutants

Translation

When and how translation is initiated in chlamydia is poorly understood. The EB is believed to be largely metabolically inactive, and cannot translate proteins *de novo*, since cell-free RBs, but not EBs, can incorporate [^{35}S]-methionine (246). However, *de novo* protein synthesis during infection was detected by 2 hpi using [^{35}S]-methionine pulse-chase experiments followed by 2D gel electrophoresis (48). Our temperature sensitive screen identified mutants with defects in multiple steps of translation, which could provide insight into how translation is controlled.

Translation requires many different proteins and substrates ranging from amino acids to tRNAs to the ribosome. We have identified mutants that are suspected to have defects in post-transcriptional modification of tRNA (HS 26; *CTL0597*^{ts}), aminoacylation of tRNA (HS 1; *gltX*^{ts}), processing of 16S rRNA (HS 13; *CTL0681*^{ts}), and a ribosomal protein (HS 17; *rpsH*^{ts}). We may have also identified a mutant (HS 10) that encodes either another temperature sensitive ribosomal protein (*rplF*) or a methionyl-tRNA formyltransferase (*fmt*). Another TS mutant that we identified suggests that some components of the *E. coli* stringent response may function in chlamydia (HS 27; *obgE*^{ts}).

Translation requires that many components act together in a highly regulated manner. tRNAs constitute a major population of RNA in EBs (197). When *de novo* tRNA transcription begins in chlamydia is not known. However, nascent tRNA transcripts are not functional until 5' and 3' cleavage, -CCA addition, and various post-

transcriptional base modifications occur, and these enzymes are not transcribed until 3 hpi (28). These steps produce tRNAs that are of the correct size, adopt the appropriate stem-loop formation, can accept an amino acid, and are structurally stable enough for accurate decoding at the ribosome. tRNA aminoacylation gives tRNAs the ability to translate mRNAs at the ribosome. Ribosomes are large nucleoprotein complexes composed of over 20 proteins and 3 rRNAs, which also contain a high percentage of modified bases (167). Stress responses can alter the proteome, and this is mediated by different components of the translational machinery. For example, IFN-γ treatment reduces the amount of tryptophan that is available to chlamydia, and this is reflected in the proteins that are preferentially synthesized (247,248); proteins that contain high proportions of tryptophan residues are downregulated while the upregulated persistence-associated proteins tend to be tryptophan poor (249,250). We identified multiple mutants that could provide insights into how translation is regulated during chlamydial development and stress responses.

CTL0597 is annotated as an O-sialoglycoprotein endopeptidase, but BLAST predicts that CTL0597 is actually a TsaB homolog and therefore a t^6A modifying enzyme. TsaB forms a heterotrimer with TsaD and TsaE. TsaD recognizes tRNAs with anticodons that decode ANN codons, while TsaB adds the threonyl group to the 6-position of A37 (251). TsaE may stabilize the complex (252). Inactivation of TsaB would be predicted to prevent modification of twelve out of 37 chlamydial tRNAs, since it would impact $tRNA^{Arg}$, $tRNA^{Asn}$, $tRNA^{Ile}$, $tRNA^{Lys}$, $tRNA^{Met}$, and $tRNA^{Thr}$ (some have multiple isoacceptors). Threonylation of A37 is believed to improve translation fidelity. Yeast mutants of the CTL0597 homolog have impaired growth (253). Consistent with

this, HS 26 (*ctl0597*^{ts}) formed smaller inclusions and fewer progeny under normal conditions, and these defects are exacerbated at 40°C (Figures 5 and 8). A Phyre2 model of CTL0597 indicates that the G69R mutation is located at the TsaB-TsaD interface (Figure 26) (252), suggesting that the temperature sensitivity of HS 26 is caused by disruption of the TsaB-TsaD complex.

Figure 26 Model of CTL0597. CTL0597 was modeled using Phyre2 software. Glycine-69 is shown in magenta space-fill. CTL0597 is a homolog of TsaB, which has been shown to interact with TsaD using the helix that the mutation is found in (252).

The impact of tRNA modification on chlamydial growth could be further investigated by identifying how tRNAs are modified *in vivo* using tRNA sequencing (185,186). How HS 26 modifies tRNAs is of particular interest. Impaired growth of HS 26 at 37°C (Figures 5 and 8) indicates that CTL0597 may not be fully functional. Further investigation will be needed to determine if the mutant *ctl0597* allele in HS 26 causes these growth defects. The number of transcripts for the serovar D homolog of *ctl0597*,

ct343, was decreased ~2-fold in a model of IFN-γ persistence (204), indicating that *ctl0597* expression is responsive to stress stimuli and that tRNA modifications may play a role in the chlamydial stress response.

How chlamydia normally modify their tRNAs is unknown, and insight into how these modifications change during stress or potentially even the developmental cycle could reveal potential drug targets. Multiple tRNA modifications occur sequentially, so inactivation of CTL0597 at 37°C could block downstream tRNA modifications. Comparison of tRNA modifications by tRNA sequencing (185) could reveal if other putative tRNA modifying enzymes are active in *Chlamydia* spp. and determine if these modifications still occur at 40°C. Additionally, because CTL0597 is predicted to act in a complex and because the CTL0597^{G69R} mutation is predicted to interrupt the TsaB-TsaD binding interface, co-immunoprecipitiation assays could be used to test if the complex is intact in HS 26 at 40°C.

Once mature tRNAs are produced, they can be aminoacylated. The rate of translation can be controlled by the availability of the different aminoacylated tRNA species. While non-synonymous mutations were identified in multiple aaRSs in our screen (HS 1, HS 2, and HS 7), only a mutation in GltX conferred temperature sensitivity, although the TS allele in HS 7 has not been mapped. HS 1 was further investigated in Chapter V and potential future directions are discussed later in this chapter.

Once aminoacyl-tRNAs are produced, the ribosome can begin translating mRNA. Several TS mutants identified in the screen have mutations in genes involved in ribosome

biogenesis. Given their large size, multiple components, and heavy level of modifications, producing ribosomes is a resource intensive process. Not having the appropriate number of active ribosomes can be detrimental: too few, and growth is inhibited from a lack of necessary proteins and an inability to adapt; too many, and nutrients will be exhausted. Therefore, the availability of free ribosomes regulates translation rate (254).

Ribosome biogenesis can be regulated at the level of synthesis of mature 16S rRNA. The first steps in generation of mature 16S rRNAs are the 5' and 3' cleavage of the primary transcript by the endoribonucleases RNase G and RNase E, respectively. A BLASTp search of CTL0681 identified that this protein shares homology with the endoribonuclease YbeY. YbeY further cleaves the 3' end of 16S rRNA transcripts in conjunction with RNase R (157,158). The TS allele in HS 13 codes for CTL0681^{P159L} that is lethal early in development (Figure 5). YbeY has been annotated as an essential bacterial gene since it is highly conserved across the bacterial kingdom, and its inactivation leaves the cell vulnerable to stresses (255).

An *E. coli ΔybeY* mutant accumulated 30S and 50S ribosomal subunits and had fewer polysomes (157). The mutant also displayed slow growth kinetics and heat shock intolerance (157). Progeny production in HS 13 is normal at 37°C, but is impaired at 40°C (Figure 8). Deletion of *ybeY* in *E. coli* decreases the number of functional ribosomes. Therefore, analysis of polysome profiles in HS 13 at 37°C and 40°C at 12 and 18 hpi could provide insight into how CTL0681^{P159L} impacts translation in *C. trachomatis*. Polysome profiling could also reveal if abnormal "damaged" ribosomes result from inadequate ribosomal maturation (158). Northern blotting could be used to

test if HS 13 produces mature 16S rRNA at 40°C. Because all of the ribosomes in HS 13 EBs should contain properly processed 16S rRNA since they were harvested from cells grown at 37°C, how frequently new ribosomes are formed and how many defective ribosomes are tolerated by the cell could be monitored by comparing the percentage of processed to non-processed 16S rRNA throughout development. We hypothesize that the percentage of processed 16S rRNA is adequate until 18 hpi, when we see that the mutant can no longer be rescued by temperature shift (Figure 5).

Functions of the protein components of the ribosome are poorly understood. It is believed that ribosomal proteins stabilize the large rRNA species, which align the mRNA and interact with tRNAs to maintain the reading frame. Our screen identified one isogenic TS mutant (HS 20), which has a missense mutation in a ribosomal protein ($RpsH^{A119V}$) (Table 7). HS 20 has decreased fitness at 37°C (Figures 5 and 8). *E. coli* RpsH stabilizes 16S rRNA of the 30S ribosomal subunit so that the mRNA will be properly aligned with the 50S ribosomal subunit and incoming tRNAs (256). Thus, the small inclusion size and inability to adapt to an increase in temperature could be expected in HS 20. HS 20 could provide insights into how RpsH interacts with 16S rRNA. Protein footprinting studies, which utilize reversible cross-linking and mass spectrometry, could be performed to identify residues that directly contact the rRNA to determine if RpsH still binds the 16S rRNA in HS20 using the same residues or if an interaction is missing at 40°C.

Cells employ many mechanisms to adapt to changes in their environments, whether that be an increase (or decrease) in temperature, sensing of immune effector mechanisms, or nutrient depletion. One classical pathway used to respond to stresses is

the stringent response. In *E. coli* and other gram-negative organisms, nutrient deprivation is signaled by production of the second messenger (p)ppGpp. The ribosome accessory protein ObgE is bound to the ribosome under normal growth conditions. When *Ec*ObgE binds ppGpp, protein synthesis is downregulated (154,155). The structure of (p)ppGpp-bound ObgE is thought to mimic a tRNA in the A-site of the ribosome (219), inhibiting incoming tRNAs from interacting with the mRNA. Binding of ObgE to the ribosome also increases the transcription of amino acid biosynthesis genes and inhibits DNA replication, although the mechanism for this is unknown (257). *Chlamydia* spp. possess a truncated ObgE homolog that can bind the ribosome, but *Ct*ObgE cannot functionally substitute *Ec*ObgE (220). However, like the *Ec*ObgE mutants, HS 27 also displays growth defects (Figure 8).

*Ec*ObgE function has been explored during induction of the stress response. In contrast, when HS 27 was shifted from 40°C to 37°C, it could not be rescued even very early (0-8 hpi) in infection, which indicates that the EB-RB transition cannot occur (Figure 5). It is possible that *Ct*ObgE inhibits translation in the spore-like EB. Co-immunoprecipitation studies could be used to investigate when ObgE interacts with the ribosome during chlamydial development. Whether chlamydia use an alternative secondary messenger to (p)ppGpp to alert the cell to nutrient stress could also be investigated. For example, other second messengers such as cyclic di-AMP, which is found in chlamydia (203), may be able to interact with *Ct*ObgE to pause translation.

Cell division and differentiation

Chlamydial cell division does not to follow the classical paradigm, and the chlamydiae lack several key *E. coli* cell division proteins. For example, *Chlamydia* spp.

lack a FtsZ homolog, so how chlamydia determine septum location and eventual fission is not known. Chlamydial homologs for FtsL and FtsQ have recently been described (66). Furthermore, how chlamydia transition between EB and RB is poorly understood. Recent studies suggest that the initial EB to RB transition may be a process more akin to budding rather than binary fission (68), but whether this same process occurs during mid-development as RB divide or runs in reverse for the RB to EB transition at the end of the developmental cycle has not been investigated. Chlamydial differentiation is also unique in that it uses histone-like proteins to compact its chromosome. These are made late in development and are thought to be important for DNA condensation during the RB-EB transition (120).

The TS allele in CS 2 mapped to *ctl0137*, and a BLAST search identified the presence of an Smc domain within *ctl0137*. Smc-domain proteins are primarily coiled-coil proteins that contain a hinge near their centers (258). The N- and C-termini are globular and can associate with each other in an ATP-dependent manner (258). Smc-domain containing proteins are involved in chromosomal segregation during cell division and function by wrapping around the chromosomal DNA and closing around it by interactions between the two globular domains. The closed protein can then pull the chromosome along with it when in contact with other cell division proteins that are attached to the membrane.

The *ctl0137* allele in CS 2 is predicted to truncate CTL0137 at position 443 of the 560 residue protein, which would result in near complete loss of the C-terminal globular domain (Table 7). Whether or not CTL0137 interacts with DNA has not been demonstrated. However, if this protein does bind DNA and localizes to the division

septum in wild type cells, a redundant mechanism for chromosomal segregation at 37°C must be present, since *ctl0137*^{ts} is truncated. This redundant pathway would be predicted to be non-functional at 32°C, leading to lethality. Gel-shift assays could determine if CTL0137^{ts} interaction is less than or equivalent to the interaction of CTL0137 with DNA. Localization of CTL0137 to the division plane could be visualized with the development of an antibody to detect CTL0137, staining of the DNA, and tagging of the division septum (67). TEM of CS 2 at 32°C could also reveal if *ctl0137*^{ts} results in defects in RB-EB differentiation or enlarged RB due to impairment of cytokinesis. If chromosomal segregation is impaired, we would anticipate that unusual sized organisms would be present and that a portion of these cells would lack a chromosome, while others would contain multiple chromosomes.

The TS allele in HS 11 mapped to *ctl0322*. This TS mutant is predicted to have defects in packaging of DNA during division and differentiation. CTL0322 is a DNA binding nucleoprotein (230). Late in development, chlamydial DNA is wrapped around histone-like proteins to produce the condensed chromosomes characteristic of EBs. The long non-coding RNA *lhtA* represses CTL0322 expression until late in development (259). Whether *ctl0137*^{ts} transcript is regulated by *lhtA* at 40°C is unknown and could be tested in a heterologous system using a reporter for translation (259). Chromatin immunoprecipitation (ChIP) experiments could determine if mutant CTL0322 can still bind to DNA at 40°C. If there are any functional differences between CTL0322 and the other chlamydial histone-like proteins HctA and HctB remains to be investigated. ChIP-seq could be used to test if CTL0322 binds similar DNA sequences to HctA and/or HctB.

DNA replication

The signal to begin genome replication in chlamydia is unknown, but, assuming that there is one complete genome per EB, at least one round of replication must precede the first cell division. Previous studies indicate that DNA replication is required for progeny production, but not for growth of the chlamydial inclusion (125). We identified a temperature sensitive *dnaE* mutant (HS 23) that we have further characterized and which is the focus of Chapter IV. This shows that inclusion expansion requires DNA replication.

Proton gradient maintenance

The proton motive force is important for securing metabolites and generating ATP. ATP generating proteins are increased in RB compared to EB, and this is associated with the high energy demands of replication and an active metabolism (199). We identified a dual HS/CS mutant (HS 19) whose TS allele mapped to the V-type ATPase subunit beta encoded by *atpB*. The V-type ATPase typically acidifies intracellular compartments. The dysfunction of this protein would be predicted to result in a more basic compartment.

To test if ATP builds up in the bacterial cells, FRET studies utilizing the ATeam system, which consists of a translationally fused cyan fluorescent protein (CFP) and Venus FRET pair linked by the ATP-binding domain of the ε-subunit of the ATPase, could be transformed into chlamydia and the levels of ATP could be measured by FRET for HS 19 and L2-GFP (260). Alternatively, it may be possible to measure pH based on fluoresecent pH indicators such as seminaphthorhodafluors (SNARFs) (261). C.SNARF-

1 is a rhodamine-based molecule with a pKa=7.5 that shows shifts in the excitation and emission spectra based on whether the molecule is in the phenol or phenolate form. Although these dyes have been shown to be dispersed evenly throughout the cell, whether or not the dye can penetrate into chlamydia is not known.

Carbohydrate metabolism

The reduced genome of chlamydia raises questions regarding what substrates can be used to generate ATP. The uptake of radiolabeled-dicarboxylate compounds into chlamydia and their subsequent ability to generate ATP has been studied (59). Later genome sequencing showed the first enzymes (citrate synthase, aconitase and isocitrate dehydrogenase) involved in the tricarboxylic acid cycle (TCA) are absent (4). If the truncated TCA cycle can produce ATP has been questioned.

Our screen identified three alleles of *ctl0456* that conferred temperature sensitivity in CS 1 (W321*), CS 3 (W442*), and HS 20 (G145R). CTL0456 is a homolog of the dicarboxylate transporter SodTi in plants (59) and of *Vc*INDY in *Vibrio cholerae*. *Vc*INDY has been recently crystalized with glutamate bound (262). Given that chlamydia was shown to import 2-oxaloacetate (59) which is classically produced by the second enzyme in the TCA cycle, isocitrate dehydrogenase, and used by the third enzyme, α-ketogluterate dehydrogenase, we hypothesize that chlamydia does utilize its truncated TCA cycle using metabolites imported from the host cell. *Chlamydia* spp. possess two potential high-affinity transporters that could feed 2-oxogluterate into the truncated TCA cycle. Direct transport of 2-oxogluterate could be achieved through CTL0456, or 2-oxogluterate could be obtained indirectly by deamination of glutamate transported via GltT. A predicted GltT null mutant was isolated from an EMS-

mutagenized L2-*rif*^{R} library (91), suggesting that GltT is non-essential. The *ctl0456* alleles in CS 1 and CS 3 are predicted to be null alleles. Taken together, these studies indicate that redundant pathways exist: either GltT and CTL0456 can substitute for each other or potentially the low-affinity 2-oxogluterate porin, PorB, could be sufficient for survival (263).

All three temperature sensitive alleles of *ctl0456* have growth defects when grown at 37°C (Figures 6 and 7), suggesting that CTL0456 is important for fitness, but is not absolutely essential unless stressed. The truncated CTL0456 mutants (CS 3 and HS 20) are dual HS/CS mutants, providing genetic evidence that host cell levels of glutamate (the GltT substrate) may be too low at 32°C or 40°C to compensate for the lack of functional CTL0456. Metabolomics studies of the available carbon sources in host cells at 32°C, 37°C, and 40°C could better inform the phenotypes of these mutants. Generation of a *ctl0456*$^{-}$*gltT*$^{-}$ double mutant using TargetTron® (96) or FRAEMing (95) may inform if the pathways are redundant or if yet another pathway, such as PorB import, can still compensate. Experiments conducted by the McClarty group (59) to define the chlamydial carbon metabolites should be revisited with the *ctl0456* (89) and *gltT* (91) mutants to determine if the TCA cycle is active or if energy is being obtained via an alternative pathway such as glycolysis or the pentose phosphate pathway.

Fatty acid biosynthesis

Chlamydia encode a bacteria-specific fatty acid biosynthetic pathway that is used to generate branched chain fatty acids at the 2-position of some phospholipids (56,229). These enzymes have been shown to be druggable targets *in vitro* in other organisms, such as *Staphylococcus aureus* (264). *C. trachomatis* FabI, which converts *trans*-2-enoyl-

ACP to acyl-ACP, is inhibited by the same inhibitor as for *Staphylococcus aureus* FabI (229). Blocking FabI activity early during *C. trachomatis* infection was lethal, since growth stops in the RB stage. We isolated a temperature sensitive FabI mutant (HS 24; $FabI^{D79N}$) that could not be rescued after being grown at 40°C for 18 hpi (Figure 5). D79 is a conserved residue in both *C. trachomatis* and *S. aureus* FabI, although it does not appear to participate in substrate binding (Figure 27; (229)).

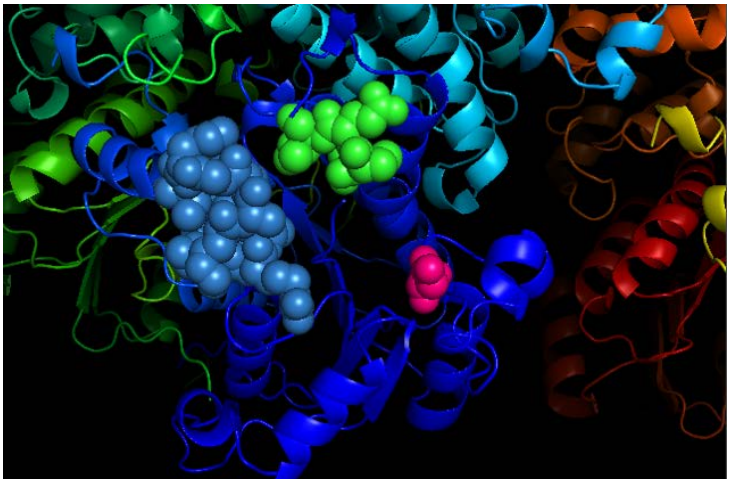

Figure 27 Model of FabI. Regions of FabI have been highlighted on the crystal structure (PDB ID 4Q9N;(229)). The "lid" loop (green spacefill) and "flipping lid" loop (blue spacefill) contact the inhibitor AFN-1252 (not shown), which binds to the catalytic cleft that is normally occupied by *trans*-2-enoyl-ACP (229). The location of D79 is colored in magenta spacefill.

Because the FabI inhibitor AFN-1252 blocked development past EB-RB differentiation, determining what developmental forms are present in cells infected with this mutant at 40°C by transmission electron microscopy would elucidate if the inhibitor and mutation inhibited growth in the same manner and to the same degree. Quantitative

mass spectrometry could be used to test if inhibition of FabI causes accumulation of *trans*-2-enoyl-ACP and a decrease in the amount of acyl-ACP in the cell (265).

Section II: TS alleles as Genetic Tools

As more genetic tools are developed, more advanced genetic manipulation strategies become feasible. Theoretically any non-essential gene can be deleted using FRAEM, which replaces a gene of interest with a *bla-gfp* cassette (95). While this cassette aids in the selection and visual identification of knock out mutants, introduction of this much foreign DNA can have notable caveats. For instance, promoter sequences for downstream genes may be destroyed or novel promoter sequences may be created by inserting *gfp* upstream of a gene, resulting in unanticipated gene products or altered expression of downstream genes. Also, antibiotic resistance cassettes have also been shown to affect fitness (232).

Ideally, deletion of a gene would be complete and leave no antibiotic resistance cassette. In *E. coli*, clean deletions can be performed by sequential allelic recombination events. In the first recombination, a suicide plasmid is designed to carry a cassette containing a positive selection marker, such as *bla*, and a negative selection marker, such as *sacB* (266), that is flanked by homologous sequence to the gene that is being deleted. After the *E. coli* is transformed with the suicide plasmid carrying the cassette, successful recombinants are selected for with ampicillin. In a second recombination event, a second suicide plasmid containing the desired sequence at that location flanked by homologous sequence is then transformed into the *E. coli bla-sacB* mutant generated from the first transformation. This sequence could simply be a clean deletion of the gene by joining of

sequence between the up- and downstream genes or be some derivative of the gene of interest, such as a catalytically inactive allele. Recombinants are selected for by growth in high sucrose media.

SacB expression is unlikely to act as a negative selection marker in *Chlamydia* spp., since the bacteria are intracellular and the high sucrose levels needed for selection are likely toxic to the host cells. However, it may be possible to engineer a selection cassette that contains *bla* and a TS allele. Because the genes identified in this screen are functional at 37°C, it is possible that additional expression of these would be detrimental to the fitness of the organism. We were unable to isolate stable transformants of six different TS alleles that were under the control of a Tet-On promoter in a pASK vector (data not shown). One possible reason for this is that the tet promoter is leaky as demonstrated by the presence of low levels of GFP from the pASK-GFP control vector even in (anhydro)tetracycline-free conditions (data not shown). Thus, overexpression of the tested TS alleles in the absence of induction may be detrimental even at 37°C. Development of tighter expression control systems may allow for direct assessment of dominant negativity of the mapped TS alleles. Alternatively, overexpression of the TS alleles may not be as severe if these were located on the chromosome. Quantification of shuttle vector copy number of a similar plasmid (pBR325::SW2) indicated that there are 16-19 plasmids/genome (92). However, only one copy of the marker would be present if inserted into the chromosome.

Section III: Understanding how DNA Replication impedes Development

Entry into the cell cycle

Previous studies showed that genome replication begins by 6 hpi (27), and our work shows that replication begins prior to 12 hpi (Figure 11). The inability to replicate the genome does not become lethal until mid-development. DNA replication can still be rescued at later time points even though immunofluorescence microscopy shows an absence of mature inclusions for infections shifted from 40°C to 37°C at 18 hpi (Figure 12 and 13). The temperature shift assays performed in this work were all stopped at the same time post-infection (34 hpi). One possibility for the discrepancy between the genome copy number and microscopy results is that if no genomes are replicated and the differentiated RB sits idly for 18 hpi or longer, then shifting to 37°C for the remaining 16 hours or less may not be enough time to generate sufficient RB populations that would subsequently result in inclusion expansion. To test this possibility, the temperature shift assays could be modified so that, after various amounts of time at 40°C, an equivalent amount of time would be spent at 37°C, such as 24 h post shift, to standardize the time for genome replication. This would allow an equivalent amount of time for cell division and inclusion expansion to occur in infections that are shifted later in development. Constant time at 37°C would allow for distinguishing between if growth at 40°C is truly lethal or if a period of lag time before re-entry into the normal cell cycle is responsible for the smaller inclusion size and minimal genome replication for infections shifted from 40°C to 37°C at 18 hpi.

TEM micrographs suggest that the EB-RB transition is completed by 32 hpi. However, the RBs have an aberrant morphology, which is characteristic of stress (Figures

15B-H). Whether these RBs have initiated *de novo* transcription or translation due to the lack of DNA replication is unknown. Temperature sensitive mutants of various DNA replication proteins in *E. coli* were identified in the 1970s by screening for the lack of radiolabeled thymine incorporation into the DNA despite the incorporation of radiolabeled leucine into the proteins of cells (236). A similar strategy could be employed here to determine if *dnaE*^{ts} is still synthesizing protein.

The beginning of the developmental cycle is characterized by the transcriptional upregulation of several early genes including *euo*, *omcA*, and the histone-like proteins. The activation of these genes could be assayed by qRT-PCR in both *dnaE* and *dnaE*^{ts} at the end of a typical developmental cycle (i.e., 34 hpi). If these genes are activated, testing of mid-cycle genes (27) should be performed. Mass spectrometry could be used to determine whether these potential defects in transcription manifest at the protein level. For example, the proteome of *dnaE*^{ts} at 40°C by 18 hpi may be characteristic of early development proteins or may be alternatively shifted to reflect upregulation of a stress response.

Requirements to set up a successful niche

Our TEM data suggests that DNA replication is required to protect the inclusion from host clearance mechanisms (Figure 15). Some inclusions formed by *dnaE*^{ts} at 40°C appeared to be in the process of being cleared (Figures 15G and 15H). The localization of both host and bacterial proteins by immunofluorescence microscopy could be studied to clarify if an active clearance mechanism is activated. Specifically, because of the numerous vacuoles, autophagic markers from the host, such as LC3, could be localizing to the inclusion. Rab4 and Rab11 have also been shown to interact with the chlamydial

inclusion early in infection, and their recruitment to the inclusion membrane is thought to label the inclusion as a typical endocytic vesicle that can intercept ER derived vesicles (267). In contrast, Rab5 and Rab7, which typically label endosomes destined for lysosomal fusion, are excluded from the inclusion (267). Which, if any, of these proteins is recruited to the inclusion membrane of *dnaE*^{ts} at 40°C by the end of development could be tested by immunofluorescence microscopy.

If secretion of type III secreted effectors that protect the inclusion from lysosomal fusion occurs in *dnaE*^{ts} is unknown. Comparison of inclusion proteomes (268) in the mutant versus its isogenic recombinant at 40°C could define what virulence factors are necessary to avoid clearance. Attempts to stain for IncA, which is normally secreted beginning at 10 hpi (269), were unsuccessful for L2-GFP inclusions grown at 40°C (data not shown). Since IncA is only required for homotypic fusion of inclusions and our assays were carried out at MOI <1, the absence of IncA would be predicted to have little, if any, effect on growth. Whether IncA is not secreted at 40°C or if the epitope is not in the proper conformation for antibody recognition is not known. Antibodies to other, earlier Incs (e.g., IncDEFG) (270) may be alternative options to stain inclusions to measure inclusion size.

Protein structure and function

The mechanism behind DNA replication inhibition in *dnaE*^{ts} at 40°C is unknown. The functions of the various DnaE domains have been investigated in model organisms. One approach to understanding the defect in *dnaE*^{ts} is to compare the function of mutant replisomes reconstituted using recombinant *Ct*DnaE or *Ct*DnaE^{P852S}. While all 20 protein components of the *E. coli* replisome are now commercially available, whether *Ct*DnaE is

compatible with the *E. coli* proteins is unknown. This could be quickly tested by ectopic expression of *Ct*DnaE in a conditional *dnaE* knock out strain of *E. coli* (such as dna*E486*) before further investing in *in vitro* complex formation studies, since purification of all the chlamydial components could prove challenging.

The ability of the mutant to polymerize DNA from a plasmid template in the presence and absence of the β-clamp *in vitro* at 37°C and 40°C would be of particular interest because P852S is in the β-clamp binding domain. The size of the resulting DNA fragments produced could be analyzed by gel electrophoresis. If $DnaE^{ts}$ is capable of binding to the β-clamp, longer DNA products should be produced. However, if $DnaE^{ts}$ cannot bind the β-clamp, processivity should be lost and short (~100 bp) DNA fragments should be present. If $DnaE^{ts}$ cannot bind DNA at all, no DNA product will be produced in the presence or absence of the β-clamp. Another possibility is that $DnaE^{ts}$ is functional, but has a drastically decreased polymerization rate. Single-molecule polymerization rates of DnaE versus $DnaE^{ts}$ could be determined using DnaE attached to a lipid bilayer in a flow cell and monitoring the quantity and length of DNA product produced in real time (271).

The interaction of $DnaE^{ts}$ with the β-clamp could be confirmed with fluorescence anisotropy experiments to verify if the β-clamp is able to bind at 40°C. A reaction of fluorescently labeled recombinant DnaE or $DnaE^{P852S}$, oligonucleotide "template", and the β-clamp could be combined and heated to 40°C. The amount of spin could then be measured. Since all reaction components would be expected to bind DnaE, a slower spin speed would be expected upon addition of the oligonucleotide and β-clamp, whereas a

relatively higher speed would be expected for the mutant if the β-clamp and/or the oligonucleotide did not bind.

The inability of DnaE^{ts} to bind to either the DNA template or the β-clamp could be due to denaturation of the protein at 40°C. Circular dichroism studies could be used to test if DnaE^{P852S} denatures at 40°C. These studies could provide insight into whether the mutation causes localized misfolding (i.e., only the β-clamp binding domain) or if more extensive structural changes are present based on the amount of α-helical character that is lost.

A previous suppressor screen for *Ec*DnaE has been performed (272). The D430K dominant negative mutant parent they used was capable of binding to the DNA template, but could not elongate (273). Five distinct suppressors that allowed for elongation were found in the editing (PHP), OB-fold, and β-clamp binding domains (272), although none of these directly corresponds to our suppressors. It may be possible to generate additional suppressors of *dnaE^{ts}* in other domains by screening larger populations. Finding suppressors for *Ct*DnaE has been logistically challenging, but, if *Ct*DnaE can fully substitute for *Ec*DnaE function and still remain temperature sensitive, these screens could be performed in *E. coli* to discover more telling suppressor mutants to further investigate the nature of the P852S defect. Performing this suppressor screen in parallel with *E. coli dnaE486* (*Ec*DnaE^{S885P}) could potentially reveal similar suppressors, since P852 and the residue analogous to *Ec*DnaE^{S885} in *Ct*DnaE (A922) potentially interact.

We identified two distinct DnaE^{P852S} suppressors (DnaE$^{D828Y\ P852S}$ and DnaE$^{P852S\ E1061K}$) that rescued DNA replication. As a precautionary measure to interpretation of these suppressors, whole genome sequencing should be performed. Although it is

unlikely that both an intragenic and extragenic suppressor appeared in the same strain, this cannot be excluded. Sequencing of the suppressor strains is also important since *E. coli dnaE486* had an increased rate of spontaneous mutation (237).

A better understanding of how DnaE$^{D828Y\ P852S}$ and DnaE$^{P852S\ E1061K}$ function could be explored using the fluorescent anisotropy and circular dichroism experiments described above.

Our TS screen identified three other strains with mutations in DnaE, although the TS alleles have not been mapped for these strains. Mutations in *dnaE* of HS 8 and HS 25 (DnaE^{A58T} and DnaE^{L89F}, respectively) are predicted to fall within the PHP domain that is responsible for proofreading and interactions with the ε and θ subunits that heighten proofreading activity. The mutation in *dnaE* from HS 16 (DnaE^{P367L}) is predicted to fall in the palm domain, which contacts the DNA template. If the TS allele in any of these three strains maps to *dnaE*, then further investigation of how DnaE functions during the developmental cycle could be gleaned by suppressor analysis of these mutants.

Relationship between DNA replication and protein synthesis in development

The existence of small inclusions that rarely contain typical RBs or that display abnormal inclusion membrane morphology in *dnaE^{ts}* at 40°C suggests that DNA replication machinery must be functional to maintain bacterial and inclusion membrane morphology (Figure 15). This same morphology is not seen in *gltX^{C1549T}* at 40°C (Figure 23), suggesting that DNA replication is required to maintain inclusion integrity, while protein synthesis is not. Temperature shifts from 37°C to 40°C also indicated that inhibition of protein synthesis via GltX is not as detrimental as inhibition of DNA

replication via DnaE (Figures 13 and 22). In both cases, genome replication ceases (Figures 11 and 21), but whether there is a difference in the transcriptome or proteome of these mutants that mediates these phenotypic differences remains to be explored by RNAseq.

The mechanism for cessation of DNA replication in cells treated with the *uhpC* inhibitor KSK120 likely differs from when the DNA polymerase is non-functional, since the same phenotypes were not observed for either $dnaE^{ts}$ and $gltX^{ts}$, which are both impaired for genome replication at 40°C. Inclusions of *C. trachomatis* serovar L2 treated with KSK120 contain normal RBs (125), but $dnaE^{ts}$ inclusions at 40°C contain RBs that appear stressed (Figure 15). Thus, the aberrant RB morphology characteristic of some of the $gltX^{ts}$ RBs at 40°C (Figure 23) and persistent inclusions from IFN-γ treated cells (228) may be dependent on active DNA replication. Whether aberrant RBs form in persistence in the absence of DNA replication in other models is unknown, but could be investigated by treatment of persistent cells with chloramphenicol. The lack of cell division during persistence would suggest that DNA replication should otherwise be expendable.

Section IV: Investigation of Protein Synthesis in a GltX Mutant

Protein inactivation

We hypothesize that truncation of GltX either removes important residues for the structural stability of the protein at higher temperatures or removes the binding site for an essential interaction partner at 40°C. If these residues are important for structural

stability, purified recombinant GltX and GltX^{Q487*} could be compared at temperatures from 37°C to 40°C using circular dichroism to detect a decrease in the α-helicity of the proteins, indicating protein denaturation. If the residues are important for an interaction partner, tagged recombinant GltX and GltX^{Q487*} could be used to pull-down these partners from chlamydial lysates that could then be identified by mass spectrometry. We hypothesize that GltX^{Q487*} is destabilized at the high temperatures, since, to our knowledge, no binding partners have been described that bind to the C-terminal region of GltX in other bacteria. Comparison of the discriminating *Ec*GluRS and *Ec*GlnRS indicates that GluRS has a more rigid structure than GlnRS, and GlnRS is thought to have evolved from GluRS after a gene duplication event (274). Evolution of GlnRS to specifically interact with a new substrate is hypothesized to be mediated by a C-terminal domain with looser structure that becomes more structured upon substrate binding (274). It is tempting to speculate that the non-discriminating GltX may represent a compromise between the two discriminating aaRSs. Whether binding of tRNA^{Glu} versus tRNA^{Gln} to a non-discriminating GltX results in different protein conformations in GltX remains to be determined.

Characterization of GltX^{Q487*} expression

A transcriptomic dataset showed that *gltX* transcripts begin to be transcribed by 8 hpi in *C. trachomatis* serovar D (28). We assume that, based on the shorter developmental cycle of serovar L2, expression of *gltX* occurs earlier in our strain. Gene expression of *gltX* in serovar L2 could be determined by qRT-PCR at 0, 2, 6, 8, 12, 18, 24, and 34 hpi. Our modeling studies suggest that GltX is truncated, but what, if any, effect this has on transcription at 37°C is unknown. Therefore, *gltX*^{ts} and *gltX*^{WT} should

also be assayed at both the permissive 37°C and the non-permissive 40°C to investigate whether the transcript is still stable throughout development.

EBs are generally not regarded as being metabolically active. EBs can take up glucose in anexic media, but glucose uptake was unable to drive EB to RB differentiation (31,32). What drives the differentiation event and what players are required has not been determined. Both proteomic and transcriptomic profiles show evidence for temporal expression of proteins and genes, respectively. There is also overlap between the proteomes of EBs and RBs despite the former being metabolically inactive (198-200). One possibility for the difference in metabolism of EBs and RBs, despite the presence of a core set of proteins involved in metabolism, is differential post-translational modifications (PTMs) such as phosphorylation (201). PTMs would support the quick activation (or inactivation) of proteins during differentiation. For example, the aaRSs may be phosphoregulated during development. Phosphopeptides from two aaRSs were found in a global phosphoproteome study of *C. caviae* (201). How any developmental cycle-linked kinase-phosphatase system is regulated and what its substrates are in chlamydia is unknown. Targeted phosphoprotein studies of aaRSs, including GltX, could elucidate whether phosphorylation of aaRSs plays a role in the EB-RB and/or RB-EB transitions. Antibodies to chlamydial aaRSs could be developed, and the presence of a post-translational modification in EBs could be seen by the presence of a doublet by western blot and confirmed by mass spectrometry of the protein bands.

Advances in genetic manipulation of *C. trachomatis* may allow for investigation of GltX function *in vivo* using tagged versions of these proteins that can be inserted into the chromosome by allelic recombination. Attempts to generate a strain with GltX-

FLAG were unsuccessful. Sequence corresponding to *gltX* and ~2 kb upstream of the 5' end of *gltX* was amplified and a C-terminal FLAG tag and ~2kb downstream of *gltX* was added by fusion PCR. This sequence was then inserted into pUC18 for expression in *E. coli*. However, no *E. coli* clones containing the entire insert were identified, and the *E. coli* colonies that did emerge grew extremely slowly, suggesting that the insert was toxic. Whether toxicity was due to overexpression of *Ct*GltX or expression of the chlamydia-specific transcription factor *euo*, a conserved chlamydial hypothetical protein *ctl0704*, or the cysteine-rich outer membrane protein *omcA* that were contained in the ~± 2 kb flanking *gltX* is unknown. Because an intact vector could not be isolated from *E. coli*, we could not transform it into $gltX^{ts}$ and select for recombinants. Future attempts to generate the FLAG-tagged mutant may include using shorter flanking regions of DNA homology that do not encode any promoters of neighboring genes to avoid toxicity in *E. coli*. More sophisticated genetic manipulation strategies to allow for ectopic expression of *gltX* while the endogenous copy is inactivated and replaced with a FLAG-tagged allele using allelic recombination could be attempted if a conditional mutant is not available for transformation.

Determination of available protein synthesis substrates

We hypothesize that $tRNA^{Glu}$ and/or $tRNA^{Gln}$ are not being aminoacylated in $gltX^{ts}$. The aminoacylation status of tRNAs in EBs can be directly probed using northern blots (275). An attached amino acid causes an approximately 100 dalton shift in the size of the tRNA that can be visualized when probing for the tRNA. The ratio of aminoacylated to non-aminoacylated tRNA can then be calculated. We have attempted to perform these blots, and have been unsuccessful at detecting the three tRNAs being

probed: $tRNA^{Met}$ (the control), $tRNA^{Glu}$, and $tRNA^{Gln}$. An alternative approach to address this question is the use of a chlamydial tRNA microarray to compare levels of aminoacylated tRNAs (276). In this assay, the 3'-OH of non-aminoacylated tRNAs are destroyed with periodate, and the aminoacylated tRNAs are then deacylated and labeled with Cy3 since their 3'-OH is functional. This sample is then compared to an identical sample representing the total number of tRNAs that has been deacylated to remove any attached amino acids before the labeling with Cy5. The relative amount of a given aminoacyl-tRNA can then be calculated as a ratio of Cy3-labeled to Cy5-labeled tRNA. Because aminoacylation levels of individual tRNA isoacceptors in chlamydia have not been previously described, this method also has the advantage of being non-biased since individual chlamydial tRNAs do not have to be used as controls. Currently, we must make the assumption that *gltX*^{ts} does not alter global aminoacyl-tRNA levels of EBs harvested at 37°C when selecting controls for northern blot analysis.

The functionality of tRNAs as protein synthesis substrates can also be investigated *in vivo* using polysome profiling assays (277). These assays use a sucrose gradient to separate ribosomal subunits, monosomes, and polysomes into fractions. The RNA in these can either be detected based on absorbance at 254 nm or by qRT-PCR. High protein synthesis rates produce multiple, strong polysome peaks; low protein synthesis rates produce weak, if any, polysome peaks and instead have an abundance of ribosomal subunits and monosomes (277). Therefore, we hypothesize that *gltX*^{ts} would have much fewer polysomes when grown at 40°C compared to at 37°C. Furthermore, if the truncation of $GltX^{ts}$ causes mischarging of tRNAs, protein synthesis should gradually decrease throughout development as toxic proteins accumulate in the cell.

Infection with *C. trachomatis* increases the amount of free amino acids in HeLa cells (Matthew M. Muramatsu, unpublished data). Whether this increase is in the host cell, the bacteria, or both has not been determined, but the increase in free amino acids could suggest that chlamydia may recruit amino acids at a rate that increases host cell production of amino acids. In *E. coli*, amino acid poor conditions activate the stringent response. While this response affects many bacterial processes, one outcome is the expression of biosynthetic genes for amino acids. In *C. trachomatis*, treatment of HeLa cells with IFN-γ induces persistence (278). IFN-γ causes a reduction of the host tryptophan pool, thus starving chlamydia for this amino acid (279). By expressing tryptophan synthase (TrpAB), chlamydia is able to synthesize tryptophan from indole and serine to survive in a viable but non-cultivatable state (280).

Whether a more general stress pathway akin to the stringent response is activated when a particular amino acid is missing in chlamydia is unknown. Both protein and RNA synthesis decreased in an *E. coli valS*^{ts} mutant at the non-permissive temperature, and deletion of *relA*, which synthesizes (p)ppGpp, restored RNA but not protein synthesis (281). While studies of tryptophan starvation give some clues as to how chlamydia respond to amino acid stress, they also require the use of IFN-γ, which alters many facets of the host cell environment (282).

The *gltX*^{ts} mutant could be used to directly investigate how amino acid starvation impacts chlamydia. RNAseq studies comparing the differences in gene expression at 40°C in *gltX*^{ts} and *gltX*^{WT} could identify genes that are alternatively regulated when either aminoacylated tRNA^{Glu} and/or tRNA^{Gln} are absent. These results could be compared to IFN-γ treatment (204) to determine if there is any overlap in the responses. Additionally,

this data would answer whether there is a coordinated downregulation of genes involved in translation—from tRNAs to the ribosome—when the necessary protein precursors are lacking as seen in other organisms, and potentially uncover a chlamydial amino acid stress response akin to the stringent response.

APPENDIX I: Generation of *C. trachomatis* x *C. muridarum* Chimeras

Power of LGT to investigate homolog functionality between species

C. muridarum and *C. trachomatis* have similar genomic synteny and share high nucleotide sequence identity; however, they exhibit distinct host and tissue tropisms. No pathogenicity islands have been described for chlamydia, although the plasticity zone was hypothesized to contribute to tropism and protect from immune clearance (283). Determining the genes that mediate host and tissue tropism are of interest, since these could serve as targets for vaccine or pharmaceutical intervention.

Genes that mediate chlamydial host and tissue tropism could potentially be identified by comparison of interspecies chimeras. Previous studies used positive selection LGT to generate chimeras, but the phenotypes of these chimeras have not been fully described, nor have they been tested in animal models. Genetic manipulation is far more advanced in *C. trachomatis* serovar L2 than *C. muridarum*, so most genetically engineered strains have only been assayed in cell culture models. Only a few *C. muridarum* mutants have been tested in the mouse model, including chlamydial plasmid variants (97,284), multiply mutated EMS mutants (90), and an *incA* knock out strain (285).

The genes required for differences in chlamydial tropism and pathogenesis are largely unexplored. For example, which genes allow L2 to become systemic? Which *C. muridarum* genes are important for sustained infection in the mouse model, and why do the *C. trachomatis* homologs not allow this? Generation of chimeric *C. trachomatis* and *C. muridarum* strains by LGT could address these questions; however, these studies are

not in the literature. We suspect that the inherent fitness defects of strains carrying the endogenous antibiotic resistance markers may have confounded interpretation of studies using these chimeric strains. Antibiotic driven LGT is also limited by the location of the genes that become resistant to the antibiotic on the chromosome. Thus, the closer a gene is to the antibiotic marker, the more likely the gene is to co-segregate, which leads to biased populations of recombinants. Since we were able to isolate recombinants using negative selection LGT, which does not introduce additional fitness defects, we wondered if we could use this strategy to generate *C. trachomatis* x *C. muridarum* chimeras.

Generation of *C. trachomatis* serovar L2 x *C. muridarum* (L2 x MoPn) chimeras

Previous work in our lab identified two *C. muridarum* TS mutants from an EMS-mutagenized plaque library that exhibited greater than 50-fold reduction in mature inclusion formation by LPS staining (Shuai Hu, unpublished data). Whole genome sequencing revealed that *Cm*HS 1 had 21 mutations while *Cm*HS 2 had 15 mutations (Table 10). Using phenotypic linkage analysis, the TS allele in *Cm*HS 1 was narrowed down to either $tc0238^{G127A}$ resulting in a G43R substitution in a hypothetical protein or $rpoB^{C3091T}$ resulting in a R1031C substitution in RNA polymerase subunit B (Figure 28). The identity of *Cm*HS 2 has been narrowed down to eight mutations that fall into proteins of diverse functions and are summarized in Figure 28. An additional set of isolates from a *Cm*HS 2 and an interferon-gamma sensitive mutant (*igs4*) confirmed that one of the eight remaining mutations should confer temperature sensitivity, but did not further decrease the number of candidate TS alleles (Amanda M. Giebel, unpublished data).

Table 10 Genome sequences of *C. muridarum* HS mutants

Reference Position	Nucleotide Change	Amino Acid Change	Gene	Function
***Cm*HS 1**				
41636	G1012A	G338R	*tc0035*	Hypothetical protein
88645	C878T	S293F	*tc0076*	GTPase Der
141409	+ A		*tc0118*	pseudogene; RNA methyltransferase
142115	C → T		*tc0118*	
182169	G1181A	R394K	*tc0149*	hypothetical protein
194644	C289T	P97S	*tc0160*	hypothetical protein
234843	G211A	G71R	*tc0199*	hypothetical protein
278107	G127A	G43R	*tc0238*	hypothetical protein
432812	G859A	E287K	*infB*	translation initiation factor IF-2
459068	C170T	A57V	*rpe*	ribulose-phosphate 3-epimerase
473544	788ΔT	V264fs	*tc0412*	hypothetical protein
548457	G443A	G148D	*tc0450*	membrane protein
588656	G119A	G40E	*tc0483*	hypothetical protein
651865	C240T		*tc0541*	hypothetical protein
705743	C3091T	R1031C	*rpoB*	DNA-directed RNA polymerase subunit beta
803183	G1301A	G434E	*proS*	proline-tRNA ligase
825043	C → T			
830078	C1922T	T641M	*pmpB/C-1*	polymorphic membrane protein
888570	C → T		*prfB*	peptide chain release factor 2
921114	G2488A	E830K	*polA*	DNA polymerase I
969645	C845T	P282L	*tc0834*	membrane protein
***Cm*HS 2**				
44872	G30A		*sctN*	ATP synthase
58829	A988G	K330E	*ompA*	porin
473675	919ΔC	P307fs	*tc0412*	hypothetical protein
563815	G203A	G68E	*tc0463*	hypothetical protein
625074	G328A	G110R	*pdhB*	pyruvate dehydrogenase subunit beta
709093	G → A			
759833	G768A		*tc0634*	hypothetical protein
772280	C329T	S110F	*aroA*	3-phosphoshikimate 1-carboxyvinyltransferase
839840	C33T		*tc0698*	metal ABC transporter permease
862608	C730T	R244*	*tc0725*	peptidase S41
883628	C137T	T46I	*tc0741*	hypothetical protein
899518	G665A	G222E	*tc0757*	hypothetical protein
978087	C417T		*tc0843*	helicase, Snf2 family
979469	C1799T	P600L	*tc0843*	helicase, Snf2 family
1042365	C270T		*tc0899*	RNA polymerase factor sigma-54

Gene	nt Change	AA Change	*Cm*HS 1	*Cm*HS 2	1[a, b]	2[a, b]	3[a, b]	4[a]
tc0035	G1012A	G338R						
sctN	G30A							
ompA	A988G	K330E						
tc0076	C878T	S293F						
tc0118	+ A							
tc0118	C → T							
tc0149	G1181A	R394K						
tc0160	C289T	P97S						
tc0199	G211A	G71R						
tc0238	G127A	G43R						
infB	G859A	E287K						
rpe	C170T	A57V						
tc0412	788ΔT	V264fs						
tc0412	919ΔC	P307fs						
tc0450	G443A	G148D						
tc0463	G203A	G68E						
tc0483	G119A	G40E						
pdhB	G328A	G110R						
tc0541	C240T							
rpoB	C3091T	R1031C						
Intergenic	G → A							
tc0634	G768A							
aroA	C329T	S110F						
proS	G1301A	G434E						
Intergenic	C → T							
pmpB/C-1	C1922T	T641M						
tc0698	C33T							
tc0725	C730T	R244*						
tc0741	C137T	T46I						
prfB	C → T							
tc0757	G665A	G222E						
polA	G2488A	E830K						
tc0834	C845T	P282L						
tc0843	C417T							
tc0843	C1799T	P600L						
tc0899	C270T							

Figure 28 Mapping of TS alleles in *C. muridarum* crosses. *Cm*HS 1 and *Cm*HS 2 were crossed using negative selection LGT. Four clonal progeny strains from independent crosses were isolated and their genomes were sequenced. Genes are listed in the order that they appear on the chromosome. Black boxes indicate the presence of the wild type allele. Purple boxes indicate the presence of the mutant allele from the *Cm*HS 1 parent. Red boxes indicate the presence of the mutant allele from the *Cm*HS 2 parent. *a*, additional mutations: G at genome coordinate 126406 is deleted and an A is inserted at genome coordinate 126416. *b*, additional C→T mutation in *tc_r02* at nucleotide 1464.

The crosses to generate interspecies chimeras were performed prior to knowing the genome sequences of the *C. muridarum* TS mutants, so *C. trachomatis* parents were selected so that the L2 TS allele would occur in different locations throughout the genome. Where multiple mapped HS alleles clustered, mutants with the strongest phenotype were selected. Six *C. trachomatis* parents were crossed with both *Cm*HS 1 and *Cm*HS 2 (Figure 29).

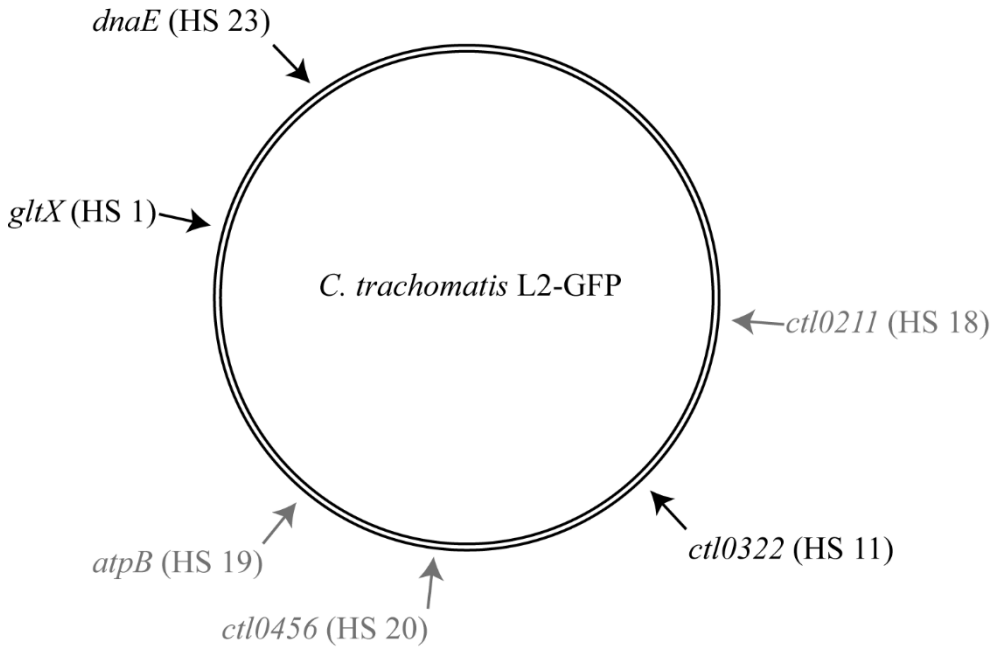

Figure 29 L2 parents used in L2 x MoPn crosses. Six mapped L2-GFP TS mutants were selected as parents for crosses with MoPn because the mapped TS alleles were dispersed throughout the genome. Arrows indicate the location of the mapped allele in the genome. Temperature resistant progeny was recovered from mutants in black type, while all progeny tested from crosses in mutants in gray type remained temperature sensitive.

Generation of L2 x MoPn crosses using negative selection LGT

Five independent wells of each cross between the six L2 and two MoPn isolates were attempted. The strains were allowed to recombine at 37°C until 34 hpi in McCoy cells. The media was then aspirated and replaced with 500 μL of SPG, and the infection was frozen at -80°C. 20 μL of thawed lysate was used to infect a fresh monolayer of McCoy cells followed by incubation at 40°C for 34 hpi before harvesting. Selection was repeated a second time. The number of inclusions present in L2 x MoPn cross wells tended to be lower than in wells with L2 x L2 or MoPn x MoPn crosses, although control wells containing either L2 or MoPn parents only showed greater decreases in inclusion number compared to the L2 x MoPn crosses (personal observation), suggesting that recombination at an interspecies level is rarer than with intraspecies crosses.

Not all wells produced progeny. Progeny from positive wells were clonally isolated by plaque cloning. The plaques were screened for temperature resistance by staining for LPS in replica plates grown at either 37°C or 40°C for 34 hpi and fixed with formaldehyde. A maximum of two isolates from each well were pursued: one that would be predicted to be an L2 recipient because it was GFP^+ and one that would be predicted to be an MoPn recipient because it was GFP^-. These plaqued populations were subjected to a second round of clonal isolation and expanded. Only three of the TS L2 strains (HS 1, HS 10, and HS 23) produced recombinants with the TS MoPn strains.

Genotyping the recombinants

Initial attempts to distinguish if a recombination event occurred relied on PCR. Since the TS allele was not mapped for the MoPn strains, the TS alleles of the L2 strains

were targeted. L2- or MoPn-locus specific primers were designed to produce approximately 700 bp amplicons. Each locus was amplified with both sets of primers, and three loci throughout the genome were assayed, however MoPn primers tended not to amplify any product despite being able to amplify specific product from wild type MoPn DNA (data not shown). We therefore turned to using whole genome sequencing of nine strains believed to phenotypically be recombinants.

Confirmation of chimera generation

A draft genome sequence for the HS 1 x *Cm*HS 2 chimera was assembled. Predicted gene coding sequences were aligned to either *C. trachomatis* serovar L2 434/Bu or *C. muridarum* Nigg reference genomes (accession numbers: AM884176 and AE002160.2, respectively). Geneious software was used to align the chimera genome sequence to each of the parents. The recombinant was largely L2 based. Interestingly, the C-terminal domain of *C. trachomatis gltX* was repaired with *C. muridarum gltX* sequence, producing a chimeric protein that further confirms that $gltX^{ts}$ is a temperature sensitive allele (Figure 30). The region of recombination extended from nt 862,694 to nt 867,696 of *C. trachomatis* L2 (Figure 30). This equates to a maximal integration of 5,003 bp of *C. muridarum* gDNA into the chimera. There are 5 deletions within the recombined regions that will need to be sequence confirmed. Four of these deletions range from 2-8 nt, and one deletion is predicted to be 74 nt.

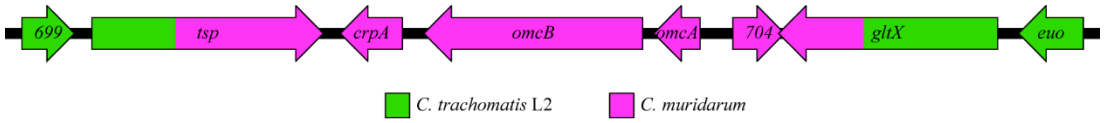

Figure 30 Region of recombination in an HS 1 x *Cm*HS2 chimera. Geneious software was used to find regions of homology between the genome of the chimeric strain and the genomes of *C. trachomatis* L2 and *C. muridarum*. The parental origin of each gene is colored green if originating from *C. trachomatis* or pink if originating from *C. muridarum*. The gene order and content are highly conserved in this locus, so hypothetical genes were labeled according to *C. trachomatis* (*ctl*) locus number. The recombination event produced chimeric Tsp and GltX proteins. No other regions of recombination were observed.

Because recombination produced two chimeric proteins, protein sequence alignments were performed for both Tsp (Figure 31) and GltX (Figure 32). The *Ct*Tsp and *Cm*Tsp homologs share 89.7% identity, while *Ct*GltX and *Cm*GltX share 94.6% identity. Recombination at nucleotide position 815 produced the chimeric *tsp* allele, which occurs in the second position of the codon that would code for alanine in *Ct*Tsp (Figure 31A). Tsp degrades proteins with nonpolar amino acid termini in *E. coli* (286) and begins to be transcribed 16 hpi in *C. trachomatis* serovar D (28). This chimeric Tsp is likely fully enzymatically active, since the proteolytic domain is completely derived from *C. muridarum* (Figure 31B). The PDZ domain is chimeric. Since this is a promiscuous binding domain and there is high homology with *Ct*Tsp, this is unlikely to negatively affect enzymatic function. Interestingly, this domain swap is likely favored due to the *Cm*HS 2 *tsp* (*tc0725*) allele coding for a truncated Tsp of only 243 amino acids in length. The truncation occurs before both the PDZ and proteolytic domains (Table 10 and Figure 31B), so Tsp in *Cm*HS 2 is most likely non-functional. Mapping efforts using *Cm*HS 1 as the other parent did not exclude tsp^{C730T} as the potential TS allele (Figure 28). Based on the region of recombination in this chimera, it is tempting to speculate that *tsp* may be the temperature sensitive allele in *Cm*HS 2.

A

```
L2       MMRFARFCLLVLTLFPQLAFSAEPLRRQDVRKTVDKLVEHHIDTQQISPYILSRSLEDYV   60
MoPn     MKRLARFCLLALTLFPQLAFSSAPLRQQDVRKTVEKLVEHHIDTKHISPHILSRSLEDYA   60
Chimera  MMRFARFCLLVLTLFPQLAFSAEPLRRQDVRKTVDKLVEHHIDTQQISPYILSRSLEDYV   60
         * *:******.**********: ***:*******:*********::***:*********.

L2       RSFDSHKAYLTQDEVFSHAFSEEATHPLFKQYQEDNFSSFKELDTCIQQSISRARERWRSS  120
MoPn     RSFDSHKAYLTQDEVLTYVFSEKATHSLFKQYQEDNFASFRELHTCIQQSISRVREWRTV  120
Chimera  RSFDSHKAYLTQDEVFSHAFSEEATHPLFKQYQEDNFSSFKELDTCIQQSISRARERWRSS  120
         ***************:::.***:*** **********:**:**.*********.****:

L2       WLTDSIRVIQDAMSHTIEKKPSAWASSIEEVKQRQYDLLLSYASIYLEDAAKNRYQGKEH  180
MoPn     WLSDAVRVIQDASSHTIPKKPTTWGSSIEEVKQRQYELLLSYASIYLEDATKNRYQGKEH  180
Chimera  WLTDSIRVIQDAMSHTIEKKPSAWASSIEEVKQRQYDLLLSYASIYLEDAAKNRYQGKEH  180
         **:*::****** **** ***::*.**********:**********:*********

L2       GLVKLCIRQIENHENPYIGINDHGYRMSPEEEANSFHVRIIKSIAHSLDAHTAYFSQEEA  240
MoPn     ALVRLCIRQIENHENPYIGINDHGLKMSLEEEANSFHIRIIKSIAHSLDAHTAYFSKEEA  240
Chimera  GLVKLCIRQIENHENPYIGINDHGYRMSPEEEANSFHVRIIKSIAHSLDAHTAYFSQEEA  240
         .**:******************** :** ********:******************:***

L2       LSMRAQLEKGMCGIGVVLKEDIDGVVVKEVLAGGPADKTGSLRVGDIIYRVNGKNIENTP  300
MoPn     LSMRAQLEKGMCGIGVVLKEDIDGVVVKEVLPGGPADKTGSLRVGDIIYRVNGKNIENTP  300
Chimera  LSMRAQLEKGMCGIGVVLKEDIDGVVVKEVLAGGPADKTGSLRVGDIIYRVNGKNIENTP  300
         ******************************** ****************************

L2       FPGVLDSLRGSPGSSVTLDIHRQNNDHVIQLRREKILLDSRRVDVSYEPYGNGIIGKITL  360
MoPn     FPGVLDSLRGLPGSSVTLDIHRQNNDHVVQLRREKILLDSRRVDVSYEPYGDGIIGKITL  360
Chimera  FPGVLDSLRGLPGSSVTLDIHRQNNDHVVQLRREKILLDSRRVDVSYEPYGDGIIGKITL  360
         ********** ****************:**********************:********

L2       HSFYEGENQVSSEQDLRKAIRELQEKNLLGLVLDIRENTGGFLSQAIKVSGLFLTNGVVV  420
MoPn     HSFYEGENQISSEQDLRRAIRELQEKNLLGLVLDIRENTGGFLSQAIKVSGLFLTNGVVV  420
Chimera  HSFYEGENQISSEQDLRRAIRELQEKNLLGLVLDIRENTGGFLSQAIKVSGLFLTNGVVV  420
         *********:*******:*******************************************

L2       VSRYADGSVKRYRTISPQKFYDGPLAVLVSKSSASAAEIVAQTLQDYGVALIVGDQQTYG  480
MoPn     VSRYADGSVKRYRTISPQKFYDGPLAVLVSKSSASAAEIVAQTLQDYGVALIVGDKQTYG  480
Chimera  VSRYADGSVKRYRTISPQKFYDGPLAVLVSKSSASAAEIVAQTLQDYGVALIVGDKQTYG  480
         ************************************************************:****

L2       KGTIQHQTITGSNSQEDFFKVTVGRYYSPSGKSTQLEGVKSDIVIPSRYAEDKLGERFLE  540
MoPn     KGTIQHQTITGNNSQEDFFKVTVGRYYSPSGKSTQLEGVKSDIVIPSRYAEDNLGERFLE  540
Chimera  KGTIQHQTITGNNSQEDFFKVTVGRYYSPSGKSTQLEGVKSDIVIPSRYAEDNLGERFLE  540
         **********.****************************************:*******

L2       YALPADQYDNVINDNLGDLDINIRPWFQKYYSPHLQKPELVWREMLPQLAHNSQERLEKN  600
MoPn     YALPADQYENVLNDNLGDLDIHIRPWFQKYYSPHLQKTELTWREMLPQLVENSQQRLEKN  600
Chimera  YALPADQYENVLNDNLGDLDIHIRPWFQKYYSPHLQKTELTWREMLPQLVENSQQRLEKN  600
         ********:**:*********:*************** **.********..***:*****

L2       KNFEIFVQHLKKTNKQDRSFGSNDLQMEESVNIVKDMILLKSISQTPAQ   649
MoPn     KNFEIFVQHLKKTDKQEQSFGSNDLQMEETVNIVKDMILLQTSLRSPAQ   649
Chimera  KNFEIFVQHLKKTDKQEQSFGSNDLQMEETVNIVKDMILLQTSLRSPAQ   649
         *************:**::***********:**********::  ::***
```

B

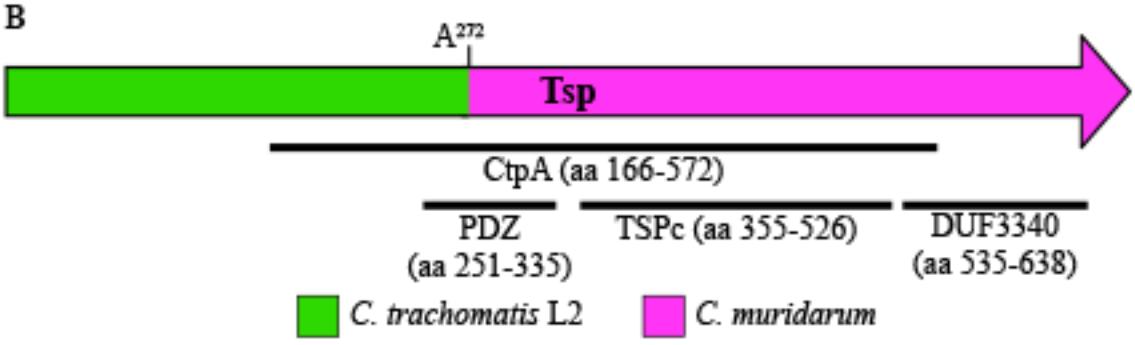

Figure 31 Protein alignment of chimeric Tsp. (A) ClustalO was used to generate a primary sequence alignment of *Ct*Tsp (L2), *Cm*Tsp (MoPn), and the chimeric Tsp. Protein sequence derived from *C. trachomatis* is in black; protein sequence from *C. muridarum* is in gray. Identical residues between *C. trachomatis* and *C. muridarum* are indicated by a *. (B) Schematic of the location of recombination in the protein with major domains labeled according to GenBank.

Because the vast majority of the genomic backbone originates from HS 1, it is interesting that the recombination event occured in the temperature sensitive allele (*gltX*^{C1459T}; GltX^{Q487*}). The recombination event produces a chimeric GltX that is derived from *C. trachomatis* until L345 and *C. muridarum* from W346 (Figure 32A). The chimeric protein contains a predicted catalytic core (residues 5-330) originating from L2, but an anticodon recognition region originating from *C. muridarum* (Figure 32B). Since the chimera is no longer temperature sensitive and since GltX is essential for aminoacylating both tRNA^{Glu} and tRNA^{Gln}, the chimeric GltX must be functional at 40°C. Because of the nearly 95% protein identity and the high likelihood that similar residues would be used to recognize the anticodons of tRNA^{Glu} and tRNA^{Gln} in such closely related organisms, it makes sense that this region could be interchangeable. Since both *C. trachomatis* and *C. muridarum* have "tails" compared to the *M. tuberculosis* (PDB ID 2O5R) and *T. maritima* (PDB ID 3AKZ) structures, the chimeric protein would be predicted to have functionally reverted this truncation.

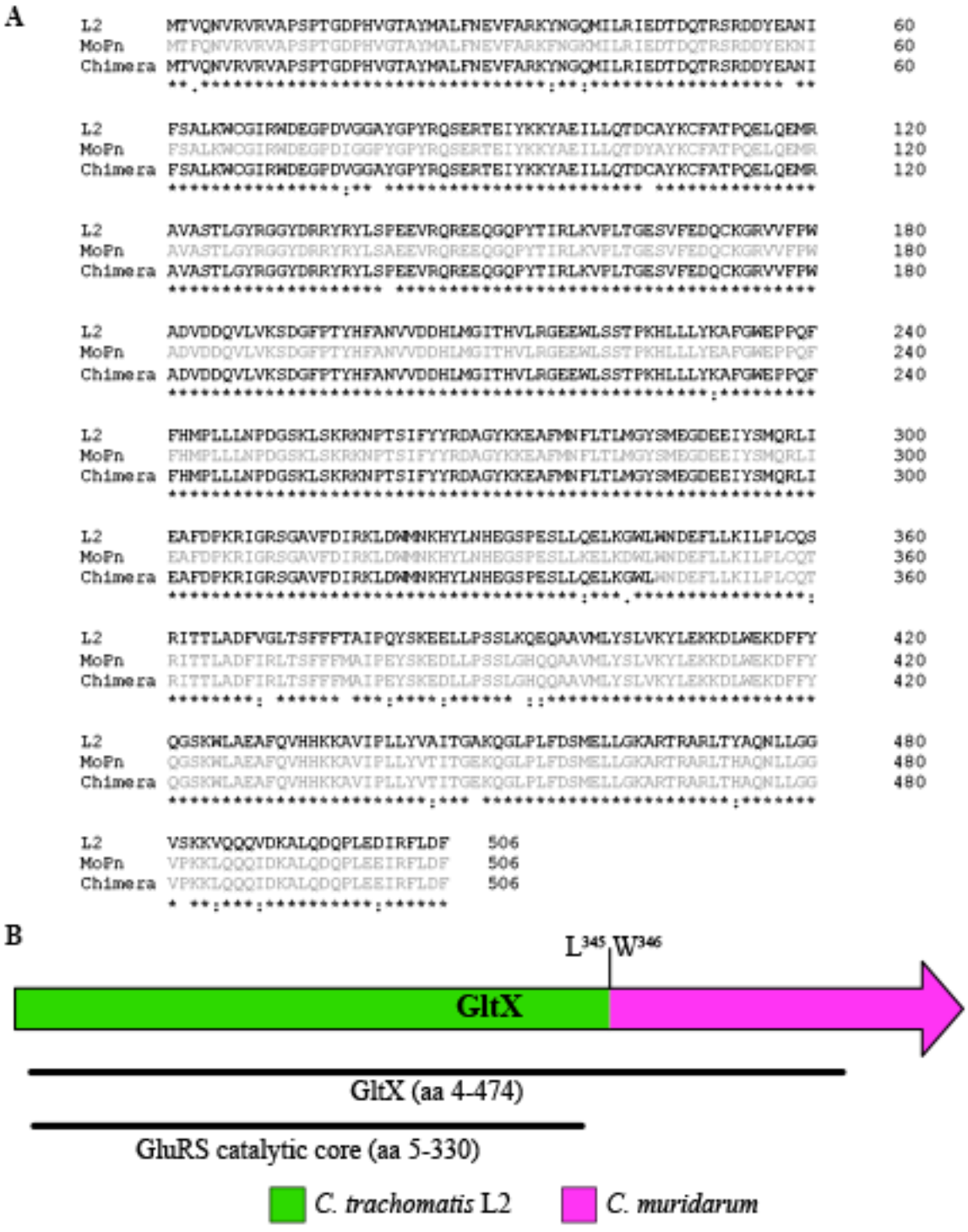

Figure 32 Protein alignment of chimeric GltX. (A) ClustalO was used to generate a primary sequence alignment of *Ct*GltX (L2), *Cm*GltX (MoPn), and the chimeric GltX. Protein sequence derived from *C. trachomatis* is in black; protein sequence from *C. muridarum* is in gray. Identical residues between *C. trachomatis* and *C. muridarum* are indicated by an *. (B) Schematic of the location of recombination in the protein with major domains labeled according to GenBank.

The other *C. muridarum* proteins that are now incorporated into the *C. trachomatis* L2 genetic background are all predicted to localize to membranes. Cysteine rich protein A (CrpA) localizes to the inclusion membrane, is immunogenic in mouse models, and is predicted to have two transmembrane helices (287,288). CrpA is located at the end of and in the same direction as the *omcAB* operon. OmcA and OmcB are known cysteine-rich proteins that are found in the outer membrane. Both are found in appreciable quantities in the COMC (198), which gives *Chlamydia* spp. EBs structural rigidity *in lieu* of peptidoglycan. Increases in CrpA and OmcB at both the transcript and protein levels have been associated with the RB to EB transition in *C. pneumoniae* (289). OmcB has also been found to be the only true substrate of CPAF, which cleaves OmcB in mid-late development (290). CTL0704 is a putative lipoprotein, although nothing is known about its function.

Because of the small area of recombination in the chimera, new studies of how the COMC forms and the important protein interactions within it can be performed. First, the chimeric nature could be confirmed with antibody staining against OmcB. OmcB processing by CPAF has been shown to occur in *C. trachomatis* (290,291) and the C-terminal cleavage fragment is secreted into the host cytoplasm (291). While CPAF from both *C. trachomatis* and *C. muridarum* can cleave the same cytoskeletal proteins in HeLa cells lysed in an SDS-based buffer (data not shown), whether *Ct*CPAF can act on *Cm*OmcB has not been shown. OmcB is the second most prevalent COMC protein and is highly immunogenic (292). Conservation of OmcB sequence across medically relevant *Chlamydia* spp. has resulted in high serocrossreactivity (292). *Ct*OmcB and *Cm*OmcB share 89.9% amino acid identity, so it is possible that there would be no effect on

seroreactivity to the *C. muridarum* OmcB peptide unless key differences exist at the cleavage site that would prevent its release. Additionally, inhibition of CPAF, and therefore OmcB processing, led to decreases in progeny production (290). The ability of the chimera to produce progeny has not yet been evaluated.

Alternatively, the composition of the COMC may be altered by the inclusion of *C. muridarum* proteins. Since the rigidity of the structure is dependent on the interprotein disulfide linkages of the COMC proteins, it may be that *Cm*OmcA and *Cm*OmcB make altered contacts with the other *Ct*COMC proteins, such as major outer membrane protein (MOMP). Alterations in COMC structure could be probed with atomic force microscopy.

Interactions with both host- and chlamydial-derived heparan sulfates is mediated at least in part by OmcB. OmcB isoforms from different *C. trachomatis* serovars have varying dependencies on OmcB to bind to heparin or heparan sulfate. For example, OmcB of *C. trachomatis* serovar E (293) or serovar B (294) do not bind heparan sulfate, whereas OmcB from *C. trachomatis* serovar L2 does despite only differing by 11 out of 553 residues compared to either the serovar E or B homologs. The ability to interact with heparan sulfate is even stronger for *C. pneumoniae* OmcB and this interaction was maximal in the presence of both heparin binding motifs (XBBXBX) and a proline that is in the immediate vicinity C-terminal of these motifs (293,295).

The ability of *Cm*OmcB to interact with host cells has not been well described. One study found that *C. muridarum* infection increases 6-*O*-sulfation of heparan sulfate via decreased expression of the heparan sulfate proteoglygan-specific endosulfatase SULF2 and this results in higher levels of attachment and entry (296). Furthermore,

intranasal infection in a murine pneumonia model with *C. muridarum* using *sulf1*$^{-/-}$*sulf2*$^{-/-}$ mice showed a 25-fold increase in the number of progeny collected from the lung (296). Thus, host expression of heparan sulfates plays an important role in chlamydial pathogenesis.

The role of *Cm*OmcB in murine infection and its ability to interact with heparan sulfates has not been investigated. OmcB isoforms are highly similar (297) especially in the C-terminal domains. An alignment of the N-terminal residues of *Ct*OmcB and *Cm*OmcB indicated that the heparin binding motif is perfectly conserved (Figure 33). The downstream proline conferring heparan sulfate binding dependence in serovar L2 versus independence in serovar E (293) is not conserved in *C. muridarum*. Since binding to heparin sulfate is through electrostatic interaction, it is also of note that the predicted pI of *Ct*OmcB is 8.4 versus 6.62 of *Cm*OmcB, indicating that *Ct*OmcB is a more basic protein, and this difference is present in the extracellularly exposed N-terminal domain.

```
L2      MRIGDPMNKLIRRAVTIFAVTSVASLFASGVLETSMAEFISTNVISLADTKAKDNTSHK-      59
MoPn    ------MNKLIRRAVTIFAVTSVASLFASGVLETSMAESLSTNVISLADTKAKETTSHQK      54
              ****************************** :*************:.***:

L2      SKKARKNHSKETPVNRKKVAPVHESKATGPKQDSCFGRMYTVKVNDDRNVEITQAVPKYA      119
MoPn    DRKARKNHQNRTSVVRKEVTAVRDTKAVEPRQDSCFGKMYTVKVNDDRNVEIVQSVPEYA      114
        .:******.::.* * **:*: *:::**. *:******:**************.*:**:**
```

Figure 33 OmcB sequence alignment. Protein sequences of OmcB from *C. trachomatis* serovar L2 and *C. muridarum* Nigg were aligned using ClustalO. The positively charged residues are colored blue and, in the case of the XBBXBX heparin binding motif (residues 63-68 in L2 and 58-63 in MoPn), are bolded. The ability of OmcB to bind heparan sulfate was found to be mediated by proline-72 (293) and this residue is underlined for L2.

Future studies with this chimera should focus on biochemical characterization of *Cm*OmcB to bind heparin in comparison to *Ct*OmcB (293-295,298). Growth kinetics

will also need to be studied to determine how compatible the *C. muridarum* locus is with *C. trachomatis*. Studying the binding properties of OmcB isoforms has relied on the expression of various OmcB constructs in *E. coli* (298) or *Saccharomyces cerevisiae* (293) and evaluating if the ability of these recombinant organisms to bind host cells was altered. This chimera permits comparison of different OmcB isoforms in a largely conserved genetic background for the first time.

Murine female genital infection models using *C. trachomatis* are limited to studies involved in the acute phase of infection, as *C. trachomatis* does not ascend to the upper genital tract or elicit hydrosalphinx. Why *C. muridarum* but not *C. trachomatis* can ascend and cause disease in mice is unclear. Differences in host IFN-γ signaling pathways have been shown to play a role (283). However, differences in IFN-γ signaling pathways do not completely account for why *C. trachomatis* cannot establish chronic infection, since some mouse lines are more permissible to *C. trachomatis* infection (299). It is possible that an adhesion factor, such as OmcB, may play a role in ascension. This could be tested using the chimera, the HS 1 parent, and wild type *C. muridarum*. We hypothesize that the *C. muridarum omcB* locus would confer a gain-of-function in progeny production and duration of infection in a murine genital tract model compared to *C. trachomatis*.

Genomes of other chimeras are still being assembled.

APPENDIX II: Recombinant Genome Sequences

Portions of this chapter were published in Brothwell JA, Muramatsu MK, Toh E, Rockey DD, Putman TE, Barta ML, Hefty PS, Suchland RJ, and Nelson DE. 2016. Interrogating Genes That Mediate *Chlamydia trachomatis* Survival in Cell Culture Using Conditional Mutants and Recombination. *J bacteriol.* **198**, 2131-2139.

Gene	Codon Position	Strain		
		Parents		Recomb.
		HS 1	HS 13	A11[a]
gspA	264	L	L	L
pmpI	777	K	R	K
CTL0323	209	A	A	A
sctU	288	V	I	V
pepF	106	S	F	S
CTL0384	58	M	V	M
CTL0456	51	L	P	L
incC	57	P	S	P
rplL	33	D	D	D
trpC	129	H	H	H
CTL0681	159	P	L	P
gltX	487	*	Q	Q
dnaB	98	L	L	L
CTL0815	345	M	V	M
gspD	87	N	S	N
uvrD	539	N	S	N

Recomb. = non-temperature sensitive progeny

[a] Whole genome sequenced

Figure 34 Recombinant mapping HS 1. An isogenic recombinant mapped HS 1 to $GltX^{Q487*}$

Gene	Codon Position	Strain					
		Parents		Recombinants			
		HS 2	HS 23	C4	C5	F1	F3
sucC	201	L	L	L	L		L
pmpG	543	M	I	I	I	I	M
CTL0255	510	L	P	P	P	P	L
dnaA	232	F	F	F	F	F	F
CTL0609	198	W	R	R	R	R	R
phnP	127	L	P	P	P	P	P
lplA	13	L	L	L	L	L	L
aspS	84	R	G	G	R	R	R
dnaE	852	P	S	P	P	P	P
copB	428	G	E	E	G	E	G

Gene	Position	Strain				
		Parents		Recombinants		
		HS 2	HS 27	55.5	58.2	74.2
CTL0255	510	L	P		L	L
dnaA	232	E	E	E	E	E
pknD	896	E	K	K	E	E
CTL0609	198	W	R	R	R	R
CTL0619	227	A	V	V	V	V
aroC	20	P	L	L	L	L
phnP	127	L	P	P	P	P
obgE	92	G	E	G	G	G
lplA	13	L	L	L	L	L
aspS	84	R	G	R	R	R

Gray box indicates not sequenced

Figure 35 Recombinants mapping HS 2. A cross between HS 2 and HS 23 narrowed down the possible TS alleles in HS 2 to *dnaA*, *ctl0609*, or *phnP*. The TS allele was unlikely to be the *dnaA* allele since it is a silent mutation. This was confirmed by a cross between HS 2 and HS 27, which definitively narrowed the TS allele to either be in *ctl0609* or *phnP*.

Gene	Codon Position	Strain		
		Parents		Recomb.
		HS 10	HS 23	G4
sucC	201	L	L	L
pmpG	543	M	I	M
rpsA	539	N	D	N
pkn1	23			
dsbG	228	C	R	C
rplF	109	E	G	G
fmt	276	N	D	D
Intergen.				
dnaE	852	P	S	P
copB	428	G	E	G

Recomb. = non-temperature sensitive progeny; Intergen. = intergenic

Figure 36 Recombinant mapping HS 10. A cross between HS 10 and HS 23 produced a recombinant that possessed the majority of the HS 10 backbone, but that had recombined in wild type alleles of *rplF* and *fmt* from HS 23.

Gene	Codon Position	Strain				
		Parents		Recombinants		
		HS 11	HS 23	F6	G4	G5
ftsK	730	L	P		P	L
Intergen.						
sucC	201	L	L	L	L	L
pmpG	543	M	I	I	I	I
CTL0322	51	I	M	M	M	M
dnaE	852	P	S	P	P	P
copB	428	G	E	G	G	G

Intergen. = intergenic

Gray box indicates not sequenced

Figure 37 Recombinants mapping HS 11. A cross between HS 11 and HS 23 produced several recombinants that mapped the TS allele to CTL0322^{M51I}, since the mutant *ftsK* allele was tolerated. The intergenic mutation could not be Sanger sequenced due to its location surrounded by duplicated sequence.

Gene	Codon Position	Strain			
		Parents		Recombinants	
		HS 13	HS 23	A6	A8[a]
gspA	264	L	L		L
sucC	201	L	L	L	L
pmpG	543	M	I	I	M
sctU	288	I	V	V	I
pepF	106	F	S	S	F
incC	57	S	P	P	S
rplL	33	D	D		D
CTL0681	159	L	P	P	P
dnaE	852	P	S	P	P
copB	428	G	E		

Recomb. = non-temperature sensitive progeny

[a] Whole genome sequenced

Gray box indicates not sequenced

Figure 38 Recombinants mapping HS 13. A cross between HS 13 and HS 23 identified an isogenic recombinant of HS 13, revealing that the TS allele coded for CTL0681^{P159L}.

Gene	Codon Position	Strain				
		Parents		Recombinants		
		HS 19	CS 1	E5	E10	G11
CTL0040	55	R	K	K	K	K
pmpF	466	N	D	D	D	N
CTL0456	321	W	*	W	W	W
nqrB	39	S	P	S	S	P
atpB	339	D	G	G	G	G
uvrA	261	S	S	S	S	S
Intergen.						
sctR	171	N	D	D	D	D
CTL0875	206	I	V	V	V	V

Gene	Codon Position	Strain				
		Parents		Recombinants		
		HS 19	HS 23	D8[a,b]	D12	E1
sucC	201	L	L	L	L	L
pmpF	466	N	D	D	N	D
pmpG	543	M	I	I	M	I
nqrB	39	S	P	P	P	P
atpB	339	D	G	G	G	G
uvrA	261	S	S	S	S	S
Intergen.						
dnaE	852	P	S	P	P	P
sctR	171	N	D	D	N	N
copB	1806	G	E	E	G	G
CTL0875	206	I	V	V	I	V

Intergen. = intergenic; Gray box indicates not sequenced

[a] Whole genome sequenced

[b] This strain definitely mapped HS 23 to *dnaE*

Figure 39 Recombinants mapping HS 19 and HS 23. A cross between HS 19 and CS 1 mapped CS 1 to the allele encoding CL0456^{W321*}. It also eliminated the possibilities of the TS allele in HS 19 being either the *pmpF* or *nqrB* alleles. Because HS 19 has dual temperature sensitivity, it was also possible to cross this mutant with HS 23. This cross identified an isogenic recombinant of HS 23 that showed that the TS allele was DnaE^{P852S} and D8 is referred to as *dnaE*^{WT} in the preceding chapters. In addition to the phenotypic linkage analysis with the CS 1 cross, it also identified the *atpB* allele as conferring temperature sensitivity in HS 19.

Gene	Codon Position	Strain				
		Parents		Recombinants		
		HS 20	CS 2	B6	B10	C1
CTL0009	369	E	G	E	E	G
CTL0137	443	Q	*	Q	Q	Q
ptr	181	Y	H	Y	Y	Y
tgt	20	W	R	R	R	W
CTL0456	145	R	G	G	G	G
murE	90	L	L	L	L	L
CTL0561	235	W	R	W	R	W
rpoB	472	K	K	K	K	K
xerC	148	G	E	G	E	G
CTL0724	14	D	N	D	D	D
Intergen.						

Intergen. = intergenic

Figure 40 Recombinants mapping HS 20. A cross between HS 20 and CS 2 yielded progeny that mapped the TS allele in HS 20 to *ctl0456* by phenotypic linkage analysis.

Gene	Codon Position	Strain			
		Parents		Recombinants	
		HS 24	HS 23	B1	B4
sucC	201	L	L	L	L
nrdA	342	H	H	H	H
pmpG	543	M	I	M	I
fabI	79	N	D	D	D
CTL0448	102	Y	H	Y	H
dnaE	852	P	S	P	P
copB	428	G	E	G	G

Figure 41 Recombinants mapping HS 24. A cross between HS 24 and HS 23 identified an isogenic recombinant of HS 24. This definitively mapped the TS allele to *fabI*.

Gene	Codon Position	Strain		
		Parents		Recomb.
		HS 26	HS 23	E5
CTL0052	35	F	S	F
CTL0144	124	C	R	C
pgsA	169	V	V	V
sucC	201	L	L	L
pmpG	543	M	I	M
truB	208	N	D	N
CTL0402	748	K	K	K
CTL0529	182	T	A	T
CTL0597	69	R	G	G
oppA4	30	S	S	S
dnaE	852	P	S	P
copB	428	G	E	G

Recomb. = non-temperature sensitive progeny

Figure 42 Recombinant mapping HS 26. Identification of an isogenic recombinant from a cross between HS 26 and HS 23 definitively mapped the TS allele in HS 26 to *CTL0597*.

Gene	Codon Position	Strain		
		Parents		Recomb.
		HS 16	HS 27	62.2
CTL0111	378	N	D	
CTL0152	17	F	L	L
dnaN	320	A	A	A
pkn1	293	I	T	T
CTL0430	14	H	R	R
gyrB	8	Y	Y	Y
pknD	896	E	K	E
pknD	321	P	L	P
Intergen.				
CTL0619	227	A	V	V
aroC	20	P	L	L
phnP	7	S	S	S
CTL0648	307	F	S	S
obgE	92	G	E	G
dnaE	367	L	P	P

Recomb. = non-temperature sensitive progeny; Intergen. = intergenic

Gray box indicates not sequenced

Figure 43 Recombinant mapping HS 27. A cross between HS 16 and HS 27 produced a near isogenic recombinant, which reduced the TS allele in HS 27 to being either in *pknD* or *obgE*. However, results of the HS 2 x HS 27 cross (Figure 23) indicate that *pknD* can be present and still allow the production of temperature resistant progeny. This maps the TS allele in HS 27 to *obgE*.

Gene	Codon Position	Strain					
		Parents		Recombinants			
		CS 2	CS 1	A1	A6[a]	C3	C8
CTL0040	55	R	K	K	K	R	R
CTL0137	443	*	Q	Q	Q	Q	Q
CTL0456	321	W	*	W	W	W	W
murE	90	L	L	L	L	L	L
rpoB	472	K	K	K	K	K	K
xerC	148	E	G	E	G	E	G
CTL0724	14	N	D	N	D	D	D

[a] Whole genome sequenced

Figure 44 Recombinants mapping CS 1 and CS 2. Crosses between CS 1 and CS 2 identify the TS allele in CS 1 as *ctl0456* and in CS 2 as *ctl0137*.

Gene	Codon Position	Strain			
		Parents		Recombinants	
		CS 3	HS 23	F1	F5
sucC	201	L	L	L	L
pmpG	543	M	I	I	M
tyrS	88	Q	Q	Q	Q
Intergen.					
devB	150	M	T	T	T
CTL0456	442	*	W	W	W
Intergen.					
Intergen.					
dnaE	852	P	S	P	P
copB	1806	G	E	G	G
rpoN	187	T	T	T	T

Gene	Codon Position	Strain				
		Parents		Recombinants		
		CS 3	CS 2	E8	F5	F9
CTL0137	443	Q	*	Q	Q	Q
tyrS	88	Q	Q	Q	Q	Q
Intergen.						
devB	150	M	T	M	T	M
CTL0456	442	*	W	W	W	W
murE	90	L	L	L	L	L
rpoB	472	K	K	K	K	K
xerC	148	G	E	G	G	G
Intergen.						
CTL0724	14	D	N	D	D	D
Intergen.						
rpoN	187	T	T	T	T	T

Intergen. = intergenic

Figure 45 Recombinants mapping CS 3. A cross between CS 3 and HS 23 narrowed down the identity of the TS allele in CS 3 to be either a mutant *devB* or *ctl0456*. The dual HS/CS phenotype allowed for crossing of CS 2 with CS 3, which showed that the temperature resistance was achieved despite variable *devB* alleles. Thus, the gene conferring temperature sensitivity in CS 3 is the mutant *ctl0456* allele.

REFERENCES

1. Fritsche, T. R., Horn, M., Wagner, M., Herwig, R. P., Schleifer, K. H., and Gautom, R. K. (2000) Phylogenetic diversity among geographically dispersed Chlamydiales endosymbionts recovered from clinical and environmental isolates of *Acanthamoeba* spp. *Applied and environmental microbiology* **66**, 2613-2619
2. Read, T. D., Brunham, R. C., Shen, C., Gill, S. R., Heidelberg, J. F., White, O., Hickey, E. K., Peterson, J., Utterback, T., Berry, K., Bass, S., Linher, K., Weidman, J., Khouri, H., Craven, B., Bowman, C., Dodson, R., Gwinn, M., Nelson, W., DeBoy, R., Kolonay, J., McClarty, G., Salzberg, S. L., Eisen, J., and Fraser, C. M. (2000) Genome sequences of *Chlamydia trachomatis* MoPn and *Chlamydia pneumoniae* AR39. *Nucleic acids research* **28**, 1397-1406
3. Read, T. D., Myers, G. S., Brunham, R. C., Nelson, W. C., Paulsen, I. T., Heidelberg, J., Holtzapple, E., Khouri, H., Federova, N. B., Carty, H. A., Umayam, L. A., Haft, D. H., Peterson, J., Beanan, M. J., White, O., Salzberg, S. L., Hsia, R. C., McClarty, G., Rank, R. G., Bavoil, P. M., and Fraser, C. M. (2003) Genome sequence of *Chlamydophila caviae* (*Chlamydia psittaci* GPIC): examining the role of niche-specific genes in the evolution of the Chlamydiaceae. *Nucleic acids research* **31**, 2134-2147
4. Stephens, R. S., Kalman, S., Lammel, C., Fan, J., Marathe, R., Aravind, L., Mitchell, W., Olinger, L., Tatusov, R. L., Zhao, Q., Koonin, E. V., and Davis, R. W. (1998) Genome sequence of an obligate intracellular pathogen of humans: *Chlamydia trachomatis*. *Science* **282**, 754-759
5. Thomson, N. R., Yeats, C., Bell, K., Holden, M. T., Bentley, S. D., Livingstone, M., Cerdeno-Tarraga, A. M., Harris, B., Doggett, J., Ormond, D., Mungall, K., Clarke, K., Feltwell, T., Hance, Z., Sanders, M., Quail, M. A., Price, C., Barrell, B. G., Parkhill, J., and Longbottom, D. (2005) The *Chlamydophila abortus* genome sequence reveals an array of variable proteins that contribute to interspecies variation. *Genome research* **15**, 629-640
6. Van Lent, S., Piet, J. R., Beeckman, D., van der Ende, A., Van Nieuwerburgh, F., Bavoil, P., Myers, G., Vanrompay, D., and Pannekoek, Y. (2012) Full genome sequences of all nine *Chlamydia psittaci* genotype reference strains. *Journal of bacteriology* **194**, 6930-6931
7. Collingro, A., Tischler, P., Weinmaier, T., Penz, T., Heinz, E., Brunham, R. C., Read, T. D., Bavoil, P. M., Sachse, K., Kahane, S., Friedman, M. G., Rattei, T., Myers, G. S., and Horn, M. (2011) Unity in variety--the pan-genome of the Chlamydiae. *Molecular biology and evolution* **28**, 3253-3270
8. Greub, G., Kebbi-Beghdadi, C., Bertelli, C., Collyn, F., Riederer, B. M., Yersin, C., Croxatto, A., and Raoult, D. (2009) High throughput sequencing and proteomics to identify immunogenic proteins of a new pathogen: the dirty genome approach. *PloS one* **4**, e8423
9. Thomson, N. R., Holden, M. T., Carder, C., Lennard, N., Lockey, S. J., Marsh, P., Skipp, P., O'Connor, C. D., Goodhead, I., Norbertzcak, H., Harris, B., Ormond, D., Rance, R., Quail, M. A., Parkhill, J., Stephens, R. S., and Clarke, I. N. (2008)

Chlamydia trachomatis: genome sequence analysis of lymphogranuloma venereum isolates. *Genome research* **18**, 161-171
10. Horn, M., Collingro, A., Schmitz-Esser, S., Beier, C. L., Purkhold, U., Fartmann, B., Brandt, P., Nyakatura, G. J., Droege, M., Frishman, D., Rattei, T., Mewes, H. W., and Wagner, M. (2004) Illuminating the evolutionary history of chlamydiae. *Science* **304**, 728-730
11. Voigt, A., Schofl, G., and Saluz, H. P. (2012) The *Chlamydia psittaci* genome: a comparative analysis of intracellular pathogens. *PloS one* **7**, e35097
12. Carlson, J. H., Hughes, S., Hogan, D., Cieplak, G., Sturdevant, D. E., McClarty, G., Caldwell, H. D., and Belland, R. J. (2004) Polymorphisms in the *Chlamydia trachomatis* cytotoxin locus associated with ocular and genital isolates. *Infection and immunity* **72**, 7063-7072
13. Aiyar, A., Quayle, A. J., Buckner, L. R., Sherchand, S. P., Chang, T. L., Zea, A. H., Martin, D. H., and Belland, R. J. (2014) Influence of the tryptophan-indole-IFNgamma axis on human genital *Chlamydia trachomatis* infection: role of vaginal co-infections. *Frontiers in cellular and infection microbiology* **4**, 72
14. Anderson, K. S., Kim, A. Y., Quillen, J. M., Sayers, E., Yang, X. J., and Miles, E. W. (1995) Kinetic characterization of channel impaired mutants of tryptophan synthase. *The Journal of biological chemistry* **270**, 29936-29944
15. Vasilevsky, S., Stojanov, M., Greub, G., and Baud, D. (2016) Chlamydial polymorphic membrane proteins: regulation, function and potential vaccine candidates. *Virulence* **7**, 11-22
16. Mishra PK, S. S., Raj SR, Chaudhry U, Saluja D. (2013) Functional Analysis of Hypothetical Proteins of *Chlamydia trachomatis*: A Bioinformatics Based Approach for Prioritizing the Targets. *Journal of Computer Science & Systems Biology* **7**
17. Falk, L., Fredlund, H., and Jensen, J. S. (2005) Signs and symptoms of urethritis and cervicitis among women with or without *Mycoplasma genitalium* or *Chlamydia trachomatis* infection. *Sexually transmitted infections* **81**, 73-78
18. Cecil, J. A., Howell, M. R., Tawes, J. J., Gaydos, J. C., McKee, K. T., Jr., Quinn, T. C., and Gaydos, C. A. (2001) Features of *Chlamydia trachomatis* and *Neisseria gonorrhoeae* infection in male Army recruits. *The Journal of infectious diseases* **184**, 1216-1219
19. Rasmussen, S. J., Eckmann, L., Quayle, A. J., Shen, L., Zhang, Y. X., Anderson, D. J., Fierer, J., Stephens, R. S., and Kagnoff, M. F. (1997) Secretion of proinflammatory cytokines by epithelial cells in response to Chlamydia infection suggests a central role for epithelial cells in chlamydial pathogenesis. *The Journal of clinical investigation* **99**, 77-87
20. Rank, R. G., Lacy, H. M., Goodwin, A., Sikes, J., Whittimore, J., Wyrick, P. B., and Nagarajan, U. M. (2010) Host chemokine and cytokine response in the endocervix within the first developmental cycle of *Chlamydia muridarum*. *Infection and immunity* **78**, 536-544
21. Cheng, W., Shivshankar, P., Li, Z., Chen, L., Yeh, I. T., and Zhong, G. (2008) Caspase-1 contributes to *Chlamydia trachomatis*-induced upper urogenital tract inflammatory pathologies without affecting the course of infection. *Infection and immunity* **76**, 515-522

22. Cheng, W., Shivshankar, P., Zhong, Y., Chen, D., Li, Z., and Zhong, G. (2008) Intracellular interleukin-1alpha mediates interleukin-8 production induced by *Chlamydia trachomatis* infection via a mechanism independent of type I interleukin-1 receptor. *Infection and immunity* **76**, 942-951
23. Manor, E., and Sarov, I. (1988) Inhibition of *Chlamydia trachomatis* replication in HEp-2 cells by human monocyte-derived macrophages. *Infection and immunity* **56**, 3280-3284
24. Ault, K. A., Kelly, K. A., Ruther, P. E., Izzo, A. A., Izzo, L. S., Sigar, I. M., and Ramsey, K. H. (2002) *Chlamydia trachomatis* enhances the expression of matrix metalloproteinases in an in vitro model of the human fallopian tube infection. *American journal of obstetrics and gynecology* **187**, 1377-1383
25. Ramsey, K. H., Sigar, I. M., Schripsema, J. H., Shaba, N., and Cohoon, K. P. (2005) Expression of matrix metalloproteinases subsequent to urogenital *Chlamydia muridarum* infection of mice. *Infection and immunity* **73**, 6962-6973
26. Byrne, G. I., and Moulder, J. W. (1978) Parasite-specified phagocytosis of *Chlamydia psittaci* and *Chlamydia trachomatis* by L and HeLa cells. *Infection and immunity* **19**, 598-606
27. Shaw, E. I., Dooley, C. A., Fischer, E. R., Scidmore, M. A., Fields, K. A., and Hackstadt, T. (2000) Three temporal classes of gene expression during the *Chlamydia trachomatis* developmental cycle. *Molecular microbiology* **37**, 913-925
28. Belland, R. J., Zhong, G., Crane, D. D., Hogan, D., Sturdevant, D., Sharma, J., Beatty, W. L., and Caldwell, H. D. (2003) Genomic transcriptional profiling of the developmental cycle of *Chlamydia trachomatis*. *Proceedings of the National Academy of Sciences of the United States of America* **100**, 8478-8483
29. Hybiske, K., and Stephens, R. S. (2007) Mechanisms of host cell exit by the intracellular bacterium Chlamydia. *Proceedings of the National Academy of Sciences of the United States of America* **104**, 11430-11435
30. Sixt, B. S., Siegl, A., Muller, C., Watzka, M., Wultsch, A., Tziotis, D., Montanaro, J., Richter, A., Schmitt-Kopplin, P., and Horn, M. (2013) Metabolic features of *Protochlamydia amoebophila* elementary bodies--a link between activity and infectivity in Chlamydiae. *PLoS pathogens* **9**, e1003553
31. Omsland, A., Sager, J., Nair, V., Sturdevant, D. E., and Hackstadt, T. (2012) Developmental stage-specific metabolic and transcriptional activity of *Chlamydia trachomatis* in an axenic medium. *Proceedings of the National Academy of Sciences of the United States of America* **109**, 19781-19785
32. Omsland, A., Sixt, B. S., Horn, M., and Hackstadt, T. (2014) Chlamydial metabolism revisited: interspecies metabolic variability and developmental stage-specific physiologic activities. *FEMS microbiology reviews* **38**, 779-801
33. Abromaitis, S., and Stephens, R. S. (2009) Attachment and entry of Chlamydia have distinct requirements for host protein disulfide isomerase. *PLoS pathogens* **5**, e1000357
34. Hall, J. V., Schell, M., Dessus-Babus, S., Moore, C. G., Whittimore, J. D., Sal, M., Dill, B. D., and Wyrick, P. B. (2011) The multifaceted role of oestrogen in enhancing *Chlamydia trachomatis* infection in polarized human endometrial epithelial cells. *Cellular microbiology* **13**, 1183-1199

35. Elwell, C. A., Ceesay, A., Kim, J. H., Kalman, D., and Engel, J. N. (2008) RNA interference screen identifies Abl kinase and PDGFR signaling in *Chlamydia trachomatis* entry. *PLoS pathogens* **4**, e1000021
36. Gerard, H. C., Fomicheva, E., Whittum-Hudson, J. A., and Hudson, A. P. (2008) Apolipoprotein E4 enhances attachment of *Chlamydophila* (*Chlamydia*) *pneumoniae* elementary bodies to host cells. *Microbial pathogenesis* **44**, 279-285
37. Puolakkainen, M., Kuo, C. C., and Campbell, L. A. (2005) *Chlamydia pneumoniae* uses the mannose 6-phosphate/insulin-like growth factor 2 receptor for infection of endothelial cells. *Infection and immunity* **73**, 4620-4625
38. Swanson, A. F., Ezekowitz, R. A., Lee, A., and Kuo, C. C. (1998) Human mannose-binding protein inhibits infection of HeLa cells by *Chlamydia trachomatis*. *Infection and immunity* **66**, 1607-1612
39. Ajonuma, L. C., Fok, K. L., Ho, L. S., Chan, P. K., Chow, P. H., Tsang, L. L., Wong, C. H., Chen, J., Li, S., Rowlands, D. K., Chung, Y. W., and Chan, H. C. (2010) CFTR is required for cellular entry and internalization of *Chlamydia trachomatis*. *Cell biology international* **34**, 593-600
40. Rosmarin, D. M., Carette, J. E., Olive, A. J., Starnbach, M. N., Brummelkamp, T. R., and Ploegh, H. L. (2012) Attachment of *Chlamydia trachomatis* L2 to host cells requires sulfation. *Proceedings of the National Academy of Sciences of the United States of America* **109**, 10059-10064
41. Clifton, D. R., Fields, K. A., Grieshaber, S. S., Dooley, C. A., Fischer, E. R., Mead, D. J., Carabeo, R. A., and Hackstadt, T. (2004) A chlamydial type III translocated protein is tyrosine-phosphorylated at the site of entry and associated with recruitment of actin. *Proceedings of the National Academy of Sciences of the United States of America* **101**, 10166-10171
42. Jewett, T. J., Dooley, C. A., Mead, D. J., and Hackstadt, T. (2008) *Chlamydia trachomatis* tarp is phosphorylated by src family tyrosine kinases. *Biochemical and biophysical research communications* **371**, 339-344
43. Hower, S., Wolf, K., and Fields, K. A. (2009) Evidence that CT694 is a novel *Chlamydia trachomatis* T3S substrate capable of functioning during invasion or early cycle development. *Molecular microbiology* **72**, 1423-1437
44. Carabeo, R. A., Grieshaber, S. S., Hasenkrug, A., Dooley, C., and Hackstadt, T. (2004) Requirement for the Rac GTPase in *Chlamydia trachomatis* invasion of non-phagocytic cells. *Traffic* **5**, 418-425
45. Grieshaber, S. S., Grieshaber, N. A., and Hackstadt, T. (2003) *Chlamydia trachomatis* uses host cell dynein to traffic to the microtubule-organizing center in a p50 dynamitin-independent process. *Journal of cell science* **116**, 3793-3802
46. Chen, Y. S., Bastidas, R. J., Saka, H. A., Carpenter, V. K., Richards, K. L., Plano, G. V., and Valdivia, R. H. (2014) The *Chlamydia trachomatis* type III secretion chaperone Slc1 engages multiple early effectors, including TepP, a tyrosine-phosphorylated protein required for the recruitment of CrkI-II to nascent inclusions and innate immune signaling. *PLoS pathogens* **10**, e1003954
47. Rockey, D. D., Scidmore, M. A., Bannantine, J. P., and Brown, W. J. (2002) Proteins in the chlamydial inclusion membrane. *Microbes and infection / Institut Pasteur* **4**, 333-340

48. Lundemose, A. G., Birkelund, S., Larsen, P. M., Fey, S. J., and Christiansen, G. (1990) Characterization and identification of early proteins in *Chlamydia trachomatis* serovar L2 by two-dimensional gel electrophoresis. *Infection and immunity* **58**, 2478-2486
49. Moulder, J. W., Novosel, D. L., and Officer, J. E. (1963) Inhibition of the Growth of Agents of the Psittacosis Group by D-Cycloserine and Its Specific Reversal by D-Alanine. *Journal of bacteriology* **85**, 707-711
50. Garrett, A. J., Harrison, M. J., and Manire, G. P. (1974) A search for the bacterial mucopeptide component, muramic acid, in Chlamydia. *Journal of general microbiology* **80**, 315-318
51. Hatch, T. P. (1996) Disulfide cross-linked envelope proteins: the functional equivalent of peptidoglycan in chlamydiae? *Journal of bacteriology* **178**, 1-5
52. Grieshaber, N. A., Fischer, E. R., Mead, D. J., Dooley, C. A., and Hackstadt, T. (2004) Chlamydial histone-DNA interactions are disrupted by a metabolite in the methylerythritol phosphate pathway of isoprenoid biosynthesis. *Proceedings of the National Academy of Sciences of the United States of America* **101**, 7451-7456
53. Cocchiaro, J. L., Kumar, Y., Fischer, E. R., Hackstadt, T., and Valdivia, R. H. (2008) Cytoplasmic lipid droplets are translocated into the lumen of the *Chlamydia trachomatis* parasitophorous vacuole. *Proceedings of the National Academy of Sciences of the United States of America* **105**, 9379-9384
54. Derre, I., Swiss, R., and Agaisse, H. (2011) The lipid transfer protein CERT interacts with the Chlamydia inclusion protein IncD and participates to ER-Chlamydia inclusion membrane contact sites. *PLoS pathogens* **7**, e1002092
55. Hackstadt, T., Rockey, D. D., Heinzen, R. A., and Scidmore, M. A. (1996) *Chlamydia trachomatis* interrupts an exocytic pathway to acquire endogenously synthesized sphingomyelin in transit from the Golgi apparatus to the plasma membrane. *The EMBO journal* **15**, 964-977
56. Wylie, J. L., Hatch, G. M., and McClarty, G. (1997) Host cell phospholipids are trafficked to and then modified by *Chlamydia trachomatis*. *Journal of bacteriology* **179**, 7233-7242
57. Harper, A., Pogson, C. I., and Pearce, J. H. (2000) Amino acid transport into cultured McCoy cells infected with *Chlamydia trachomatis*. *Infection and immunity* **68**, 5439-5442
58. Tjaden, J., Winkler, H. H., Schwoppe, C., Van Der Laan, M., Mohlmann, T., and Neuhaus, H. E. (1999) Two nucleotide transport proteins in *Chlamydia trachomatis*, one for net nucleoside triphosphate uptake and the other for transport of energy. *Journal of bacteriology* **181**, 1196-1202
59. Iliffe-Lee, E. R., and McClarty, G. (2000) Regulation of carbon metabolism in *Chlamydia trachomatis*. *Molecular microbiology* **38**, 20-30
60. Nicholson, T. L., Olinger, L., Chong, K., Schoolnik, G., and Stephens, R. S. (2003) Global stage-specific gene regulation during the developmental cycle of *Chlamydia trachomatis*. *Journal of bacteriology* **185**, 3179-3189
61. Mathews, S. A., Volp, K. M., and Timms, P. (1999) Development of a quantitative gene expression assay for *Chlamydia trachomatis* identified temporal expression of sigma factors. *FEBS letters* **458**, 354-358

62. Niehus, E., Cheng, E., and Tan, M. (2008) DNA supercoiling-dependent gene regulation in Chlamydia. *Journal of bacteriology* **190**, 6419-6427
63. Zhang, L., Douglas, A. L., and Hatch, T. P. (1998) Characterization of a *Chlamydia psittaci* DNA binding protein (EUO) synthesized during the early and middle phases of the developmental cycle. *Infection and immunity* **66**, 1167-1173
64. Grieshaber, N. A., Grieshaber, S. S., Fischer, E. R., and Hackstadt, T. (2006) A small RNA inhibits translation of the histone-like protein Hc1 in *Chlamydia trachomatis*. *Molecular microbiology* **59**, 541-550
65. Ouellette, S. P., Karimova, G., Subtil, A., and Ladant, D. (2012) Chlamydia co-opts the rod shape-determining proteins MreB and Pbp2 for cell division. *Molecular microbiology* **85**, 164-178
66. Ouellette, S. P., Rueden, K. J., AbdelRahman, Y. M., Cox, J. V., and Belland, R. J. (2015) Identification and Partial Characterization of Potential FtsL and FtsQ Homologs of Chlamydia. *Frontiers in microbiology* **6**, 1264
67. Liechti, G. W., Kuru, E., Hall, E., Kalinda, A., Brun, Y. V., VanNieuwenhze, M., and Maurelli, A. T. (2014) A new metabolic cell-wall labelling method reveals peptidoglycan in *Chlamydia trachomatis*. *Nature* **506**, 507-510
68. Abdelrahman, Y., Ouellette, S. P., Belland, R. J., and Cox, J. V. (2016) Polarized Cell Division of *Chlamydia trachomatis*. *PLoS pathogens* **12**, e1005822
69. Nans, A., Saibil, H. R., and Hayward, R. D. (2014) Pathogen-host reorganization during Chlamydia invasion revealed by cryo-electron tomography. *Cellular microbiology* **16**, 1457-1472
70. Wilson, D. P., Whittum-Hudson, J. A., Timms, P., and Bavoil, P. M. (2009) Kinematics of intracellular chlamydiae provide evidence for contact-dependent development. *Journal of bacteriology* **191**, 5734-5742
71. Shaw, J. H., Behar, A. R., Snider, T. A., Allen, N. A., and Lutter, E. I. (2017) Comparison of Murine Cervicovaginal Infection by Chlamydial Strains: Identification of Extrusions Shed In vivo. *Frontiers in cellular and infection microbiology* **7**, 18
72. Marrazzo, J., and Suchland, R. (2014) Recent advances in understanding and managing *Chlamydia trachomatis* infections. *F1000prime reports* **6**, 120
73. Kumar, Y., and Valdivia, R. H. (2008) Reorganization of the host cytoskeleton by the intracellular pathogen *Chlamydia trachomatis*. *Communicative & integrative biology* **1**, 175-177
74. Olivares-Zavaleta, N., Whitmire, W., Gardner, D., and Caldwell, H. D. (2010) Immunization with the attenuated plasmidless *Chlamydia trachomatis* L2(25667R) strain provides partial protection in a murine model of female genitourinary tract infection. *Vaccine* **28**, 1454-1462
75. Suchland, R. J., Jeffrey, B. M., Xia, M., Bhatia, A., Chu, H. G., Rockey, D. D., and Stamm, W. E. (2008) Identification of concomitant infection with *Chlamydia trachomatis* IncA-negative mutant and wild-type strains by genomic, transcriptional, and biological characterizations. *Infection and immunity* **76**, 5438-5446
76. Gong, S., Yang, Z., Lei, L., Shen, L., and Zhong, G. (2013) Characterization of *Chlamydia trachomatis* plasmid-encoded open reading frames. *Journal of bacteriology* **195**, 3819-3826

77. O'Connell, C. M., Ingalls, R. R., Andrews, C. W., Jr., Scurlock, A. M., and Darville, T. (2007) Plasmid-deficient *Chlamydia muridarum* fail to induce immune pathology and protect against oviduct disease. *Journal of immunology* **179**, 4027-4034
78. O'Connell, C. M., and Nicks, K. M. (2006) A plasmid-cured *Chlamydia muridarum* strain displays altered plaque morphology and reduced infectivity in cell culture. *Microbiology* **152**, 1601-1607
79. Fields, K. A., Fischer, E., and Hackstadt, T. (2002) Inhibition of fusion of *Chlamydia trachomatis* inclusions at 32°C correlates with restricted export of IncA. *Infection and immunity* **70**, 3816-3823
80. Suchland, R. J., Rockey, D. D., Bannantine, J. P., and Stamm, W. E. (2000) Isolates of *Chlamydia trachomatis* that occupy nonfusogenic inclusions lack IncA, a protein localized to the inclusion membrane. *Infection and immunity* **68**, 360-367
81. Moulder, J. W. (1966) The relation of the psittacosis group (Chlamydiae) to bacteria and viruses. *Annual review of microbiology* **20**, 107-130
82. Hybiske, K. (2015) Expanding the Molecular Toolkit for Chlamydia. *Cell host & microbe* **18**, 11-13
83. DeMars, R., and Weinfurter, J. (2008) Interstrain gene transfer in *Chlamydia trachomatis in vitro*: mechanism and significance. *Journal of bacteriology* **190**, 1605-1614
84. Suchland, R. J., Sandoz, K. M., Jeffrey, B. M., Stamm, W. E., and Rockey, D. D. (2009) Horizontal transfer of tetracycline resistance among *Chlamydia* spp. *in vitro*. *Antimicrobial agents and chemotherapy* **53**, 4604-4611
85. Binet, R., and Maurelli, A. T. (2009) Transformation and isolation of allelic exchange mutants of *Chlamydia psittaci* using recombinant DNA introduced by electroporation. *Proceedings of the National Academy of Sciences of the United States of America* **106**, 292-297
86. Burall, L. S., Rodolakis, A., Rekiki, A., Myers, G. S., and Bavoil, P. M. (2009) Genomic analysis of an attenuated *Chlamydia abortus* live vaccine strain reveals defects in central metabolism and surface proteins. *Infection and immunity* **77**, 4161-4167
87. Kari, L., Goheen, M. M., Randall, L. B., Taylor, L. D., Carlson, J. H., Whitmire, W. M., Virok, D., Rajaram, K., Endresz, V., McClarty, G., Nelson, D. E., and Caldwell, H. D. (2011) Generation of targeted *Chlamydia trachomatis* null mutants. *Proceedings of the National Academy of Sciences of the United States of America* **108**, 7189-7193
88. Nguyen, B. D., and Valdivia, R. H. (2012) Virulence determinants in the obligate intracellular pathogen *Chlamydia trachomatis* revealed by forward genetic approaches. *Proceedings of the National Academy of Sciences of the United States of America* **109**, 1263-1268
89. Brothwell, J. A., Muramatsu, M. K., Toh, E., Rockey, D. D., Putman, T. E., Barta, M. L., Hefty, P. S., Suchland, R. J., and Nelson, D. E. (2016) Interrogating Genes That Mediate *Chlamydia trachomatis* Survival in Cell Culture Using Conditional Mutants and Recombination. *Journal of bacteriology* **198**, 2131-2139

90. Rajaram, K., Giebel, A. M., Toh, E., Hu, S., Newman, J. H., Morrison, S. G., Kari, L., Morrison, R. P., and Nelson, D. E. (2015) Mutational Analysis of the *Chlamydia muridarum* Plasticity Zone. *Infection and immunity* **83**, 2870-2881
91. Kokes, M., Dunn, J. D., Granek, J. A., Nguyen, B. D., Barker, J. R., Valdivia, R. H., and Bastidas, R. J. (2015) Integrating chemical mutagenesis and whole-genome sequencing as a platform for forward and reverse genetic analysis of Chlamydia. *Cell Host Microbe* **17**, 716-725
92. Wang, Y., Kahane, S., Cutcliffe, L. T., Skilton, R. J., Lambden, P. R., and Clarke, I. N. (2011) Development of a transformation system for *Chlamydia trachomatis*: restoration of glycogen biosynthesis by acquisition of a plasmid shuttle vector. *PLoS pathogens* **7**, e1002258
93. Wickstrum, J., Sammons, L. R., Restivo, K. N., and Hefty, P. S. (2013) Conditional gene expression in *Chlamydia trachomatis* using the tet system. *PloS one* **8**, e76743
94. Agaisse, H., and Derre, I. (2013) A *C. trachomatis* cloning vector and the generation of *C. trachomatis* strains expressing fluorescent proteins under the control of a C. trachomatis promoter. *PloS one* **8**, e57090
95. Mueller, K. E., Wolf, K., and Fields, K. A. (2016) Gene Deletion by Fluorescence-Reported Allelic Exchange Mutagenesis in *Chlamydia trachomatis*. *mBio* **7**, e01817-01815
96. Johnson, C. M., and Fisher, D. J. (2013) Site-specific, insertional inactivation of incA in *Chlamydia trachomatis* using a group II intron. *PloS one* **8**, e83989
97. Huang, Y., Zhang, Q., Yang, Z., Conrad, T., Liu, Y., and Zhong, G. (2015) Plasmid-Encoded Pgp5 Is a Significant Contributor to *Chlamydia muridarum* Induction of Hydrosalpinx. *PloS one* **10**, e0124840
98. Setlow, P., Brutlag, D., and Kornberg, A. (1972) Deoxyribonucleic acid polymerase: two distinct enzymes in one polypeptide. I. A proteolytic fragment containing the polymerase and 3' leads to 5' exonuclease functions. *The Journal of biological chemistry* **247**, 224-231
99. Setlow, P., and Kornberg, A. (1972) Deoxyribonucleic acid polymerase: two distinct enzymes in one polypeptide. II. A proteolytic fragment containing the 5' leads to 3' exonuclease function. Restoration of intact enzyme functions from the two proteolytic fragments. *The Journal of biological chemistry* **247**, 232-240
100. McHenry, C., and Kornberg, A. (1977) DNA polymerase III holoenzyme of *Escherichia coli*. Purification and resolution into subunits. *The Journal of biological chemistry* **252**, 6478-6484
101. McInerney, P., Johnson, A., Katz, F., and O'Donnell, M. (2007) Characterization of a triple DNA polymerase replisome. *Molecular cell* **27**, 527-538
102. Fukuoka, T., Moriya, S., Yoshikawa, H., and Ogasawara, N. (1990) Purification and characterization of an initiation protein for chromosomal replication, DnaA, in *Bacillus subtilis*. *Journal of biochemistry* **107**, 732-739
103. Speck, C., and Messer, W. (2001) Mechanism of origin unwinding: sequential binding of DnaA to double- and single-stranded DNA. *The EMBO journal* **20**, 1469-1476
104. Naktinis, V., Onrust, R., Fang, L., and O'Donnell, M. (1995) Assembly of a chromosomal replication machine: two DNA polymerases, a clamp loader, and

sliding clamps in one holoenzyme particle. II. Intermediate complex between the clamp loader and its clamp. *The Journal of biological chemistry* **270**, 13358-13365

105. Onrust, R., Finkelstein, J., Naktinis, V., Turner, J., Fang, L., and O'Donnell, M. (1995) Assembly of a chromosomal replication machine: two DNA polymerases, a clamp loader, and sliding clamps in one holoenzyme particle. I. Organization of the clamp loader. *The Journal of biological chemistry* **270**, 13348-13357
106. Onrust, R., Finkelstein, J., Turner, J., Naktinis, V., and O'Donnell, M. (1995) Assembly of a chromosomal replication machine: two DNA polymerases, a clamp loader, and sliding clamps in one holoenzyme particle. III. Interface between two polymerases and the clamp loader. *The Journal of biological chemistry* **270**, 13366-13377
107. Debyser, Z., Tabor, S., and Richardson, C. C. (1994) Coordination of leading and lagging strand DNA synthesis at the replication fork of bacteriophage T7. *Cell* **77**, 157-166
108. Rannou, O., Le Chatelier, E., Larson, M. A., Nouri, H., Dalmais, B., Laughton, C., Janniere, L., and Soultanas, P. (2013) Functional interplay of DnaE polymerase, DnaG primase and DnaC helicase within a ternary complex, and primase to polymerase hand-off during lagging strand DNA replication in *Bacillus subtilis*. *Nucleic acids research* **41**, 5303-5320
109. Sakabe, K., and Okazaki, R. (1966) A unique property of the replicating region of chromosomal DNA. *Biochimica et biophysica acta* **129**, 651-654
110. Gefter, M. L., Hirota, Y., Kornberg, T., Wechsler, J. A., and Barnoux, C. (1971) Analysis of DNA polymerases II and 3 in mutants of *Escherichia coli* thermosensitive for DNA synthesis. *Proceedings of the National Academy of Sciences of the United States of America* **68**, 3150-3153
111. Wing, R. A., Bailey, S., and Steitz, T. A. (2008) Insights into the replisome from the structure of a ternary complex of the DNA polymerase III alpha-subunit. *Journal of molecular biology* **382**, 859-869
112. Nelson, D. L. and Cox, M. M. (2008) *Lehninger Principles of Biochemistry*, Fifth ed.,
113. Dohrmann, P. R., and McHenry, C. S. (2005) A bipartite polymerase-processivity factor interaction: only the internal beta binding site of the alpha subunit is required for processive replication by the DNA polymerase III holoenzyme. *Journal of molecular biology* **350**, 228-239
114. Kim, D. R., and McHenry, C. S. (1996) Identification of the beta-binding domain of the alpha subunit of *Escherichia coli* polymerase III holoenzyme. *The Journal of biological chemistry* **271**, 20699-20704
115. Mulugu, S., Potnis, A., Shamsuzzaman, Taylor, J., Alexander, K., and Bastia, D. (2001) Mechanism of termination of DNA replication of *Escherichia coli* involves helicase-contrahelicase interaction. *Proceedings of the National Academy of Sciences of the United States of America* **98**, 9569-9574
116. Kim, D. R., and McHenry, C. S. (1996) In vivo assembly of overproduced DNA polymerase III. Overproduction, purification, and characterization of the alpha, alpha-epsilon, and alpha-epsilon-theta subunits. *The Journal of biological chemistry* **271**, 20681-20689

117. Jergic, S., Horan, N. P., Elshenawy, M. M., Mason, C. E., Urathamakul, T., Ozawa, K., Robinson, A., Goudsmits, J. M., Wang, Y., Pan, X., Beck, J. L., van Oijen, A. M., Huber, T., Hamdan, S. M., and Dixon, N. E. (2013) A direct proofreader-clamp interaction stabilizes the Pol III replicase in the polymerization mode. *The EMBO journal* **32**, 1322-1333
118. Georgescu, R. E., Yao, N., Indiani, C., Yurieva, O., and O'Donnell, M. E. (2014) Replisome mechanics: lagging strand events that influence speed and processivity. *Nucleic acids research* **42**, 6497-6510
119. Hatch, T. P. (1999) *Developmental Biology*, American Society for Microbiology
120. Hackstadt, T., Baehr, W., and Ying, Y. (1991) *Chlamydia trachomatis* developmentally regulated protein is homologous to eukaryotic histone H1. *Proceedings of the National Academy of Sciences of the United States of America* **88**, 3937-3941
121. Barry, C. E., 3rd, Brickman, T. J., and Hackstadt, T. (1993) Hc1-mediated effects on DNA structure: a potential regulator of chlamydial development. *Molecular microbiology* **9**, 273-283
122. Beatty, W. L., Morrison, R. P., and Byrne, G. I. (1995) Reactivation of persistent *Chlamydia trachomatis* infection in cell culture. *Infection and immunity* **63**, 199-205
123. Lewis, M. E., Belland, R. J., AbdelRahman, Y. M., Beatty, W. L., Aiyar, A. A., Zea, A. H., Greene, S. J., Marrero, L., Buckner, L. R., Tate, D. J., McGowin, C. L., Kozlowski, P. A., O'Brien, M., Lillis, R. A., Martin, D. H., and Quayle, A. J. (2014) Morphologic and molecular evaluation of *Chlamydia trachomatis* growth in human endocervix reveals distinct growth patterns. *Frontiers in cellular and infection microbiology* **4**, 71
124. Byrne, G. I., Ouellette, S. P., Wang, Z., Rao, J. P., Lu, L., Beatty, W. L., and Hudson, A. P. (2001) *Chlamydia pneumoniae* expresses genes required for DNA replication but not cytokinesis during persistent infection of HEp-2 cells. *Infection and immunity* **69**, 5423-5429
125. Engstrom, P., Bergstrom, M., Alfaro, A. C., Syam Krishnan, K., Bahnan, W., Almqvist, F., and Bergstrom, S. (2015) Expansion of the *Chlamydia trachomatis* inclusion does not require bacterial replication. *International journal of medical microbiology : IJMM* **305**, 378-382
126. Engstrom, P., Krishnan, K. S., Ngyuen, B. D., Chorell, E., Normark, J., Silver, J., Bastidas, R. J., Welch, M. D., Hultgren, S. J., Wolf-Watz, H., Valdivia, R. H., Almqvist, F., and Bergstrom, S. (2015) A 2-pyridone-amide inhibitor targets the glucose metabolism pathway of *Chlamydia trachomatis*. *mBio* **6**, e02304-02314
127. Liu, Y., Beyer, A., and Aebersold, R. (2016) On the Dependency of Cellular Protein Levels on mRNA Abundance. *Cell* **165**, 535-550
128. Belasco, J. G. (2010) All things must pass: contrasts and commonalities in eukaryotic and bacterial mRNA decay. *Nature reviews. Molecular cell biology* **11**, 467-478
129. Petrelli, D., LaTeana, A., Garofalo, C., Spurio, R., Pon, C. L., and Gualerzi, C. O. (2001) Translation initiation factor IF3: two domains, five functions, one mechanism? *The EMBO journal* **20**, 4560-4569

130. Carter, A. P., Clemons, W. M., Jr., Brodersen, D. E., Morgan-Warren, R. J., Hartsch, T., Wimberly, B. T., and Ramakrishnan, V. (2001) Crystal structure of an initiation factor bound to the 30S ribosomal subunit. *Science* **291**, 498-501
131. Dahlquist, K. D., and Puglisi, J. D. (2000) Interaction of translation initiation factor IF1 with the E. coli ribosomal A site. *Journal of molecular biology* **299**, 1-15
132. Yusupova, G. Z., Yusupov, M. M., Cate, J. H., and Noller, H. F. (2001) The path of messenger RNA through the ribosome. *Cell* **106**, 233-241
133. Selmer, M., Dunham, C. M., Murphy, F. V. t., Weixlbaumer, A., Petry, S., Kelley, A. C., Weir, J. R., and Ramakrishnan, V. (2006) Structure of the 70S ribosome complexed with mRNA and tRNA. *Science* **313**, 1935-1942
134. Marshall, R. A., Aitken, C. E., and Puglisi, J. D. (2009) GTP hydrolysis by IF2 guides progression of the ribosome into elongation. *Molecular cell* **35**, 37-47
135. Steitz, T. A. (2008) A structural understanding of the dynamic ribosome machine. *Nature reviews. Molecular cell biology* **9**, 242-253
136. Valle, M., Sengupta, J., Swami, N. K., Grassucci, R. A., Burkhardt, N., Nierhaus, K. H., Agrawal, R. K., and Frank, J. (2002) Cryo-EM reveals an active role for aminoacyl-tRNA in the accommodation process. *The EMBO journal* **21**, 3557-3567
137. Schmeing, T. M., Huang, K. S., Strobel, S. A., and Steitz, T. A. (2005) An induced-fit mechanism to promote peptide bond formation and exclude hydrolysis of peptidyl-tRNA. *Nature* **438**, 520-524
138. Watson, J. D. (1963) Involvement of RNA in the synthesis of proteins. *Science* **140**, 17-26
139. Petry, S., Brodersen, D. E., Murphy, F. V. t., Dunham, C. M., Selmer, M., Tarry, M. J., Kelley, A. C., and Ramakrishnan, V. (2005) Crystal structures of the ribosome in complex with release factors RF1 and RF2 bound to a cognate stop codon. *Cell* **123**, 1255-1266
140. Gaal, T., Bartlett, M. S., Ross, W., Turnbough, C. L., Jr., and Gourse, R. L. (1997) Transcription regulation by initiating NTP concentration: rRNA synthesis in bacteria. *Science* **278**, 2092-2097
141. Green, C. J., and Vold, B. S. (1992) A cluster of nine tRNA genes between ribosomal gene operons in *Bacillus subtilis*. *Journal of bacteriology* **174**, 3147-3151
142. Rudner, R., Chevrestt, A., Buchholz, S. R., Studamire, B., White, A. M., and Jarvis, E. D. (1993) Two tRNA gene clusters associated with rRNA operons rrnD and rrnE in *Bacillus subtilis*. *Journal of bacteriology* **175**, 503-509
143. Condon, C., Grunberg-Manago, M., and Putzer, H. (1996) Aminoacyl-tRNA synthetase gene regulation in *Bacillus subtilis*. *Biochimie* **78**, 381-389
144. Miller, M. R., and Buskirk, A. R. (2014) An unusual mechanism for EF-Tu activation during tmRNA-mediated ribosome rescue. *Rna* **20**, 228-235
145. Starosta, A. L., Lassak, J., Jung, K., and Wilson, D. N. (2014) The bacterial translation stress response. *FEMS microbiology reviews* **38**, 1172-1201
146. Cook, G. M., Robson, J. R., Frampton, R. A., McKenzie, J., Przybilski, R., Fineran, P. C., and Arcus, V. L. (2013) Ribonucleases in bacterial toxin-antitoxin systems. *Biochimica et biophysica acta* **1829**, 523-531

147. Neubauer, C., Gao, Y. G., Andersen, K. R., Dunham, C. M., Kelley, A. C., Hentschel, J., Gerdes, K., Ramakrishnan, V., and Brodersen, D. E. (2009) The structural basis for mRNA recognition and cleavage by the ribosome-dependent endonuclease RelE. *Cell* **139**, 1084-1095
148. Moll, I., and Engelberg-Kulka, H. (2012) Selective translation during stress in *Escherichia coli*. *Trends in biochemical sciences* **37**, 493-498
149. Rojiani, M. V., Jakubowski, H., and Goldman, E. (1989) Effect of variation of charged and uncharged tRNA(Trp) levels on ppGpp synthesis in *Escherichia coli*. *Journal of bacteriology* **171**, 6493-6502
150. Tanner, D. R., Cariello, D. A., Woolstenhulme, C. J., Broadbent, M. A., and Buskirk, A. R. (2009) Genetic identification of nascent peptides that induce ribosome stalling. *The Journal of biological chemistry* **284**, 34809-34818
151. Boel, G., Smith, P. C., Ning, W., Englander, M. T., Chen, B., Hashem, Y., Testa, A. J., Fischer, J. J., Wieden, H. J., Frank, J., Gonzalez, R. L., Jr., and Hunt, J. F. (2014) The ABC-F protein EttA gates ribosome entry into the translation elongation cycle. *Nature structural & molecular biology* **21**, 143-151
152. Kint, C., Verstraeten, N., Hofkens, J., Fauvart, M., and Michiels, J. (2014) Bacterial Obg proteins: GTPases at the nexus of protein and DNA synthesis. *Critical reviews in microbiology* **40**, 207-224
153. Raskin, D. M., Judson, N., and Mekalanos, J. J. (2007) Regulation of the stringent response is the essential function of the conserved bacterial G protein CgtA in *Vibrio cholerae*. *Proceedings of the National Academy of Sciences of the United States of America* **104**, 4636-4641
154. Jiang, M., Datta, K., Walker, A., Strahler, J., Bagamasbad, P., Andrews, P. C., and Maddock, J. R. (2006) The *Escherichia coli* GTPase CgtAE is involved in late steps of large ribosome assembly. *Journal of bacteriology* **188**, 6757-6770
155. Sato, A., Kobayashi, G., Hayashi, H., Yoshida, H., Wada, A., Maeda, M., Hiraga, S., Takeyasu, K., and Wada, C. (2005) The GTP binding protein Obg homolog ObgE is involved in ribosome maturation. *Genes to cells : devoted to molecular & cellular mechanisms* **10**, 393-408
156. Madhugiri, R., and Evguenieva-Hackenberg, E. (2009) RNase J is involved in the 5'-end maturation of 16S rRNA and 23S rRNA in Sinorhizobium meliloti. *FEBS letters* **583**, 2339-2342
157. Davies, B. W., Kohrer, C., Jacob, A. I., Simmons, L. A., Zhu, J., Aleman, L. M., Rajbhandary, U. L., and Walker, G. C. (2010) Role of *Escherichia coli* YbeY, a highly conserved protein, in rRNA processing. *Molecular microbiology* **78**, 506-518
158. Jacob, A. I., Kohrer, C., Davies, B. W., RajBhandary, U. L., and Walker, G. C. (2013) Conserved bacterial RNase YbeY plays key roles in 70S ribosome quality control and 16S rRNA maturation. *Molecular cell* **49**, 427-438
159. Yoshida, H., and Wada, A. (2014) The 100S ribosome: ribosomal hibernation induced by stress. *Wiley interdisciplinary reviews. RNA* **5**, 723-732
160. Endres, L., Dedon, P. C., and Begley, T. J. (2015) Codon-biased translation can be regulated by wobble-base tRNA modification systems during cellular stress responses. *RNA biology* **12**, 603-614

161. Slagter-Jager, J. G., Puzis, L., Gutgsell, N. S., Belfort, M., and Jain, C. (2007) Functional defects in transfer RNAs lead to the accumulation of ribosomal RNA precursors. *Rna* **13**, 597-605
162. Ran, W., and Higgs, P. G. (2012) Contributions of speed and accuracy to translational selection in bacteria. *PloS one* **7**, e51652
163. Dana, A., and Tuller, T. (2014) The effect of tRNA levels on decoding times of mRNA codons. *Nucleic acids research* **42**, 9171-9181
164. Dong, H., Nilsson, L., and Kurland, C. G. (1996) Co-variation of tRNA abundance and codon usage in *Escherichia coli* at different growth rates. *Journal of molecular biology* **260**, 649-663
165. Rojas-Benitez, D., Thiaville, P. C., de Crecy-Lagard, V., and Glavic, A. (2015) The Levels of a Universally Conserved tRNA Modification Regulate Cell Growth. *The Journal of biological chemistry* **290**, 18699-18707
166. Ishida, K., Kunibayashi, T., Tomikawa, C., Ochi, A., Kanai, T., Hirata, A., Iwashita, C., and Hori, H. (2011) Pseudouridine at position 55 in tRNA controls the contents of other modified nucleotides for low-temperature adaptation in the extreme-thermophilic eubacterium *Thermus thermophilus*. *Nucleic acids research* **39**, 2304-2318
167. Wang, X., and He, C. (2014) Dynamic RNA modifications in posttranscriptional regulation. *Molecular cell* **56**, 5-12
168. Gu, C., Begley, T. J., and Dedon, P. C. (2014) tRNA modifications regulate translation during cellular stress. *FEBS letters* **588**, 4287-4296
169. Kinghorn, S. M., O'Byrne, C. P., Booth, I. R., and Stansfield, I. (2002) Physiological analysis of the role of *truB* in *Escherichia coli*: a role for tRNA modification in extreme temperature resistance. *Microbiology* **148**, 3511-3520
170. Helm, M., and Alfonzo, J. D. (2014) Posttranscriptional RNA Modifications: playing metabolic games in a cell's chemical Legoland. *Chemistry & biology* **21**, 174-185
171. Urbonavicius, J., Durand, J. M., and Bjork, G. R. (2002) Three modifications in the D and T arms of tRNA influence translation in *Escherichia coli* and expression of virulence genes in *Shigella flexneri*. *Journal of bacteriology* **184**, 5348-5357
172. Kirsebom, L. A., and Trobro, S. (2009) RNase P RNA-mediated cleavage. *IUBMB life* **61**, 189-200
173. Zhang, J. R., and Deutscher, M. P. (1988) Transfer RNA is a substrate for RNase D in vivo. *The Journal of biological chemistry* **263**, 17909-17912
174. Tomita, K., and Yamashita, S. (2014) Molecular mechanisms of template-independent RNA polymerization by tRNA nucleotidyltransferases. *Frontiers in genetics* **5**, 36
175. Cantara, W. A., Crain, P. F., Rozenski, J., McCloskey, J. A., Harris, K. A., Zhang, X., Vendeix, F. A., Fabris, D., and Agris, P. F. (2011) The RNA Modification Database, RNAMDB: 2011 update. *Nucleic acids research* **39**, D195-201
176. Arnez, J. G., and Steitz, T. A. (1994) Crystal structure of unmodified tRNA(Gln) complexed with glutaminyl-tRNA synthetase and ATP suggests a possible role for pseudo-uridines in stabilization of RNA structure. *Biochemistry* **33**, 7560-7567

177. Thiaville, P. C., El Yacoubi, B., Kohrer, C., Thiaville, J. J., Deutsch, C., Iwata-Reuyl, D., Bacusmo, J. M., Armengaud, J., Bessho, Y., Wetzel, C., Cao, X., Limbach, P. A., RajBhandary, U. L., and de Crecy-Lagard, V. (2015) Essentiality of threonylcarbamoyladenosine (t(6)A), a universal tRNA modification, in bacteria. *Molecular microbiology* **98**, 1199-1221
178. Machnicka, M. A., Olchowik, A., Grosjean, H., and Bujnicki, J. M. (2014) Distribution and frequencies of post-transcriptional modifications in tRNAs. *RNA biology* **11**, 1619-1629
179. Grosjean, H., Droogmans, L., Roovers, M., and Keith, G. (2007) Detection of enzymatic activity of transfer RNA modification enzymes using radiolabeled tRNA substrates. *Methods in enzymology* **425**, 55-101
180. Jackman, J. E., Kotelawala, L., Grayhack, E. J., and Phizicky, E. M. (2007) Identification and characterization of modification enzymes by biochemical analysis of the proteome. *Methods in enzymology* **425**, 139-152
181. Chernyakov, I., Baker, M. A., Grayhack, E. J., and Phizicky, E. M. (2008) Chapter 11. Identification and analysis of tRNAs that are degraded in *Saccharomyces cerevisiae* due to lack of modifications. *Methods in enzymology* **449**, 221-237
182. Alexandrov, A., Chernyakov, I., Gu, W., Hiley, S. L., Hughes, T. R., Grayhack, E. J., and Phizicky, E. M. (2006) Rapid tRNA decay can result from lack of nonessential modifications. *Molecular cell* **21**, 87-96
183. Hori, H. (2014) Methylated nucleosides in tRNA and tRNA methyltransferases. *Frontiers in genetics* **5**, 144
184. Durairaj, A., and Limbach, P. A. (2008) Matrix-assisted laser desorption/ionization mass spectrometry screening for pseudouridine in mixtures of small RNAs by chemical derivatization, RNase digestion and signature products. *Rapid communications in mass spectrometry : RCM* **22**, 3727-3734
185. Li, S., and Limbach, P. A. (2012) Method for comparative analysis of ribonucleic acids using isotope labeling and mass spectrometry. *Analytical chemistry* **84**, 8607-8613
186. Castleberry, C. M., and Limbach, P. A. (2010) Relative quantitation of transfer RNAs using liquid chromatography mass spectrometry and signature digestion products. *Nucleic acids research* **38**, e162
187. Tomikawa, C., Yokogawa, T., Kanai, T., and Hori, H. (2010) N7-Methylguanine at position 46 (m7G46) in tRNA from *Thermus thermophilus* is required for cell viability at high temperatures through a tRNA modification network. *Nucleic acids research* **38**, 942-957
188. Farmer, T. H., Gilbart, J., and Elson, S. W. (1992) Biochemical basis of mupirocin resistance in strains of *Staphylococcus aureus*. *The Journal of antimicrobial chemotherapy* **30**, 587-596
189. Tan, M., Zhu, B., Zhou, X. L., He, R., Chen, X., Eriani, G., and Wang, E. D. (2010) tRNA-dependent pre-transfer editing by prokaryotic leucyl-tRNA synthetase. *The Journal of biological chemistry* **285**, 3235-3244
190. Jockel, S., Nees, G., Sommer, R., Zhao, Y., Cherkasov, D., Hori, H., Ehm, G., Schnare, M., Nain, M., Kaufmann, A., and Bauer, S. (2012) The 2'-O-methylation

status of a single guanosine controls transfer RNA-mediated Toll-like receptor 7 activation or inhibition. *The Journal of experimental medicine* **209**, 235-241
191. Sarin, L. P., and Leidel, S. A. (2014) Modify or die?--RNA modification defects in metazoans. *RNA biology* **11**, 1555-1567
192. Hou, Y. M., and Schimmel, P. (1988) A simple structural feature is a major determinant of the identity of a transfer RNA. *Nature* **333**, 140-145
193. Das, M., Vargas-Rodriguez, O., Goto, Y., Suga, H., and Musier-Forsyth, K. (2014) Distinct tRNA recognition strategies used by a homologous family of editing domains prevent mistranslation. *Nucleic acids research* **42**, 3943-3953
194. Raczniak, G., Ibba, M., and Soll, D. (2001) Genomics-based identification of targets in pathogenic bacteria for potential therapeutic and diagnostic use. *Toxicology* **160**, 181-189
195. Raczniak, G., Becker, H. D., Min, B., and Soll, D. (2001) A single amidotransferase forms asparaginyl-tRNA and glutaminyl-tRNA in *Chlamydia trachomatis*. *The Journal of biological chemistry* **276**, 45862-45867
196. Ito, T., and Yokoyama, S. (2010) Two enzymes bound to one transfer RNA assume alternative conformations for consecutive reactions. *Nature* **467**, 612-616
197. Albrecht, M., Sharma, C. M., Reinhardt, R., Vogel, J., and Rudel, T. (2010) Deep sequencing-based discovery of the *Chlamydia trachomatis* transcriptome. *Nucleic acids research* **38**, 868-877
198. Liu, X., Afrane, M., Clemmer, D. E., Zhong, G., and Nelson, D. E. (2010) Identification of *Chlamydia trachomatis* outer membrane complex proteins by differential proteomics. *Journal of bacteriology* **192**, 2852-2860
199. Saka, H. A., Thompson, J. W., Chen, Y. S., Kumar, Y., Dubois, L. G., Moseley, M. A., and Valdivia, R. H. (2011) Quantitative proteomics reveals metabolic and pathogenic properties of *Chlamydia trachomatis* developmental forms. *Molecular microbiology* **82**, 1185-1203
200. Skipp, P., Robinson, J., O'Connor, C. D., and Clarke, I. N. (2005) Shotgun proteomic analysis of *Chlamydia trachomatis*. *Proteomics* **5**, 1558-1573
201. Fisher, D. J., Adams, N. E., and Maurelli, A. T. (2015) Phosphoproteomic analysis of the *Chlamydia caviae* elementary body and reticulate body forms. *Microbiology* **161**, 1648-1658
202. Pendergast, A. M., and Traugh, J. A. (1985) Alteration of aminoacyl-tRNA synthetase activities by phosphorylation with casein kinase I. *The Journal of biological chemistry* **260**, 11769-11774
203. Barker, J. R., Koestler, B. J., Carpenter, V. K., Burdette, D. L., Waters, C. M., Vance, R. E., and Valdivia, R. H. (2013) STING-dependent recognition of cyclic di-AMP mediates type I interferon responses during *Chlamydia trachomatis* infection. *mBio* **4**, e00018-00013
204. Belland, R. J., Nelson, D. E., Virok, D., Crane, D. D., Hogan, D., Sturdevant, D., Beatty, W. L., and Caldwell, H. D. (2003) Transcriptome analysis of chlamydial growth during IFN-gamma-mediated persistence and reactivation. *Proceedings of the National Academy of Sciences of the United States of America* **100**, 15971-15976
205. Scidmore, M. A., Rockey, D. D., Fischer, E. R., Heinzen, R. A., and Hackstadt, T. (1996) Vesicular interactions of the *Chlamydia trachomatis* inclusion are

determined by chlamydial early protein synthesis rather than route of entry. *Infection and immunity* **64**, 5366-5372
206. Matsumoto, A., Izutsu, H., Miyashita, N., and Ohuchi, M. (1998) Plaque formation by and plaque cloning of *Chlamydia trachomatis* biovar trachoma. *Journal of clinical microbiology* **36**, 3013-3019
207. Nelson, D. E., Taylor, L. D., Shannon, J. G., Whitmire, W. M., Crane, D. D., McClarty, G., Su, H., Kari, L., and Caldwell, H. D. (2007) Phenotypic rescue of *Chlamydia trachomatis* growth in IFN-gamma treated mouse cells by irradiated *Chlamydia muridarum*. *Cellular microbiology* **9**, 2289-2298
208. Schindelin, J., Arganda-Carreras, I., Frise, E., Kaynig, V., Longair, M., Pietzsch, T., Preibisch, S., Rueden, C., Saalfeld, S., Schmid, B., Tinevez, J. Y., White, D. J., Hartenstein, V., Eliceiri, K., Tomancak, P., and Cardona, A. (2012) Fiji: an open-source platform for biological-image analysis. *Nature methods* **9**, 676-682
209. Jeffrey, B. M., Suchland, R. J., Eriksen, S. G., Sandoz, K. M., and Rockey, D. D. (2013) Genomic and phenotypic characterization of *in vitro*-generated *Chlamydia trachomatis* recombinants. *BMC microbiology* **13**, 142
210. Putman, T. E., Suchland, R. J., Ivanovitch, J. D., and Rockey, D. D. (2013) Culture-independent sequence analysis of *Chlamydia trachomatis* in urogenital specimens identifies regions of recombination and in-patient sequence mutations. *Microbiology* **159**, 2109-2117
211. Kearse, M., Moir, R., Wilson, A., Stones-Havas, S., Cheung, M., Sturrock, S., Buxton, S., Cooper, A., Markowitz, S., Duran, C., Thierer, T., Ashton, B., Meintjes, P., and Drummond, A. (2012) Geneious Basic: an integrated and extendable desktop software platform for the organization and analysis of sequence data. *Bioinformatics* **28**, 1647-1649
212. Kamentsky, L., Jones, T. R., Fraser, A., Bray, M. A., Logan, D. J., Madden, K. L., Ljosa, V., Rueden, C., Eliceiri, K. W., and Carpenter, A. E. (2011) Improved structure, function and compatibility for CellProfiler: modular high-throughput image analysis software. *Bioinformatics* **27**, 1179-1180
213. Osaka, I., Hills, J. M., Kieweg, S. L., Shinogle, H. E., Moore, D. S., and Hefty, P. S. (2012) An automated image-based method for rapid analysis of *Chlamydia infection* as a tool for screening antichlamydial agents. *Antimicrobial agents and chemotherapy* **56**, 4184-4188
214. Caldwell, H. D., Kromhout, J., and Schachter, J. (1981) Purification and partial characterization of the major outer membrane protein of *Chlamydia trachomatis*. *Infection and immunity* **31**, 1161-1176
215. Yu, J., Rossi, R., Hale, C., Goulding, D., and Dougan, G. (2009) Interaction of enteric bacterial pathogens with murine embryonic stem cells. *Infection and immunity* **77**, 585-597
216. Engel, J. N., Pollack, J., Perara, E., and Ganem, D. (1990) Heat shock response of murine *Chlamydia trachomatis*. *Journal of bacteriology* **172**, 6959-6972
217. Van Ooij, C., Homola, E., Kincaid, E., and Engel, J. (1998) Fusion of *Chlamydia trachomatis*-containing inclusions is inhibited at low temperatures and requires bacterial protein synthesis. *Infection and immunity* **66**, 5364-5371
218. Paul, B. J., Barker, M. M., Ross, W., Schneider, D. A., Webb, C., Foster, J. W., and Gourse, R. L. (2004) DksA: a critical component of the transcription

initiation machinery that potentiates the regulation of rRNA promoters by ppGpp and the initiating NTP. *Cell* **118**, 311-322
219. Feng, B., Mandava, C. S., Guo, Q., Wang, J., Cao, W., Li, N., Zhang, Y., Zhang, Y., Wang, Z., Wu, J., Sanyal, S., Lei, J., and Gao, N. (2014) Structural and functional insights into the mode of action of a universally conserved Obg GTPase. *PLoS biology* **12**, e1001866
220. Polkinghorne, A., and Vaughan, L. (2011) *Chlamydia abortus* YhbZ, a truncated Obg family GTPase, associates with the *Escherichia coli* large ribosomal subunit. *Microbial pathogenesis* **50**, 200-206
221. Fields, K. A., and Hackstadt, T. (2002) The chlamydial inclusion: escape from the endocytic pathway. *Annual review of cell and developmental biology* **18**, 221-245
222. Kumar, Y., and Valdivia, R. H. (2008) Actin and intermediate filaments stabilize the *Chlamydia trachomatis* vacuole by forming dynamic structural scaffolds. *Cell host & microbe* **4**, 159-169
223. Tan, J., Jakob, U., and Bardwell, J. C. (2002) Overexpression of two different GTPases rescues a null mutation in a heat-induced rRNA methyltransferase. *Journal of bacteriology* **184**, 2692-2698
224. McHenry, C. S. (2011) Bacterial replicases and related polymerases. *Current opinion in chemical biology* **15**, 587-594
225. Georgescu, R. E., Yurieva, O., Kim, S. S., Kuriyan, J., Kong, X. P., and O'Donnell, M. (2008) Structure of a small-molecule inhibitor of a DNA polymerase sliding clamp. *Proceedings of the National Academy of Sciences of the United States of America* **105**, 11116-11121
226. Stukenberg, P. T., Studwell-Vaughan, P. S., and O'Donnell, M. (1991) Mechanism of the sliding beta-clamp of DNA polymerase III holoenzyme. *The Journal of biological chemistry* **266**, 11328-11334
227. Pavlov, A. R., Belova, G. I., Kozyavkin, S. A., and Slesarev, A. I. (2002) Helix-hairpin-helix motifs confer salt resistance and processivity on chimeric DNA polymerases. *Proceedings of the National Academy of Sciences of the United States of America* **99**, 13510-13515
228. Muramatsu, M. K., Brothwell, J. A., Stein, B. D., Putman, T. E., Rockey, D. D., and Nelson, D. E. (2016) Beyond tryptophan synthase: identification of genes that contribute to *Chlamydia trachomatis* survival during IFN-gamma induced persistence and reactivation. *Infection and immunity*
229. Yao, J., Abdelrahman, Y. M., Robertson, R. M., Cox, J. V., Belland, R. J., White, S. W., and Rock, C. O. (2014) Type II fatty acid synthesis is essential for the replication of *Chlamydia trachomatis*. *The Journal of biological chemistry* **289**, 22365-22376
230. Sisko, J. L., Spaeth, K., Kumar, Y., and Valdivia, R. H. (2006) Multifunctional analysis of Chlamydia-specific genes in a yeast expression system. *Molecular microbiology* **60**, 51-66
231. Kurland, C. G., Canback, B., and Berg, O. G. (2003) Horizontal gene transfer: a critical view. *Proceedings of the National Academy of Sciences of the United States of America* **100**, 9658-9662

232. Binet, R., Bowlin, A. K., Maurelli, A. T., and Rank, R. G. (2010) Impact of azithromycin resistance mutations on the virulence and fitness of *Chlamydia caviae* in guinea pigs. *Antimicrobial agents and chemotherapy* **54**, 1094-1101
233. Dugan, J., Rockey, D. D., Jones, L., and Andersen, A. A. (2004) Tetracycline resistance in *Chlamydia suis* mediated by genomic islands inserted into the chlamydial inv-like gene. *Antimicrobial agents and chemotherapy* **48**, 3989-3995
234. Jacob, F., and Wollman, E. L. (1958) Genetic and physical determinations of chromosomal segments in *Escherichia coli*. *Symposia of the Society for Experimental Biology* **12**, 75-92
235. Derbyshire, K. M., and Gray, T. A. (2014) Distributive Conjugal Transfer: New Insights into Horizontal Gene Transfer and Genetic Exchange in Mycobacteria. *Microbiology spectrum* **2**
236. Wechsler, J. A., and Gross, J. D. (1971) *Escherichia coli* mutants temperature-sensitive for DNA synthesis. *Molecular & general genetics : MGG* **113**, 273-284
237. Vandewiele, D., Fernandez de Henestrosa, A. R., Timms, A. R., Bridges, B. A., and Woodgate, R. (2002) Sequence analysis and phenotypes of five temperature sensitive mutator alleles of *dnaE*, encoding modified alpha-catalytic subunits of *Escherichia coli* DNA polymerase III holoenzyme. *Mutation research* **499**, 85-95
238. Zyskind, J. W., Deen, L. T., and Smith, D. W. (1977) Temporal sequence of events during the initiation process in *Escherichia coli* deoxyribonucleic acid replication: roles of the *dnaA* and *dnaC* gene products and ribonucleic acid polymerase. *Journal of bacteriology* **129**, 1466-1475
239. Durfee, T., Hansen, A. M., Zhi, H., Blattner, F. R., and Jin, D. J. (2008) Transcription profiling of the stringent response in *Escherichia coli*. *Journal of bacteriology* **190**, 1084-1096
240. Germain, E., Castro-Roa, D., Zenkin, N., and Gerdes, K. (2013) Molecular mechanism of bacterial persistence by HipA. *Molecular cell* **52**, 248-254
241. Kaspy, I., Rotem, E., Weiss, N., Ronin, I., Balaban, N. Q., and Glaser, G. (2013) HipA-mediated antibiotic persistence via phosphorylation of the glutamyl-tRNA-synthetase. *Nature communications* **4**, 3001
242. Hinnebusch, A. G. (1988) Mechanisms of gene regulation in the general control of amino acid biosynthesis in *Saccharomyces cerevisiae*. *Microbiological reviews* **52**, 248-273
243. Hinnebusch, A. G. (1993) Gene-specific translational control of the yeast GCN4 gene by phosphorylation of eukaryotic initiation factor 2. *Molecular microbiology* **10**, 215-223
244. Buchan, J. R., and Parker, R. (2009) Eukaryotic stress granules: the ins and outs of translation. *Molecular cell* **36**, 932-941
245. Jakubowski, H., and Goldman, E. (1984) Quantities of individual aminoacyl-tRNA families and their turnover in *Escherichia coli*. *Journal of bacteriology* **158**, 769-776
246. Hatch, T. P., Miceli, M., and Silverman, J. A. (1985) Synthesis of protein in host-free reticulate bodies of *Chlamydia psittaci* and *Chlamydia trachomatis*. *Journal of bacteriology* **162**, 938-942

247. Shaw, A. C., Christiansen, G., and Birkelund, S. (1999) Effects of interferon gamma on *Chlamydia trachomatis* serovar A and L2 protein expression investigated by two-dimensional gel electrophoresis. *Electrophoresis* **20**, 775-780
248. Molestina, R. E., Klein, J. B., Miller, R. D., Pierce, W. H., Ramirez, J. A., and Summersgill, J. T. (2002) Proteomic analysis of differentially expressed *Chlamydia pneumoniae* genes during persistent infection of HEp-2 cells. *Infection and immunity* **70**, 2976-2981
249. Ouellette, S. P., Hatch, T. P., AbdelRahman, Y. M., Rose, L. A., Belland, R. J., and Byrne, G. I. (2006) Global transcriptional upregulation in the absence of increased translation in Chlamydia during IFNgamma-mediated host cell tryptophan starvation. *Molecular microbiology* **62**, 1387-1401
250. Ouellette, S. P., Rueden, K. J., and Rucks, E. A. (2016) Tryptophan Codon-Dependent Transcription in *Chlamydia pneumoniae* during Gamma Interferon-Mediated Tryptophan Limitation. *Infection and immunity* **84**, 2703-2713
251. Lauhon, C. T. (2012) Mechanism of N6-threonylcarbamoyladenonsine (t(6)A) biosynthesis: isolation and characterization of the intermediate threonylcarbamoyl-AMP. *Biochemistry* **51**, 8950-8963
252. El Yacoubi, B., Hatin, I., Deutsch, C., Kahveci, T., Rousset, J. P., Iwata-Reuyl, D., Murzin, A. G., and de Crecy-Lagard, V. (2011) A role for the universal Kae1/Qri7/YgjD (COG0533) family in tRNA modification. *The EMBO journal* **30**, 882-893
253. El Yacoubi, B., Lyons, B., Cruz, Y., Reddy, R., Nordin, B., Agnelli, F., Williamson, J. R., Schimmel, P., Swairjo, M. A., and de Crecy-Lagard, V. (2009) The universal YrdC/Sua5 family is required for the formation of threonylcarbamoyladenosine in tRNA. *Nucleic acids research* **37**, 2894-2909
254. Jinks-Robertson, S., Gourse, R. L., and Nomura, M. (1983) Expression of rRNA and tRNA genes in *Escherichia coli*: evidence for feedback regulation by products of rRNA operons. *Cell* **33**, 865-876
255. Gil, R., Silva, F. J., Pereto, J., and Moya, A. (2004) Determination of the core of a minimal bacterial gene set. *Microbiology and molecular biology reviews : MMBR* **68**, 518-537, table of contents
256. Wower, I., Kowaleski, M. P., Sears, L. E., and Zimmermann, R. A. (1992) Mutagenesis of ribosomal protein S8 from *Escherichia coli*: defects in regulation of the spc operon. *Journal of bacteriology* **174**, 1213-1221
257. Persky, N. S., Ferullo, D. J., Cooper, D. L., Moore, H. R., and Lovett, S. T. (2009) The ObgE/CgtA GTPase influences the stringent response to amino acid starvation in *Escherichia coli*. *Molecular microbiology* **73**, 253-266
258. Nolivos, S., and Sherratt, D. (2014) The bacterial chromosome: architecture and action of bacterial SMC and SMC-like complexes. *FEMS microbiology reviews* **38**, 380-392
259. Grieshaber, N. A., Tattersall, J. S., Liguori, J., Lipat, J. N., Runac, J., and Grieshaber, S. S. (2015) Identification of the base-pairing requirements for repression of *hctA* translation by the small RNA *IhtA* leads to the discovery of a new mRNA target in *Chlamydia trachomatis*. *PloS one* **10**, e0116593
260. Imamura, H., Nhat, K. P., Togawa, H., Saito, K., Iino, R., Kato-Yamada, Y., Nagai, T., and Noji, H. (2009) Visualization of ATP levels inside single living

cells with fluorescence resonance energy transfer-based genetically encoded indicators. *Proceedings of the National Academy of Sciences of the United States of America* **106**, 15651-15656
261. Balut, C., vandeVen, M., Despa, S., Lambrichts, I., Ameloot, M., Steels, P., and Smets, I. (2008) Measurement of cytosolic and mitochondrial pH in living cells during reversible metabolic inhibition. *Kidney international* **73**, 226-232
262. Mancusso, R., Gregorio, G. G., Liu, Q., and Wang, D. N. (2012) Structure and mechanism of a bacterial sodium-dependent dicarboxylate transporter. *Nature* **491**, 622-626
263. Kubo, A., and Stephens, R. S. (2001) Substrate-specific diffusion of select dicarboxylates through *Chlamydia trachomatis* PorB. *Microbiology* **147**, 3135-3140
264. Kaplan, N., Albert, M., Awrey, D., Bardouniotis, E., Berman, J., Clarke, T., Dorsey, M., Hafkin, B., Ramnauth, J., Romanov, V., Schmid, M. B., Thalakada, R., Yethon, J., and Pauls, H. W. (2012) Mode of action, in vitro activity, and in vivo efficacy of AFN-1252, a selective antistaphylococcal FabI inhibitor. *Antimicrobial agents and chemotherapy* **56**, 5865-5874
265. Vick, J. E., Clomburg, J. M., Blankschien, M. D., Chou, A., Kim, S., and Gonzalez, R. (2015) *Escherichia coli* enoyl-acyl carrier protein reductase (FabI) supports efficient operation of a functional reversal of beta-oxidation cycle. *Applied and environmental microbiology* **81**, 1406-1416
266. Blomfield, I. C., Vaughn, V., Rest, R. F., and Eisenstein, B. I. (1991) Allelic exchange in *Escherichia coli* using the *Bacillus subtilis sacB* gene and a temperature-sensitive pSC101 replicon. *Molecular microbiology* **5**, 1447-1457
267. Rzomp, K. A., Scholtes, L. D., Briggs, B. J., Whittaker, G. R., and Scidmore, M. A. (2003) Rab GTPases are recruited to chlamydial inclusions in both a species-dependent and species-independent manner. *Infection and immunity* **71**, 5855-5870
268. Mirrashidi, K. M., Elwell, C. A., Verschueren, E., Johnson, J. R., Frando, A., Von Dollen, J., Rosenberg, O., Gulbahce, N., Jang, G., Johnson, T., Jager, S., Gopalakrishnan, A. M., Sherry, J., Dunn, J. D., Olive, A., Penn, B., Shales, M., Cox, J. S., Starnbach, M. N., Derre, I., Valdivia, R., Krogan, N. J., and Engel, J. (2015) Global Mapping of the Inc-Human Interactome Reveals that Retromer Restricts Chlamydia Infection. *Cell host & microbe* **18**, 109-121
269. Hackstadt, T., Scidmore-Carlson, M. A., Shaw, E. I., and Fischer, E. R. (1999) The *Chlamydia trachomatis* IncA protein is required for homotypic vesicle fusion. *Cellular microbiology* **1**, 119-130
270. Scidmore-Carlson, M. A., Shaw, E. I., Dooley, C. A., Fischer, E. R., and Hackstadt, T. (1999) Identification and characterization of a *Chlamydia trachomatis* early operon encoding four novel inclusion membrane proteins. *Molecular microbiology* **33**, 753-765
271. Georgescu, R. E., Langston, L., Yao, N. Y., Yurieva, O., Zhang, D., Finkelstein, J., Agarwal, T., and O'Donnell, M. E. (2014) Mechanism of asymmetric polymerase assembly at the eukaryotic replication fork. *Nature structural & molecular biology* **21**, 664-670

272. Lindow, J. C., Dohrmann, P. R., and McHenry, C. S. (2015) DNA Polymerase alpha Subunit Residues and Interactions Required for Efficient Initiation Complex Formation Identified by a Genetic Selection. *The Journal of biological chemistry* **290**, 16851-16860
273. Kim, D. R., and McHenry, C. S. (1996) Biotin tagging deletion analysis of domain limits involved in protein-macromolecular interactions. Mapping the tau binding domain of the DNA polymerase III alpha subunit. *The Journal of biological chemistry* **271**, 20690-20698
274. Saha, R., Dasgupta, S., Banerjee, R., Mitra-Bhattacharyya, A., Soll, D., Basu, G., and Roy, S. (2012) A functional loop spanning distant domains of glutaminyl-tRNA synthetase also stabilizes a molten globule state. *Biochemistry* **51**, 4429-4437
275. Jester, B. C., Levengood, J. D., Roy, H., Ibba, M., and Devine, K. M. (2003) Nonorthologous replacement of lysyl-tRNA synthetase prevents addition of lysine analogues to the genetic code. *Proceedings of the National Academy of Sciences of the United States of America* **100**, 14351-14356
276. Dittmar, K. A., Sorensen, M. A., Elf, J., Ehrenberg, M., and Pan, T. (2005) Selective charging of tRNA isoacceptors induced by amino-acid starvation. *EMBO reports* **6**, 151-157
277. Picard, F., Loubiere, P., Girbal, L., and Cocaign-Bousquet, M. (2013) The significance of translation regulation in the stress response. *BMC genomics* **14**, 588
278. Beatty, W. L., Byrne, G. I., and Morrison, R. P. (1993) Morphologic and antigenic characterization of interferon gamma-mediated persistent *Chlamydia trachomatis* infection *in vitro*. *Proceedings of the National Academy of Sciences of the United States of America* **90**, 3998-4002
279. Beatty, W. L., Belanger, T. A., Desai, A. A., Morrison, R. P., and Byrne, G. I. (1994) Tryptophan depletion as a mechanism of gamma interferon-mediated chlamydial persistence. *Infection and immunity* **62**, 3705-3711
280. Xie, G., Bonner, C. A., and Jensen, R. A. (2002) Dynamic diversity of the tryptophan pathway in chlamydiae: reductive evolution and a novel operon for tryptophan recapture. *Genome biology* **3**, research0051
281. Dennis, P. P., and Nomura, M. (1974) Stringent control of ribosomal protein gene expression in *Escherichia coli*. *Proceedings of the National Academy of Sciences of the United States of America* **71**, 3819-3823
282. Trost, M., English, L., Lemieux, S., Courcelles, M., Desjardins, M., and Thibault, P. (2009) The phagosomal proteome in interferon-gamma-activated macrophages. *Immunity* **30**, 143-154
283. Nelson, D. E., Virok, D. P., Wood, H., Roshick, C., Johnson, R. M., Whitmire, W. M., Crane, D. D., Steele-Mortimer, O., Kari, L., McClarty, G., and Caldwell, H. D. (2005) Chlamydial IFN-gamma immune evasion is linked to host infection tropism. *Proceedings of the National Academy of Sciences of the United States of America* **102**, 10658-10663
284. Liu, Y., Huang, Y., Yang, Z., Sun, Y., Gong, S., Hou, S., Chen, C., Li, Z., Liu, Q., Wu, Y., Baseman, J., and Zhong, G. (2014) Plasmid-encoded Pgp3 is a major

virulence factor for *Chlamydia muridarum* to induce hydrosalpinx in mice. *Infection and immunity* **82**, 5327-5335
285. Lowden, N. M., Yeruva, L., Johnson, C. M., Bowlin, A. K., and Fisher, D. J. (2015) Use of aminoglycoside 3' adenyltransferase as a selection marker for *Chlamydia trachomatis* intron-mutagenesis and in vivo intron stability. *BMC research notes* **8**, 570
286. Silber, K. R., Keiler, K. C., and Sauer, R. T. (1992) Tsp: a tail-specific protease that selectively degrades proteins with nonpolar C-termini. *Proceedings of the National Academy of Sciences of the United States of America* **89**, 295-299
287. Roan, N. R., and Starnbach, M. N. (2006) Antigen-specific CD8+ T cells respond to *Chlamydia trachomatis* in the genital mucosa. *Journal of immunology* **177**, 7974-7979
288. Starnbach, M. N., Loomis, W. P., Ovendale, P., Regan, D., Hess, B., Alderson, M. R., and Fling, S. P. (2003) An inclusion membrane protein from *Chlamydia trachomatis* enters the MHC class I pathway and stimulates a CD8+ T cell response. *Journal of immunology* **171**, 4742-4749
289. Mukhopadhyay, S., Good, D., Miller, R. D., Graham, J. E., Mathews, S. A., Timms, P., and Summersgill, J. T. (2006) Identification of *Chlamydia pneumoniae* proteins in the transition from reticulate to elementary body formation. *Molecular & cellular proteomics : MCP* **5**, 2311-2318
290. Hou, S., Lei, L., Yang, Z., Qi, M., Liu, Q., and Zhong, G. (2013) *Chlamydia trachomatis* outer membrane complex protein B (OmcB) is processed by the protease CPAF. *Journal of bacteriology* **195**, 951-957
291. Qi, M., Gong, S., Lei, L., Liu, Q., and Zhong, G. (2011) A *Chlamydia trachomatis* OmcB C-terminal fragment is released into the host cell cytoplasm and is immunogenic in humans. *Infection and immunity* **79**, 2193-2203
292. Frikha-Gargouri, O., Gdoura, R., Znazen, A., Gargouri, B., Gargouri, J., Rebai, A., and Hammami, A. (2008) Evaluation of an *in silico* predicted specific and immunogenic antigen from the OmcB protein for the serodiagnosis of *Chlamydia trachomatis* infections. *BMC microbiology* **8**, 217
293. Moelleken, K., and Hegemann, J. H. (2008) The Chlamydia outer membrane protein OmcB is required for adhesion and exhibits biovar-specific differences in glycosaminoglycan binding. *Molecular microbiology* **67**, 403-419
294. Stephens, R. S., Koshiyama, K., Lewis, E., and Kubo, A. (2001) Heparin-binding outer membrane protein of chlamydiae. *Molecular microbiology* **40**, 691-699
295. Fechtner, T., Stallmann, S., Moelleken, K., Meyer, K. L., and Hegemann, J. H. (2013) Characterization of the interaction between the chlamydial adhesin OmcB and the human host cell. *Journal of bacteriology* **195**, 5323-5333
296. Kim, J. H., Chan, C., Elwell, C., Singer, M. S., Dierks, T., Lemjabbar-Alaoui, H., Rosen, S. D., and Engel, J. N. (2013) Endosulfatases SULF1 and SULF2 limit *Chlamydia muridarum* infection. *Cellular microbiology* **15**, 1560-1571
297. Millman, K. L., Tavare, S., and Dean, D. (2001) Recombination in the ompA gene but not the omcB gene of Chlamydia contributes to serovar-specific differences in tissue tropism, immune surveillance, and persistence of the organism. *Journal of bacteriology* **183**, 5997-6008

298. Fadel, S., and Eley, A. (2007) *Chlamydia trachomatis* OmcB protein is a surface-exposed glycosaminoglycan-dependent adhesin. *Journal of medical microbiology* **56**, 15-22
299. Bernstein-Hanley, I., Balsara, Z. R., Ulmer, W., Coers, J., Starnbach, M. N., and Dietrich, W. F. (2006) Genetic analysis of susceptibility to *Chlamydia trachomatis* in mouse. *Genes and immunity* **7**, 122-129

CURRICULUM VITAE

Julie Ann Brothwell

EDUCATION

Ph.D.—Microbiology and Immunology
Indiana University, Indianapolis, IN, 2017
Dissertation: Genetic Dissection of Essential Gene Function in *Chlamydia trachomatis*

B.S.—Microbiology, *summa cum laude*
Barrett Honors College, Arizona State University, 2010
Thesis: Characterization of the Opioid Peptide Dynorphin A as a Novel Ligand for Leukocyte Integrin $\alpha_M\beta_2$ (Mac-1)

RESEARCH EXPERIENCE

Jan. 2013-April 2017 Graduate Microbiology Research Assistant
Department of Microbiology and Immunology, School of Medicine, Indiana University, Indianapolis, IN
Principal Investigator: Dr. David Nelson
Project: Genetic Manipulation of the Obligate Intracellular Pathogen *Chlamydia trachomatis*

Aug. 2010-Dec. 2012 Graduate Biochemistry Research Assistant
Department of Biology, Indiana University—Bloomington, Bloomington, IN
Principal Investigator: Dr. David Nelson
Project: The Effect of Chlamydial Infection on the Host Intermediate Filament Cytoskeleton

Aug. 2008-June 2010 Undergraduate Researcher, School of Life Sciences Undergraduate Research (SOLUR) Program
School of Life Sciences, Arizona State University, Tempe, AZ
Mentor: Dr. Tatiana Ugarova
Project: An Unexpected Link between the Immune and Nervous systems: the Effects of Dynorphin on Integrin $\alpha_M\beta_2$ in Neutrophils

TEACHING EXPERIENCE

Fall 2013	Teaching Assistant, Introduction to Microbiology for Nurses Laboratory (J210) Indiana University, Indianapolis, IN Professor: Dr. Götz-Ulrich von Bulow Invited to guest lecture on RNA viruses to main class (100 students)
Spr 2009-Spr 2010	Teaching Assistant, Cell Biology (BIO 353) Arizona State University, Tempe, AZ Professors: Drs. Dawn Coletta, Robert Roberson & Tatiana Ugarova Invited to guest lecture on cell signaling each semester to classes of 100+

PUBLICATIONS

1. M. K. Muramatsu, **J. A. Brothwell**, B. D. Stein, T. E. Putman, D. D. Rockey, D. E. Nelson. Beyond tryptophan synthase: identification of genes that contribute to *Chlamydia trachomatis* survival during IFN-γ induced persistence and reactivation. *Infect and Immun*. 2016 Sep 19. 84(10):2791-801. doi: 10.1128/IAI.00356-16

2. **J. A. Brothwell**, M. K. Muramatsu, E. Toh, D. D. Rockey, T. E. Putman, M. L. Barta, P. S. Hefty, R. J. Suchland, and D. E. Nelson. Interrogating genes that mediate *Chlamydia trachomatis* survival in cell culture using conditional mutants and recombination. *J Bacteriol*. 2016 Jul 13. 198(15):2131-9. doi: 10.1128/JB.00161-16.

3. N. P. Podolnikova, **J. A. Brothwell**, and T. P. Ugarova. The opioid peptide dynorphin A induces leukocyte responses via integrin Mac-1 (αMβ2, CD11b/CD18). *Mol Pain*. 2015 Jun 3; 11(1):33. doi: 10.1186/s12990-015-0027-0.

ORAL PRESENTATIONS

1. Characterization of a temperature sensitive aminoacyl-tRNA synthetase *Chlamydia trachomatis* mutant. 8th Meeting of the European Society of Chlamydia Research, Oxford, UK, September 2016.

2. Exploiting temperature sensitive alleles to investigate chlamydial essential gene functions and generate isogenic recombinants. 7th Meeting of the Chlamydia Basic Research Society, New Orleans, LA, USA, March 2015.

POSTER PRESENTATIONS

1. **J. A. Brothwell**, B. D. Stein, and D. E. Nelson. Characterization of a Temperature Sensitive Aminoacyl-tRNA Synthetase *Chlamydia trachomatis* Mutant. American Society for Microbiology Microbe, Boston, MA, June 2016.

2. **J. A. Brothwell**, M. K. Muramatsu, E. Toh, T. E. Putman, D. D. Rockey, and D. E. Nelson. Generation of *Chlamydia trachomatis* recombinants via negative selection. Midwest Microbial Pathogenesis Conference, Indianapolis, IN, August 2015.

3. **J. A. Brothwell**, M. K. Muramatsu, E. Toh, and D. E. Nelson. Uncovering chlamydial essential genes: screen and genetic analysis of temperature sensitive *Chlamydia trachomatis* mutants. Midwest Microbial Pathogenesis Conference, Chicago, IL, September 2014.

4. **J. A. Brothwell**, B. Fan, and D. E. Nelson. The Role of Intermediate Filaments in *Chlamydia trachomatis* Infection. Genetics, Cellular, and Molecular Sciences Symposium, Bloomington, IN, May 2013.

5. **J. A. Brothwell**, B. Fan, E. Toh, F. Liu, S. Easwaran, and D. E. Nelson. The Role of Cytokeratin 17 in *Chlamydia trachomatis* Infection. American Society for Microbiology General Meeting, San Francisco, CA, July 2012.

6. **J. A. Brothwell**, B. Fan, S. Easwaran, and D. E. Nelson. The Role of Cytokeratin 17 in *Chlamydia trachomatis* Infection. Midwest Microbial Pathogenesis, Ann Arbor, MI, October 2011.

7. **J. A. Brothwell**, N. P. Podolnikova, and T. P. Ugarova. Characterization of the Opioid Peptide Dynorphin A as a Novel Ligand for Leukocyte Integrin αMβ2 (Mac-1). Experimental Biology Conference, Anaheim, CA, April 2010.
   *Abstract published in: *The FASEB Journal* (24): 1 Supplement 953.7

8. **J. A. Brothwell**, N. P. Podolnikova, and T. P. Ugarova. Characterization of the Opioid Peptide Dynorphin A as a Novel Ligand for Leukocyte Integrin αMβ2 (Mac-1). Arizona State University Undergraduate Research Symposium, Tempe, AZ, March 2010.

9. **J. A. Brothwell**, N. P. Podolnikova, and T. P. Ugarova. Characterization of the Opioid Peptide Dynorphin A as a Novel Ligand for Leukocyte Integrin αMβ2 (Mac-1). Arizona State University Undergraduate Research Symposium, Tempe, AZ, March 2009.

AWARDS

IUSM Travel Grant, January 2015
Genetics, Cellular, and Molecular Sciences Predoctoral Training Grant (NIGMS 5T32GM007757-32), July 2011-May 2013
Abstract Honorable Mention, Midwest Microbial Pathogenesis Conference 2011, October 2011
Peglow Travel Award, October 2011
SOLUR Program Appointment, funded by an HHMI training grant to the SOLUR program/R. L. Rutowski, Fall 2008-2010
Arizona State University President's Scholarship, Fall 2007-Spring 2010
Dean's List, Arizona State University, Tempe, AZ, Fall 2007-Spring 2010

ORGANIZATIONS

Chair, Fong-Clontech Award Search Committee, 2016
Student Representative, IUSM Dept. of Microbiology and Immunology, Indiana University-Purdue University-Indianapolis, Fall 2015-Summer 2016
Member, American Society for Microbiology, January 2012-present
Mentor, Barrett Mentor Program, Barrett Honors College, Arizona State University, Tempe, AZ, Fall 2009